Publication No. 101

MANAGEMENT METHODS FOR IMPOUNDED FLORIDA COASTAL MARSHES

Final Report

by

M. Eileen Rowan, James P. Heaney,
Mark D. Shafer, Thomas G. Potter, S. Wayne Miles,
and Michael A. O'Connell

Publication No. 101

MANAGEMENT METHODS FOR IMPOUNDED FLORIDA COASTAL MARSHES

Final Report

by

M. Eileen Rowan, James P. Heaney,
Mark D. Shafer, Thomas G. Potter, S. Wayne Miles,
and Michael A. O'Connell

Florida Water Resources Research Center
and
Department of Environmental Engineering Sciences
University of Florida
Gainesville, Florida 32611

November 11, 1987

ACKNOWLEDGEMENTS

The authors would like to thank the following people for their cooperation and assistance with this project:

Douglas Carlson and Peter O'Bryan, Indian River Mosquito Control District, Vero Beach; Grant Gilmore, Ned Smith, Peter Hood, and Dennis Peters, Harbor Branch Foundation, Inc., Fort Pierce; Jorge Rey, Florida Medical Entomology Laboratory, Institute of Food and Agricultural Sciences, University of Florida; Clay Montague and Wayne Huber, Department of Environmental Engineering Sciences, University of Florida, Gainesville; William Leenhouts, Merritt Island National Wildlife Refuge, Titusville; Frank Evans and Jim David, St. Lucie County Mosquito Control District, Fort Pierce; Jack Salmella, Brevard County Mosquito Control District, Titusville; Carl Goodwin, U. S. Geological Survey, Tampa; Scott Ritchie, Department of Entomology, University of Florida, Gainesville; Doris Smithson and James Wittig, Department of Environmental Engineering Sciences, University of Florida, Gainesville; Dan Klein, Insects Affecting Man and Animals Laboratory, U. S. Department of Agriculture, Gainesville; and James Cato and William Seaman, Florida Sea Grant College Program, Gainesville.

This report was developed under the auspices of the Florida Sea Grant College Program with support from the National Oceanic and Atmospheric Administration, Office of Sea Grant, U. S. Department of Commerce, Grant No. R/C-E-23. The authors also wish to acknowledge

financial support from the Engineering and Industrial Experiment Station, College of Engineering, University of Florida, Gainesville, Project No. 4910-4510-044.

PREFACE

Chapters 1 through 5 and Chapter 8 are the contribution of M. E. Rowan. M. D. Shafer provided Chapter 7, "Economics of Impounded Coastal Marshes for Mosquito Control." Chapter 6, "Incorporating Spatial Analysis into Mosquito Impoundment Simulation," was written primarily by T. G. Potter, with surface mapping/spreadsheet topographic analysis and discussion contributed by S. Wayne Miles. Appendix A was prepared by Michael A. O'Connell.

This project was conducted under the general supervision of James P. Heaney, Professor of Environmental Engineering Sciences and Director, Florida Water Resources Research Center.

CONTENTS

CONTENTS

CONTENTS

LIST OF TABLES

LIST OF FIGURES

CHAPTER 1
INTRODUCTION

The goals of this project are to develop a continuous simulation model to predict water levels, salinity, and associated impacts of mosquito impoundments on fisheries, wildlife, and vegetation under different management strategies; to estimate the benefits, costs, and risks of these alternative strategies; and to test this model using impoundments along the east central coast of Florida for which data are available.

The following specific tasks will be addressed:

1) create a simulation model of a typical impoundment to predict hydrologic, water quality, and mosquito breeding responses to impoundment design and management practices;

2) analyze existing data from study areas to establish correlations between hydrologic events, water level, and brood production in salt marsh impoundments;

3) analyze benefits, costs, and risks in order to compare design and management methods; and

4) create an expert system to assist in making design and management decisions based upon a given description of marsh area and desired use, including considerations for impacts on wildlife, vegetation, marsh and estuarine water quality and interchange.

In Chapter 2 the concept of a microcomputer-based decision support

system is presented. A brief overview of Florida's coastal wetlands is presented in Chapter 3, including the salt marsh mosquito problem and the use of impoundments in its control. The remaining chapters detail possible components of a decision support system for the management of impounded salt marshes.

Hydrologic analysis and simulation of a salt-marsh impoundment are performed in Chapter 4, generating time series indicating hydrologic responses to varying control methods. Chapters 5 and 6 offer techniques to expand upon the spatial distribution capabilities of this model.

Chapter 7 reviews mosquito production at the study area, and an analysis of costs and benefits associated with mosquito control is found in Chapter and 8. Chapter 9 summarizes and presents conclusions.

CHAPTER 2
DECISION SUPPORT SYSTEMS

As researchers work to develop new and better models, several groups are directing their efforts to improving the usability of existing models. The problem of managers and engineers too short on time or expertise to fully take advantage of the modeling techniques is creating a rapidly growing need for such developments. This has led to the current work in decision support systems (DSS), defined by Sprague and Carlson (1982) as "an interactive computer-based system that helps decision-makers utilize data and models to solve unstructured or underspecified problems."

Paralleling these developments has been the increased interest in expert systems. These employ a knowledge base of simple rules to deduce a series of user-directed queries in order to arrive at an optimal decision or solution. Appendix A presents an expert system for mosquito control impoundment management (O'Connell, 1985) which, although designed as only a rudimentary demonstration, exhibits the expert system's advantages and disadvantages. This user-friendly program can be expanded or refined with the addition of more rules to the knowledge base. It can describe the rules it used in arriving at decisions when requested. The focus is clearly solution-oriented; for applications with clearly-defined objectives, this may be an appropriate process.

The goals in management of impounded salt marshes, however, are numerous and complex, as is often the case in water management problems. The expert system typically deals with qualitative rules and goals; the interests here are of a quantitative nature. Often the prioritizing of objectives is in a state of flux and can be subjective. A more flexible system is needed which permits the user to remain closer to the modeling process without extensive computer experience, continually shaping and directing the operation.

The path for the development of DSS's has been paved by work in interactive data management (IDM). Fedra and Loucks (1985) discussed the structure of an interactive computer workstation for environmental planning and policy-making applications. This concept includes a general knowledge database with handbook-type information, a project-specific database, applications programs, and methods for formatting generated information. One recurring emphasis is that "an important element is the direct interaction. What we are proposing is the development and transfer of tools and skills rather than 'solutions.'"

Interactive tools that seem most promising may come from the proliferating availability of graphics processors and software. Until recently, sophisticated graphics were far too costly for single-user workstations. The past two years, however, have seen the introduction of a large array of graphics products stimulated by the growing computer-aided-design (CAD) market. Graphics expansion for the microcomputer is expected to continue at this accelerated pace with lowering prices (Knorr and Koessel, 1986).

The employment of graphics in the development of interactive data management systems at Cornell University is described by Loucks et al.

(1985). They observed that graphical and pictorial displays can "substantially improve effective communication of spatial information...they also can aid in human-model-computer interaction."

Adding to the toolkit of the DSS designer will soon be a variety of software packages that link with graphics software for graphics input, editing, or information extraction. Another type of software is the engineering database management system (EDBMS) which accepts program input, sorts the data, and transmits these to the next program (Basta, 1986). These integrated packages are currently limited in their availability, but assurances of their development should encourage the graphics user.

Electronic Spreadsheets in Decision Support Systems

All components of the decision support system -- database management, modeling and other applications programs, analysis, and graphical output can be supported with varying degrees of success within the electronic spreadsheet environment. Hancock and Heaney (1987) note that spreadsheet modeling can lead to better understanding of a specific water resources problem than large generic "black box" models; all assumptions and equations are visible and can be documented with text. Model pre- and post-processing and graphical analysis can be performed within the same spreadsheet with ease.

Lotus 1-2-3, a popular spreadsheet package, is therefore utilized extensively for the hydrological analysis and modeling described in the following chapters. Although a basic understanding of this or a similar software package will be assumed, each new spreadsheet function or feature mentioned will be explained briefly. It should be possible to

follow this narrative in performing similar analyses, adapting models presented here, or building new ones for specific problems.

Advanced Computer Graphics

Graphics are extremely useful in providing a more intuitive grasp of a physical problem. One of the most successful of these software packages is AutoCAD, by Autodesk of Sausalito, California. AutoCAD is widely used by engineers in most fields; the popularity of this and other CAD packages is quickly making the hardware necessary to support this software an industry standard, and at steadily dropping prices. Basic hardware requirements are 512 K of memory, a graphics controller card, a pointing device, a graphics monitor, and a plotter or printer-plotter.

AutoCAD is a completely menu-driven program; the novice user may quickly prepare simple sketches with it. More sophisticated work requires greater familiarity, however. This situation can be improved through the use of custom menus, which make possible the design of AutoCAD-based application programs which do not require the user to become an expert computer drafter. AutoCAD's ability to both transfer data to and receive data from a spreadsheet makes it a useful component in a decision support system such as described here.

The next chapter is a general presentation of impoundment management concepts. Applications of the tools described above within the framework of a general decision support system for impoundment management are described in the following chapters.

References

Basta, N. 1986. Computer aided design zeroes in on Ch.E. needs. Chemical Engineering September 1: 14-17.

Fedra, K. and D. P. Loucks. 1985. Interactive computer technology for planning and policy modeling. Water Resources Research 2: 114-122.

Hancock, M. C. and J. P. Heaney. 1987. Water resources analysis using electronic spreadsheets. Journal of Water Resources Planning and Management, 113 (5): 639-658.

Johnson, L. E. 1986. Water resource management decision support systems. Journal of Water Resources Planning and Management, American Society of Civil Engineers, 112 (3): 308-325.

Knorr, E. and K. Koessel. 1986. Seven up on EGA. PC World, August: 210-219.

Loucks, D. P., M. R. Taylor and P. N. French. 1985. Interactive data management for resource planning and analysis. Water Resources Research, 21(2):131-142.

CHAPTER 3
IMPOUNDED COASTAL MARSHES FOR MOSQUITO CONTROL

Estuarine Wetlands of Florida

Florida's coastal wetlands cover approximately 1390 square miles, or approximately 20 percent of the coastal wetlands in the United States. About 60% of these wetlands are salt or brackish marshes, which are defined as tidally flooded (either regularly or irregularly) and dominated by salt-tolerant marsh grasses. These marshes are concentrated along Florida's Atlantic coast extending northward from Martin County, and along the Gulf Coast northward from Pasco County (Figure 3-1). Mangrove swamps comprise the remaining coastal wetlands, fringing South Florida's shoreline and creating large dense forested areas along the Gulf of Mexico (Fish and Wildlife Service, 1984).

Within the coastal marsh there is usually a natural levee at the mean high water mark which roughly separates low marsh, that area washed daily by diurnal high tides, from high marsh, the area further upland that is tidally washed only by seasonal high tides (Provost, 1958). The ratio of high to low marsh, which is related to elevation and the amount of fresh water flowing into the marsh, holds some significance for mosquito control. A similar though equally rough zonation may be noted in the mangrove swamps. This "high swamp" is irregularly flooded and dominated by black mangroves. Florida's high marsh to low marsh ratio is 3.3; that is, approximately 77% of its coastal marshes are high marsh (U. S. Fish and Wildlife Service, 1982).

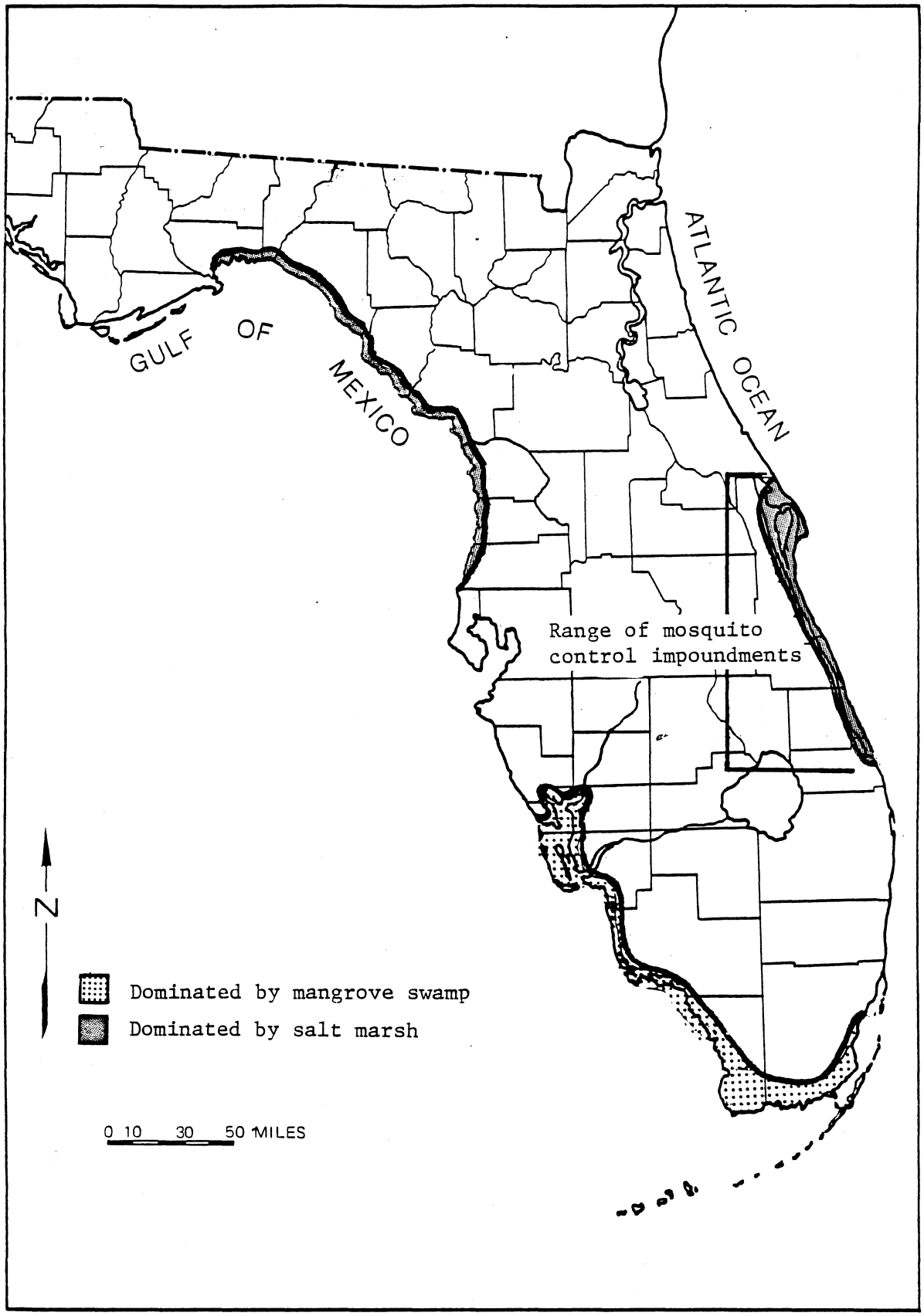

Figure 3-1. Distribution of coastal wetlands and mosquito control impoundments. Provost (1958); Fish and Wildlife Service (1984).

Mosquito Breeding Patterns

The mosquitoes that dominate Florida's coastlines and mosquito control budgets are those associated with salt marsh and mangrove swamp habitat, primarily Aedes taenyiorhynchus and Aedes sollicitans (Nayar, 1984). Aedes mosquitoes deposit their eggs in moist soil where they may remain for several months until inundation triggers larval hatching. Four to seven days later the adult mosquitoes emerge as a brood following the flooding event (Provost, 1958).

The facts that oviposition never occurs in water and that the larvae require up to a week of standing water for development rule out most low marsh and mangrove swamp as mosquito breeding grounds. Thus soil is not exposed long enough for oviposition, and the daily tides flush out any larvae that may have been produced. The higher elevations, however, are exposed for extended periods of time. When seasonal high tides or rains flood these upper areas, the water is trapped in many pools, creating excellent areas for brood production (Provost, 1958).

Balling and Resh (1983a) found the occurrence and abundance of Aedes mosquito larvae in San Francisco Bay marshes to correlate significantly with pond inundation height, defined to be the minimum tidal height above mean lower low water (MLLW) necessary to inundate a marsh pond. In a further report (1983b), the same authors provide a simple method for determining pond inundation height. When surveying from a nearby tidal benchmark is impossible or impractical, a tidal marker is placed in the pond when a flooding tide is expected. After flooding, 12-14 hours are allowed for the pond to drain to basin-full level before significant evaporation occurs. The difference between the high water mark and the pond surface, when subtracted from the known height of the

tide (taken from tide tables or a tide gauge) yields an acceptable estimate of pond inundation height. The assumption may be made that differences in inundation height within and between marshes are relatively constant.

Bidlingmayer and Klock (1955) looked at the influence of tidal action upon the inundation of two salt marsh areas in Georgia known as good Aedes breeding sites. Lower water levels in marsh sloughs than those predicted from tide tables indicated complicating hydraulic factors. They concluded that in evaluating an area for mosquito breeding potential, elevation should not be relied upon completely and emphasized the value of marsh vegetation as a breeding indicator.

Ritchie (1984) examined rainfall, water table and mosquito records for Lee and Collier Counties, Florida, noting an inverse relationship between winter rainfall and mosquito landing rates. He observed that winter rainfall and water table measurements may be useful indicators of mosquito populations.

Haile and Weidhaas (1977) have developed a simulation model for predicting mosquito populations. For a more in-depth review of the mosquitoes themselves, Nayar has edited a useful compendium (1984) covering mosquito biology, development, distribution, behavior, transmitted diseases, and control.

Methods for Mosquito Control

Florida's large high-to-low-marsh ratio, in association with the state's southern latitudes, have helped create sizeable salt-marsh mosquito troubles (Provost, 1967). Aedes breeding can be reduced in salt marshes by draining and filling above high tide lines, by preventing

water from standing long enough to permit larval development, or by keeping the marsh flooded to prevent oviposition. Draining and filling are now generally considered unacceptable due to destruction of marsh and high cost (Provost, 1967).

Prevention of standing water has typically been accomplished by ditching methods. Open marsh water management (OMWM), which improves upon older ditching methods to eliminate mosquito breeding depressions, has been developed and reported in New Jersey by Ferrigno and Jobbins (1968), and Ferrigno, Slavin and Jobbins (1975). OMWM to increase tidal circulation in San Francisco Bay salt marshes was reported by Balling and Resh (1983a).

Diking and flooding of marshes to create mosquito control impoundments has been shown to be very effective in preventing the breeding of Aedes. Clements and Rogers (1964) studied an impounded area of both high and low marsh in Indian River County from 1958 to 1963, comparing three different management methods. In one section, the impoundment was flooded continuously with only artesian water; in a second, flooding with artesian water occurred only seasonally until fall high tides flooded the marsh, after which the tide gates were continually open; in a third, natural marsh conditions were represented with seasonal tidal flooding only.

In both the permanent and the seasonally flooded impoundments, Aedes mosquitoes were almost completely eliminated. The conversion to fresh water for some periods did not produce significant numbers of freshwater mosquitoes. Year-long flooding, however, destroyed most salt marsh vegetation and greatly reduced fish and shellfish by denying them ingress and egress.

In the seasonally flooded impoundment, damage to vegetation and reduction of fish and shellfish were somewhat lessened, and birds seemed to prefer this area over both the permanent impoundment and natural marsh.

Clements and Rogers concluded that seasonal flooding was an acceptable method of marsh management for mosquito control. Flooding could be restricted to March through August or early September to keep costs down; this was aided by trapping rainwater which falls most heavily outside high tide periods.

Further confirmations of impoundment effectiveness may be found in Florschutz (1959) and LaSalle and Knight (1984). The use of open culverts through impoundment dikes vs. retaining water with flapgate risers, and their effects on marsh flooding and mosquito production, were examined over two years at Impoundment No. 12 in Indian River County by Carlson and Vigliano (1984). Their study confirmed Clements and Rogers' finding that some degree of artificial flooding is almost always a requirement for mosquito control.

Further studies refined this and other methods of mosquito source reduction, which to a large extent have replaced chemical control in Florida. Chemicals as a primary control have pronounced disadvantages, which include buildup of mosquito resistance, numerous environmental problems, and higher costs (Breeland and Mulrennan, 1983).

Florida's Coastal Impoundments

Almost 33 thousand acres of salt marsh are now impounded in Florida, virtually all of which are located on Florida's east central coast. Nineteen thousand acres of these impoundments are contained within Mer-

ritt Island National Wildlife Refuge (MINWR), where the average impoundment size is approximately 300 acres (Leenhouts, 1982).

Bidlingmayer (1983) surveyed the approximately 13 thousand acres of Florida impoundments on private lands, recording an average size of 200 acres. A breakdown of these impoundments by ownership, river system, and county is given in Table 3-1.

Florida's coastal impoundments are concentrated along the Indian River system of saltwater lagoons stretching from Ponce de Leon Inlet in Volusia County to St. Lucie Inlet in Martin County and including Mosquito Lagoon and the Banana River (Figure 3-1). The Indian River Lagoon is approximately 120 miles long, averaging 1.2-2.5 miles wide and 3-6.5 feet deep. Due to few inlets to the ocean, only the roughly 50% of the lagoon extending south from Melbourne experiences daily tidal fluctuations (Smith, 1985). Daily tides have been found of little significance in high marsh impoundments, especially in bays, lagoons, and estuaries; wind-generated tides and rainfall are more influential (Provost, 1973; Smith, 1980; Carlson and Vigliano, 1984).

The most important parameter in the management of diked and flooded areas is water level. Although mosquitoes will not oviposit in even the thinnest film of water (Provost, 1968), several additional inches of water as a safety margin against irregular bottom topography and water fluctuations must be kept. A minimum of ten to twelve inches has been found best for breeding prevention (Florschutz, 1958; Clements and Rogers, 1964). This maximizes the advantages of higher water levels in reducing dense vegetative mats at the surface which act as cover for larvae and in providing better access to larvivorous fish (Dukes, Axtell and Knight, 1974; LaSalle and Knight, 1974) without excessively pene-

Table 3-1. Location of impounded coastal marshes in Florida.

Privately Owned

County	Halifax River	Mosquito Lagoon	Banana River	Indian River	Total
Volusia	1100	478	0	0	1578
Brevard	0	0	2608	970	3578
Indian River	0	0	0	2944	2944
St. Lucie	0	0	0	4508	4508
Martin	0	0	0	603	603
Subtotal	1100	478	2608	9025	13211

Federally Owned

County	Halifax River	Mosquito Lagoon	Banana River	Indian River	Total
Volusia	0	1430	0	0	1430
Brevard	0	3861	2432	11584	17877
Indian River	0	0	0	0	0
St. Lucie	0	0	0	0	0
Martin	0	0	0	20	20
Subtotal	0	5291	2432	11604	19327
Total	1100	5769	5040	20629	32538

Sources: Information on privately-owned lands from Bidlingmayer and McCoy, 1978.

All federally-owned lands in Volusia and Brevard Counties are within Merritt Island National Wildlife Refuge (MINWR). Estimates are approximate; total acreage for MINWR of 19307 from Leenhouts, 1983.

Federally-owned land in Martin County is within Hobe Sound National Wildlife Refuge (HSNWR). Acreage estimate is per S. Marcus, HSNWR, personal communication 1986.

trating into uplands or fatally inundating black mangrove pneumatophores or other high marsh vegetation (Carlson and Vigliano, 1984).

According to Provost (1968), low marsh salinity typically reflects lagoon waters and rarely exceeds 35 ppt. High marsh salinity, however, varies widely since tidewater or rainwater can be trapped. During rainless periods, salinity can surpass 60 ppt. Excessive salinity limits marsh productivity; too little salinity promotes invasion of freshwater vegetation, altering the salt marsh ecosystem from its natural state to a freshwater wetlands community. Salinity itself is not a direct factor in mosquito breeding, however, and as has been mentioned before, the problem of converting a saltwater mosquito problem into a freshwater mosquito problem which has harassed managers elsewhere has not been experienced in Florida (Provost, 1968).

Environmental Considerations

Many studies of estuarine marsh management and the impacts of impoundments have been performed or are in progress. Rather than mentioning the numerous key papers here, the reader is referred to two reports by Montague et al.: a comprehensive, categorized bibliography of salt-marsh literature (1984), and an ecologically-integrated conceptual model of salt marsh management for Merritt Island National Wildlife Refuge (MINWR) (1985) which refers to a large body of work. Some significant considerations of impoundment management beyond mosquito control discussed in the latter report are reviewed below.

Attraction of Waterfowl and Other Birds

Montague et al. (1985) have reviewed available literature on attraction of waterfowl and other waterbirds and spoken with a number of

Florida mosquito impoundment managers and wildlife biologists, focusing on Merritt Island salt marshes. This survey indicates that managing for waterfowl involves the maintenance of a desired vegetative balance through control over water level and salinity. Desirable emergent vegetation increases in number of species with decreasing salinity and requires a minimum water level. Submerged vegetation is not dependent upon water level, but must be maintained within high and low salinity limits. In practice, if the salinity of available water is too high for desired emergents, water level is kept high enough to reduce undesired emergents with all focus being shifted to submergent production.

Most emergents and submergents require a complete drawdown in spring for seeding. Sufficient water circulation is necessary not only to maintain the required salinity range but to prevent overgrowth of phytoplankton which reduces light available to submergents.

Enhancement of Fish and Shellfish

Recommendations on fish and shellfish management techniques focus on the necessity of providing ingress and egress. Suggested methods include: more submerged cross-sectional area of open access; more time open during high water periods; keeping culverts open during January's water level drop to allow marsh drainage where possible; breaching or removing water control structures where possible; adding more ditches; and pumping while leaving culverts partially open.

Summary

Impounded salt marshes represent a significant management concern for Florida. Attaining numerous mosquito control objectives while main-

taining a sensitive ecological balance is a challenging task. The increasing use of rotational impoundment management will require a deeper understanding of the pertinent hydrology and hydrodynamics.

Chapter 4 presents such an analysis of one impoundment, explaining the methods used so that similar studies can be performed elsewhere or general characteristics extrapolated.

References

Balling, S. S. and V. H. Resh. 1983. Mosquito control and salt marsh management: factors influencing the presence of Aedes larvae. Mosquito News 43: 212-218.

Balling, S. S. and V. H. Resh. 1983b. A method for determining pond inundation height for use in salt marsh mosquito control. Mosquito News 43: 239-240.

Bidlingmayer, W. L. and Klock, J. W. 1955. Notes on the influence of salt-marsh topography on tidal action. Mosquito News 15: 231-235.

Carlson, D. B. and R. R. Vigliano. 1984. The effects of two different management regimes using water control structures on flooding and mosquito production in a naturally-flooded salt-marsh impoundment. Unpublished. Indian River Mosquito Control District, Vero Beach, Florida.

Clements, B. W., Jr. and A. J. Rogers. 1964. Studies of impounding for the control of salt marsh mosquitoes in Florida, 1958-1963. Mosquito News 24: 265-276.

Ferrigno, F. and D. M. Jobbins. 1968. Open marsh water management. Proceedings from the Annual Meeting, New Jersey Mosquito Exterminators Association 53: 97-112.

Ferrigno, F., P. Slavin and D. M. Jobbins. 1975. Saltmarsh water management for mosquito control. Proceedings from the Annual Meeting, New Jersey Mosquito Exterminators Association 62: 30-38.

Fish and Wildlife Service, U. S. Department of the Interior. 1982. The ecology of New England high salt marshes: a community profile. Biological Services Program Publication #FWS/OBS-81/55.

Fish and Wildlife Service, U.S. Department of the Interior. 1984. Florida wetland acreage. National Wetlands Inventory, St. Petersburg, Florida.

Florschutz, O., Jr. 1959. Mosquito production and wildlife usage in impounded, ditched and unditched tidal marshes at Assawoman Wildlife Area, Delaware, 1957-58. Proceedings from the Annual Meeting, New Jersey Mosquito Exterminators Association 46: 103-111.

Hail, D. G. and D. E. Weidhaas. 1977. Computer simulation of mosquito populations (Anopheles albimanus) for comparing the effectiveness of control technologies. Journal of Medical Entomology 13: 553-567.

LaSalle, R. N. and K. L. Knight. 1974. Effects of salt marsh impoundments on mosquito populations. Report No. 92, Water Resources Research Institute, University of North Carolina, Raleigh, N. C.

Leenhouts, W. P. 1983. Marsh and water management plan, Merritt Island National Wildlife Refuge, Titusville, Florida. An unpublished report for the U. S. Department of the Interior, Fish and Wildlife Service, Titusville, FL.

Montague, C. L., A. V. Zale and H. F. Percival. 1984a. A categorized bibliography for a conceptual model of salt marsh management on Merritt Island, Florida. Technical Report No. 9, Florida Cooperative Fish and Wildlife Research Unit, University of Florida, Gainesville, Florida.

Montague, C. L., A. V. Zale and H. F. Percival. 1985. A conceptual model of salt marsh management on Merritt Island National Wildlife Refuge, Florida. Technical Report No. 17, Florida Cooperative Fish and Wildlife Research Unit, University of Florida, Gainesville, FL.

Nayar, J. K. (ed.). 1984. Bionomics and physiology of Aedes taenyiorhynchus and Aedes sollicitans, the salt marsh mosquitoes of Florida. An unpublished report by the Florida Agricultural Experiment Stations, Institute of Food and Agricultural Sciences, University of Florida, Gainesville, FL.

Provost, M. W. 1968. Managing impounded salt marsh for mosquito control and estuarine resource conservation. Proceedings, Louisiana State University, Marsh and Estuary Management Symposium, J. D. Newson, ed. 163-171. Louisiana State University, Division of Continuing Education, Baton Rouge, LA.

Ritchie, S. A. 1984. Record winter rains and the minimal populations of Aedes taenyiorhynchus (Wiedemann): cause and effect? Journal of the Florida Anti-Mosquito Association 55: 14-21.

Smith, N. P. (in press). An introduction to the tides of Florida's Indian River Lagoon. Part I: water level variations. Florida Scientist.

CHAPTER 4
SPREADSHEET SIMULATION OF IMPOUNDED COASTAL MARSH HYDROLOGY

Introduction

In order to quantitatively predict the behavior of an impoundment salt marsh under varying management schemes, its behavior may be observed under one set of known conditions. Dominating hydrologic factors and their interrelationship with impoundment dynamics may then become apparent. If so, new dynamics may then be predicted given expected environmental conditions. When this can be shown to be successful, one has an excellent tool for developing a management strategy.

Water levels and associated constituents such as salinity and dissolved oxygen are the primary physical characteristics of interest in managing salt marshes. Prediction or simulation of these should consider the marsh's physical descriptors, the hydrologic budget components, and water control structures. Such a model may be used for long-term statistical analysis of marsh activity in which seasonal patterns may be seen, or for shorter periods where a more precise picture of marsh response is needed for a highly specific set of conditions. A combination of widely used and relatively easy to master personal computer tools makes this type of analysis readily feasible.

A microcomputer-based simulation model for Indian River County Impoundment No. 12 (IRC-12) using general purpose software is described in this section. Given the representative nature of this marsh, it is

hoped that this model may serve as a template for other impoundments along the Indian River Lagoon system, and possibly other estuarine systems.

Description of Study Area

Selection and Location of Site

Numerous studies on impounded salt marshes in Florida have focused upon Indian River County Impoundment No. 12 (IRC-12), located on the barrier island shore of the Indian River Lagoon at the Indian River - St. Lucie county line (Figures 4-1 and 4-2).

Originally this was high marshland vegetated with saltwort (Batis maritima), glasswort (Salicornia perennis), and black mangrove (Avicennia germinans), edged with a combination of black mangrove, red mangrove (Rhizophora mangle), white mangrove (Laguncularia racemosa), sea oxe-eye (Borrichia frutescens), and buttonwood (Conocarpus erectus) (Rey, et al., 1986).

In 1966 the marsh was impounded with the construction of a dike approximately ten feet in width sealing off a 50-acre area on its western, southern, and part of its northern sides. The undiked portion of the northern side and entire eastern side slope gradually into upland hammock. A perimeter ditch three to ten feet in width rims the inner side of the dike (Carlson and Vigliano, 1984). Currently the impoundment is vegetated over less than 20% of its surface area with saltwort, perennial glasswort (Salicornia virginica), annual glasswort (Salicornia bigelovii), and very few black and white mangroves. Numerous open

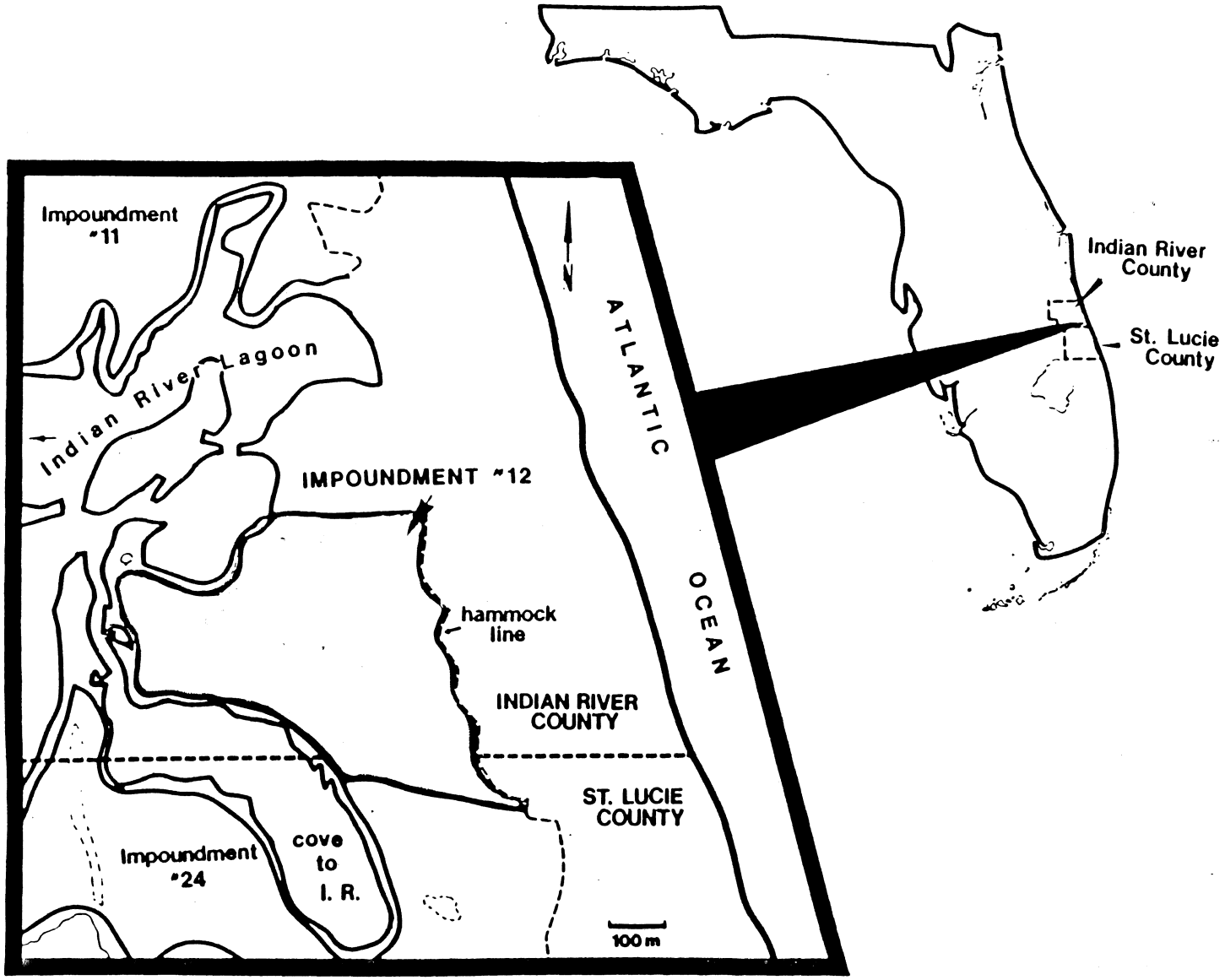

Figure 4-1. Indian River County Impoundment No. 12 locator map. Source: Carlson and O'Bryan, 1986.

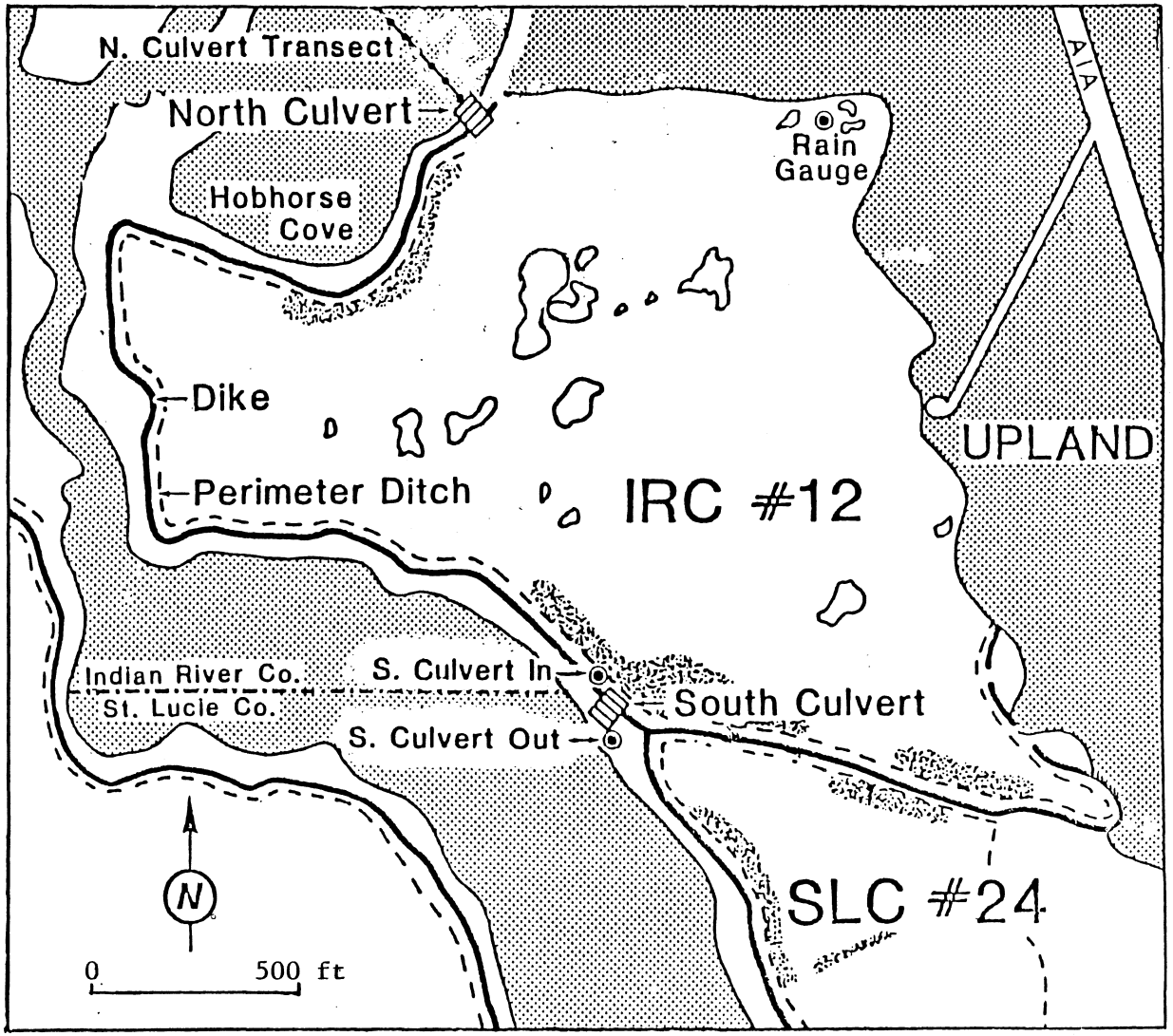

Figure 4-2. Indian River County Impoundment No. 12. Source: Rey et al., 1986.

unvegetated ponds and depressions, some of which retain water perennially, dot the impoundment (Carlson and O'Bryan, 1986).

The relative extent of available data for this area, its physical features which typify impoundment salt marshes along the Indian River system, and the fact that it has been operated under several different management regimes have led to its selection for this particular study.

Background and Operation History

While privately owned, IRC-12 is managed by the Indian River Mosquito Control District (IRMCD) primarily for the control of mosquitoes. A brief chronology of IRMCD operations at this impoundment is summarized in Table 4-1. IRC-12 was diked in 1966 and kept artificially flooded with water pumped from the Indian River. Within two years almost all vegetation (chiefly grasses and mangroves) was dead from flooding and fauna were greatly reduced. In 1978 pumping ceased at the property owners' requests; after this point, the only inputs and outputs of water were rainfall, evaporation and infiltration. In 1982, an 18" open culvert (South Culvert) was installed, permitting free exchange with the Indian River (Figure 4-3). During July 1983 a flapgate riser was attached to trap rainfall and tidal inflow. The riser was set at 1 foot NGVD (National Geodetic Vertical Datum), allowing spillage from the impoundment when water levels reached that height. A second 18" culvert (North Culvert) was placed at the northwest corner in September 1983 with the riser set so that no spillage from the impoundment into the lagoon could occur. The flapgate riser was removed from the south culvert in January 1984 (Carlson & Vigliano, 1985).

Table 4-1. IRC-12 management history.

Begin Date	End Date	Culverts	Pumping	Comments
1966	1978	None	Yes	
1978	03/08/82	None	No	
03/09/82	07/12/83	S: Open	No	South culvert installed.
07/13/83	09/27/83	S: FR 1'	No	
09/28/83	01/18/84	S: FR 1' N: FR NS	No	North culvert installed.
01/19/84	01/30/84	S: Open N: FR NS	No	
01/31/84	05/21/86	S: Open N: Open	No	
05/22/86	09/16/86	S: FR 1' N: FR 1'	Yes	Rotational impoundment management (RIM) begins.
09/17/86	05/20/87	S: Open N: Open	No	

Notes: FR 1' = flapgate riser set at 1 foot NGVD.

FR NS = riser set to prevent all spillage from impoundment.

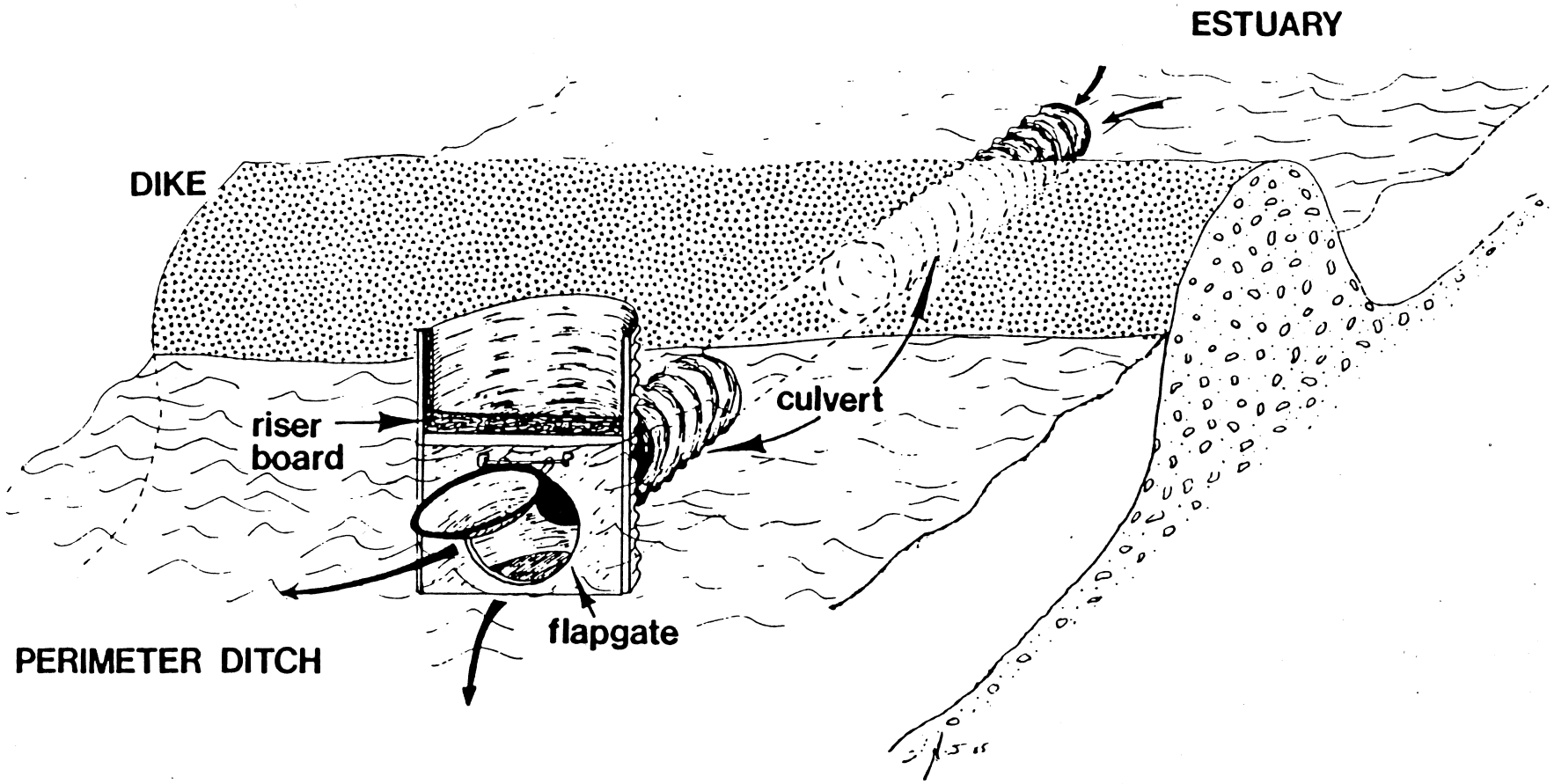

Figure 4-3. Typical culvert. Source: Carlson and O'Bryan, 1986.

Both culverts remained open and unmanaged until May 1986, when flapgate risers were set on both culverts for 1 feet. and the Indian River Mosquito Control District (IRMCD) resumed pumping. This strategy continued through September 1986, at which point the risers were removed until the following May (Gilmore, 1986).

This seasonal flooding during mosquito breeding season (in this case from May until September) alternating with a period of free exchange with the estuary is termed Rotational Impoundment Management (RIM). IRC-12 is scheduled for continued RIM, including the installation of two thirty-inch culverts with flowmeters.

All Florida east coast counties with impounded salt marshes are utilizing RIM to varying degrees (Gilmore, 1986). Statistics are not currently available on the number or acreages involved with RIM or other management methods; however, a study to update the Bidlingmayer & McCoy impoundment inventory of 1978 which would address such questions has been proposed.

Climate and Hydrology

For long-term records the nearest climatological stations are designated by the National Oceanic and Atmospheric Administration (NOAA) as Vero Beach 4W and Vero Beach Municipal Airport. Vero Beach 4W is located at latitude 27° 38' north and longitude 80° 27' west, at an elevation of 20 feet above mean sea level and at a distance of 9.2 miles northwest of IRC-12. Vero Beach Municipal Airport is at latitude 27° 39'north and longitude 80° 25' west, at an elevation of 24 feet, placing it 8.5 miles northwest of IRC-12 and 2.6 miles northeast of the Vero Beach 4W station (Figure 4-4).

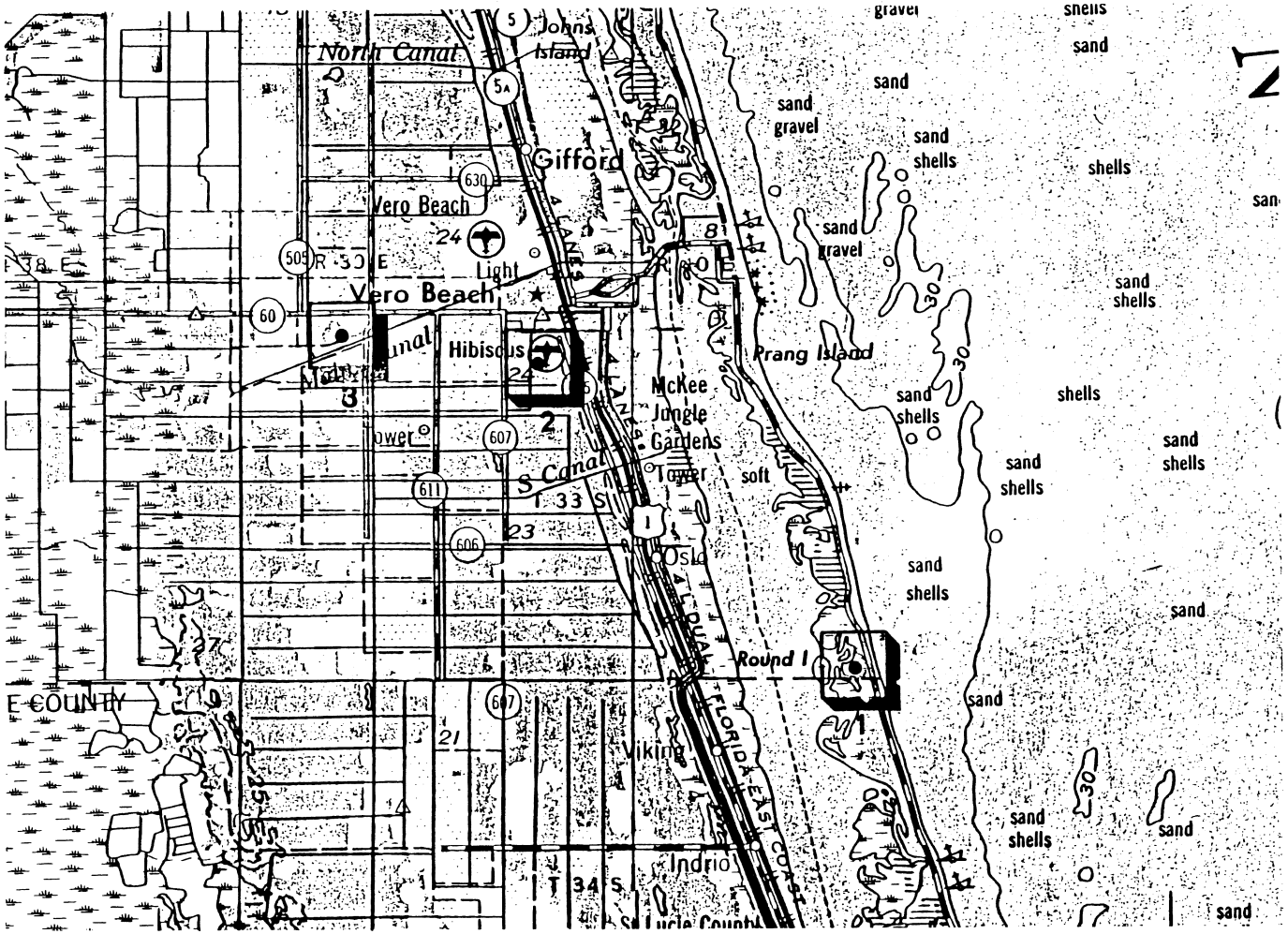

1 IRC-12 **2** Vero Beach Municipal Airport **3** Vero Beach 4W

0 5 miles

Figure 4-4. Location of climatological stations. From USGS topo map, 1956.

Daily records from Vero Beach 4W are available from the National Oceanic and Atmospheric Administration (NOAA) from May 1965 to August 1986 for pan evaporation, wind movement, average maximum and minimum temperatures, and temperature extremes. Records from Vero Beach 4W are more complete for the study periods chosen than those available from Vero Beach Municipal Airport and are thus utilized here.

Rainfall. For long-term trends, annual and monthly statistics through 1979 were obtained using the Hydrologic Information Storage and Retrieval System (HISARS) at the University of Florida (Portier, 1981). After 1979, daily records from NOAA's Climatological Data: Florida were used.

Rainfall measurements made within Indian River County Impoundment No. 12 (IRC-12) are available from 1982 to 1987. These are taken by the Indian River Mosquito Control District (IRMCD) who record accumulated rainfall approximately twice weekly from a gauge located in the northern part of the impoundment. Since the time distribution between measurements is unknown, monthly totals of these records are difficult to compare directly with monthly totals from daily or hourly stations. For a better comparison, hourly or daily records were summed to match IRC-12 collection dates; study periods could then be chosen that corresponded well in rainfall. These results are discussed further later in this chapter.

Long-term rainfall totals and averages for both Vero Beach 4W and IRC-12 are listed in Table 4-2. The mean annual rainfall for Vero Beach 4W over the 22-year period of record was 54.02 inches, with a low of 37.86 inches in 1967 and a high of 81.74 inches in 1982 (Figure 4-5).

Table 4-2. Annual and average monthly rainfall--Vero Beach 4W (1965-1986) and IRC-12 (1982-1986).

Year	Annual Rainfall, inches		Month	Average Monthly Rainfall, inches	
	IRC-12	VB4W		IRC-12	VB4W
1965		48.10	Jan	3.55	2.35
1966		65.58	Feb	2.41	3.00
1967		37.86	Mar	5.46	3.00
1968		67.01	Apr	3.04	2.15
1969		62.79	May	4.61	4.78
1970		45.96	Jun	4.25	7.37
1971		51.93	Jul	4.33	6.44
1972		50.70	Aug	5.06	6.50
1973		68.31	Sep	9.11	7.20
1974		50.68	Oct	5.54	5.53
1975		45.55	Nov	6.05	3.50
1976		47.48	Dec	2.30	2.20
1977		47.86			
1978		46.26			
1979		49.90	Annual	55.71	54.02
1980		39.70			
1981		44.73			
1982	52.66	81.74			
1983	61.80	67.14			
1984	60.90	61.81			
1985	55.75	54.23			
1986	47.44	53.10			
Avg	55.71	54.02			

Notes: IRC-12 data collected approximately semiweekly by Indian River Mosquito Control District.

Vero Beach 4W statistics through 1979 compiled by HISARS; those for 1980 and thereafter obtained from NOAA's Climatological Data: Florida. Long-term averages used for missing months in computing annual sums.

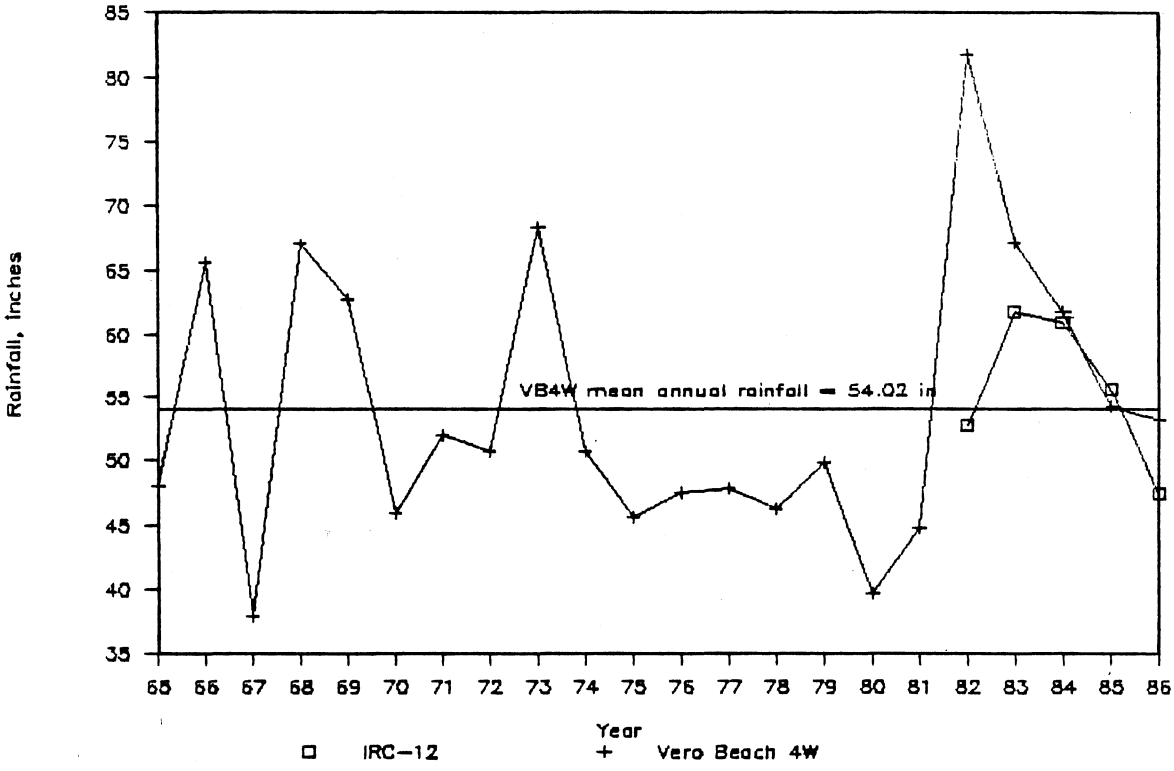

Figure 4-5. Annual rainfall--Vero Beach 4W (1965-1986) and IRC-12 (1982-1986).

IRC-12 showed a five-year mean of 55.71 inches, reporting similar annual totals with the exception of a marked 28-inch difference in Vero Beach 4W's wet year of 1982. Most areas of the state reported rainfall in 1982 as well above average. It is not known if IRC-12's much lower total for this year represents a true local variation or possible error with the impoundment data. Both long-term means typify the Indian River Lagoon area, where mean annual rainfall ranges from 52 to 56 inches per year (Fernald and Patton, 1984).

Monthly variation at Vero Beach 4W (Figure 4-6) based on long-term averages ranges from 2.15 inches in April to 7.37 inches in June. Although the overall seasonal profile appears similar to IRC-12, the impoundment averaged a minimum of 2.30 inches in December and a maximum of 9.11 inches in September.

Hourly data from 1965 to 1979 were analyzed for rainfall event characteristics using SYNOP, a USEPA computer program. A rainfall event is defined as a continuous series of hours in which rainfall occurs, separated from an adjacent series by a minimum interevent time (MIT). The MIT is chosen according to regional patterns and analysis needs; in this case an MIT of 5 hours was chosen. Each event may be described by the total volume of rain that falls during the event; the duration, or length of the event; the average intensity of rainfall throughout the event; and the time elapsed since the previous event, or interevent time.

SYNOP's statistics by year for these storm characteristics are given in Table 4-3. Seasonal variations for each of the parameters are listed in Table 4-4 and plotted in Figures 4-7 through 4-10. For the

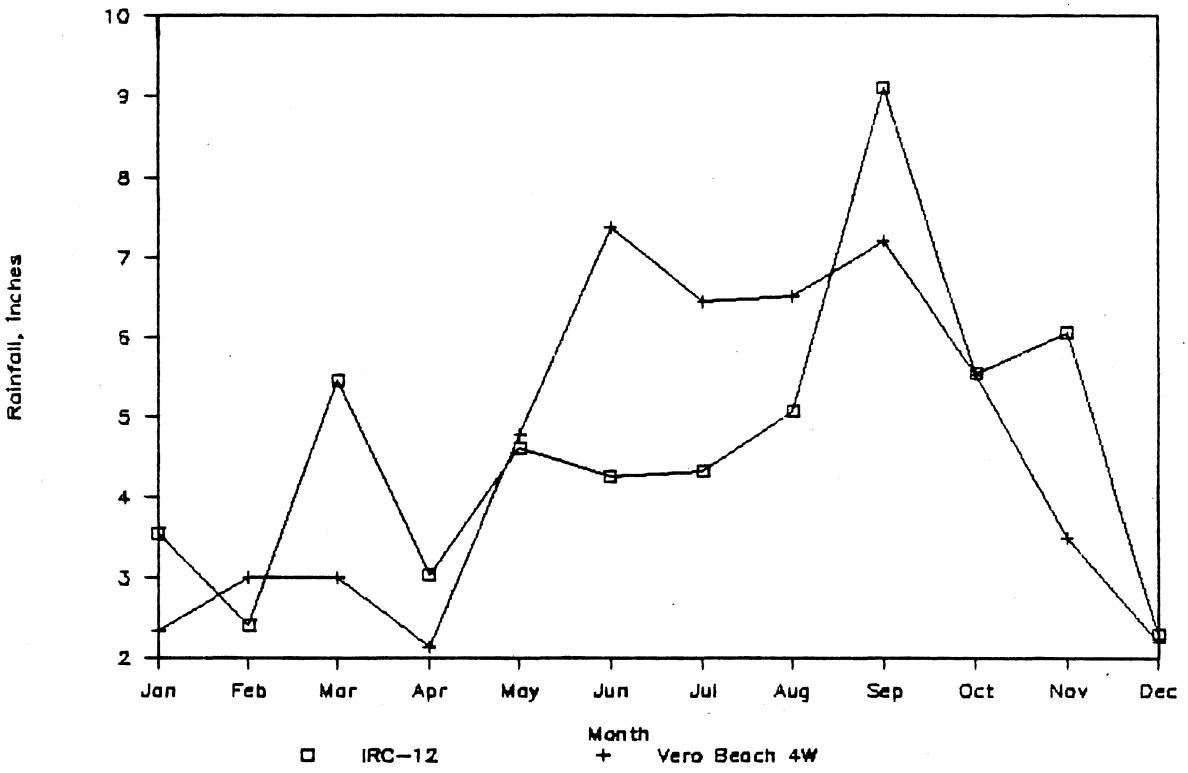

Figure 4-6. Average monthly rainfall--Vero Beach 4W (1965-1986) and IRC-12 (1982-1986).

Table 4-3. Annual rainfall event statistics--Vero Beach 4W (1965-1979).

Year	Duration, hrs		Intensity, in/hr		Volume, in		Interevent time, hrs	
	Avg	Std	Avg	Std	Avg	Std	Avg	Std
65	4.58	5.46	0.1187	0.1617	0.44	0.58	64	69
66	5.15	5.86	0.0962	0.1238	0.49	0.93	66	66
67	4.64	3.27	0.0830	0.0992	0.34	0.47	85	106
68	4.92	4.47	0.1262	0.1502	0.59	0.71	83	102
69	4.57	4.82	0.1003	0.1318	0.42	0.64	62	67
70	4.61	4.08	0.0878	0.1124	0.43	0.64	88	126
71	2.77	2.56	0.1836	0.1893	0.47	0.58	79	106
72	9.46	70.31	0.1781	0.1405	0.46	0.71	86	110
73	2.61	2.65	0.2228	0.2387	0.56	0.73	69	79
74	2.73	4.21	0.2045	0.1997	0.47	0.61	84	104
75	2.20	1.81	0.2271	0.2253	0.43	0.44	87	114
76	2.78	3.02	0.1795	0.1640	0.48	0.61	95	119
77	2.39	2.24	0.1963	0.1968	0.43	0.53	84	117
78	3.36	4.02	0.1559	0.1347	0.46	0.60	98	113
79	2.75	3.81	0.1928	0.2323	0.56	1.26	84	105
Avg Year	4.22	3.88	0.1633	0.1672	0.49	0.50	84	86

Note: An event ends when it has not rained for five consecutive hours.

Table 4-4. Monthly rainfall event statistics--Vero Beach 4W (1965-1979).

Month	Duration, hrs		Intensity, in/hr		Volume, in		Interevent time, hrs	
	Avg	Std	Avg	Std	Avg	Std	Avg	Std
Jan	4.72	5.02	0.1068	0.0947	0.41	0.48	126	129
Feb	4.14	4.86	0.1395	0.1326	0.47	0.56	141	164
Mar	4.28	4.39	0.1096	0.1125	0.45	0.71	130	112
Apr	14.19	90.28	0.1354	0.1455	0.41	0.76	171	194
May	3.06	2.90	0.1904	0.2269	0.50	0.70	79	122
Jul	3.96	4.83	0.1728	0.1857	0.59	0.79	53	52
Jul	3.08	2.54	0.1911	0.2463	0.48	0.58	56	52
Aug	2.57	2.29	0.1807	0.1819	0.41	0.53	58	64
Sep	3.59	4.41	0.1583	0.1796	0.49	0.95	51	53
Oct	4.30	4.70	0.1284	0.1240	0.49	0.80	66	68
Nov	3.91	5.02	0.1029	0.0861	0.37	0.48	109	108
Dec	3.39	3.69	0.1088	0.1069	0.34	0.53	124	120
Avg Storm	4.00	18.44	0.1550	0.1776	0.47	0.70	80	101

Note: Mean of years does not equal mean of months.

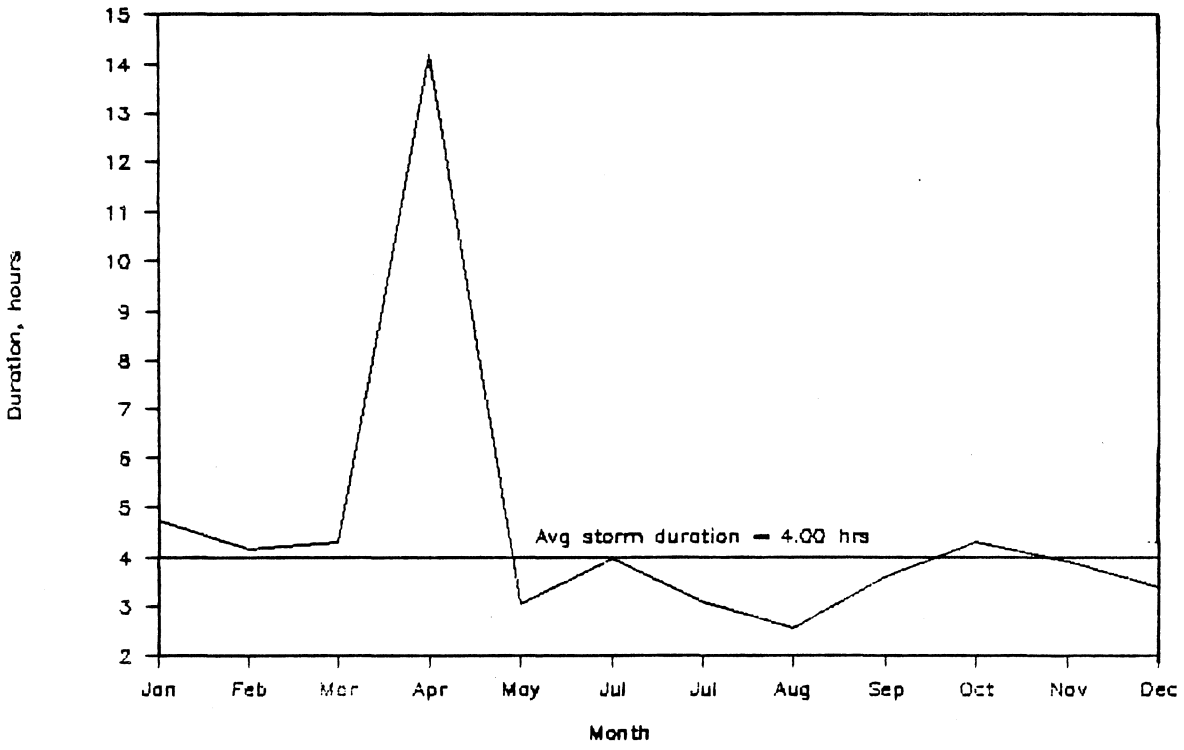

Figure 4-7. Rainfall event duration seasonal trend--Vero Beach 4W (1965-1979).

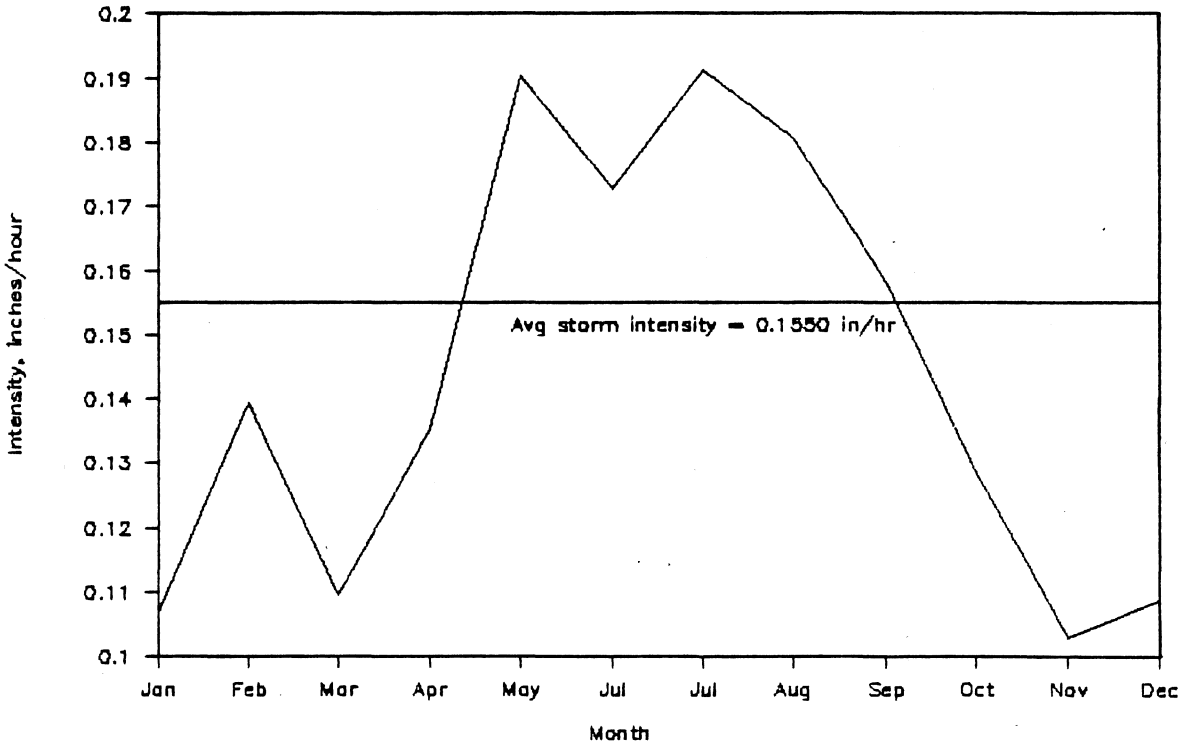

Figure 4-8. Rainfall event intensity seasonal trend--Vero Beach 4W (1965-1979).

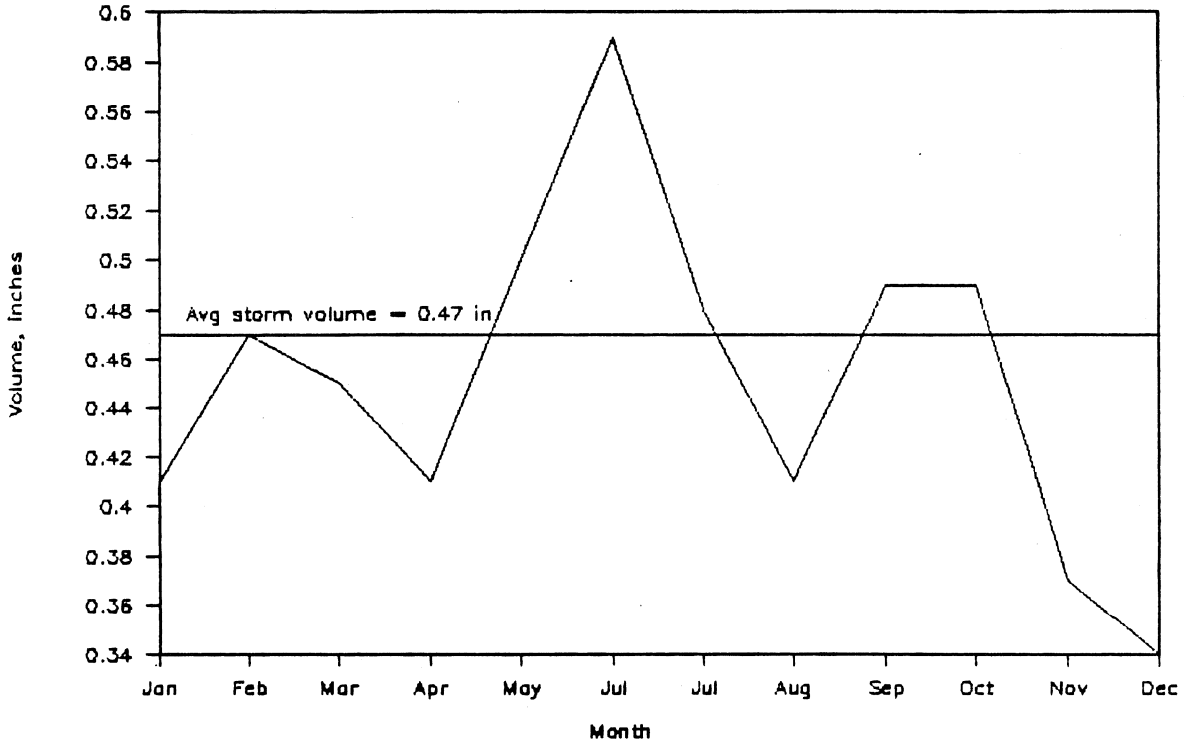

Figure 4-9. Rainfall event volume seasonal trend--Vero Beach 4W (1965-1979).

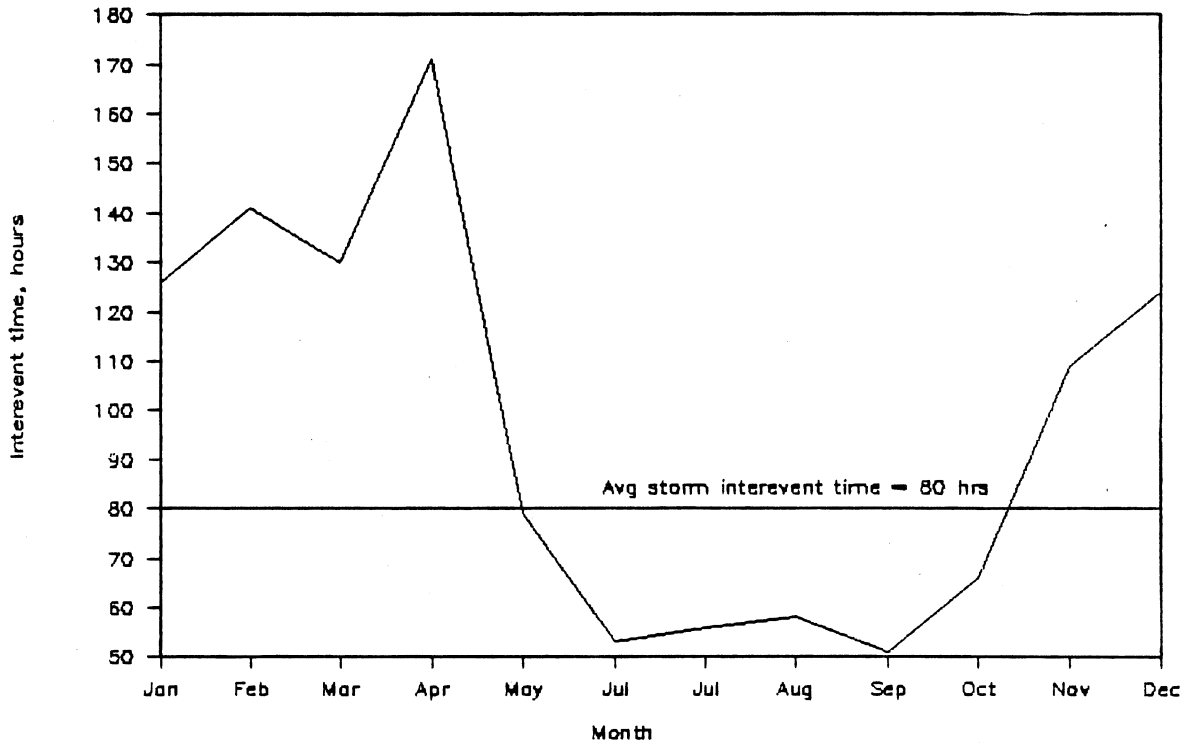

Figure 4-10. Rainfall event interevent time seasonal trend--Vero Beach 4W (1965-1979).

period of record, the average storm at Vero Beach 4W was calculated to have a duration of 22 hours, an intensity of 0.163 inches per hour, a volume of 0.49 inches, and an interevent time of 84 hours.

Temperature. Mean annual temperatures calculated from the previously-described NOAA databases (Table 4-5) range from 70.6°F in 1968 to 73.9°F in 1982, yielding a long-term mean annual temperature for Vero Beach 4W of 72.0°F for the years 1965 to 1986. An increasing trend may exist (Figure 4-11). In order to smooth out annual variation to reveal longer-term trends, a five-year moving average was plotted. An increasing trends remains apparent in this graph until 1973, after which no clear trend is visible. A study of earlier records may aid in verifying the pre-1973 trends. Average monthly temperatures vary from 60.8°F in January to 81.0°F in August (Figure 4-12).

Wind movement. An analysis of NOAA's wind movement database (Table 4-6) indicates a decreasing trend over the years 1965 to 1986 (Figure 4-13); a five-year moving average further illustrates this trend. A maximum of 16159 miles per year of wind movement occurred in 1966; a minimum of 9036 miles per year occurred in 1974. Mean annual wind movement for the entire period totaled 12333 miles per year. Seasonal variation in winds results in a maximum total wind movement in March of 1409 miles per year and a minimum in August of 700 miles per year (Figure 4-14).

Evaporation. Pan evaporation at Vero Beach 4W has averaged 60.05 inches per year from 1965 to 1986, ranging from a low in 1969 of 50.73

Table 4-5. Annual and average monthly temperatures--Vero Beach 4W (1965-1986) and IRC-12 (1982-1986).

Year	Average annual temperature, degrees F	5-Yr moving average, degrees F
1965	71.7	
1966	70.9	
1967	72.2	71.3
1968	70.6	71.2
1969	71.2	71.5
1970	71.2	71.6
1971	72.3	71.9
1972	72.8	72.1
1973	72.0	72.6
1974	72.4	72.5
1975	73.5	72.2
1976	71.6	72.2
1977	71.6	72.2
1978	72.0	71.9
1979	72.4	71.9
1980	72.2	72.4
1981	71.5	72.4
1982	73.9	72.4
1983	72.1	72.4
1984	72.1	72.5
1985	72.5	
1986	72.0	
Avg	72.0	

Month	Average monthly temperature, degrees F
Jan	60.8
Feb	61.9
Mar	66.6
Apr	71.2
May	75.6
Jun	79.2
Jul	80.8
Aug	81.0
Sep	79.7
Oct	75.4
Nov	68.7
Dec	63.5
Annual	72.0

Notes: Statistics through 1979 compiled by HISARS; those for 1980 and thereafter obtained from NOAA's Climatological Data: Florida. Long-term averages used for missing months in computing annual sums.

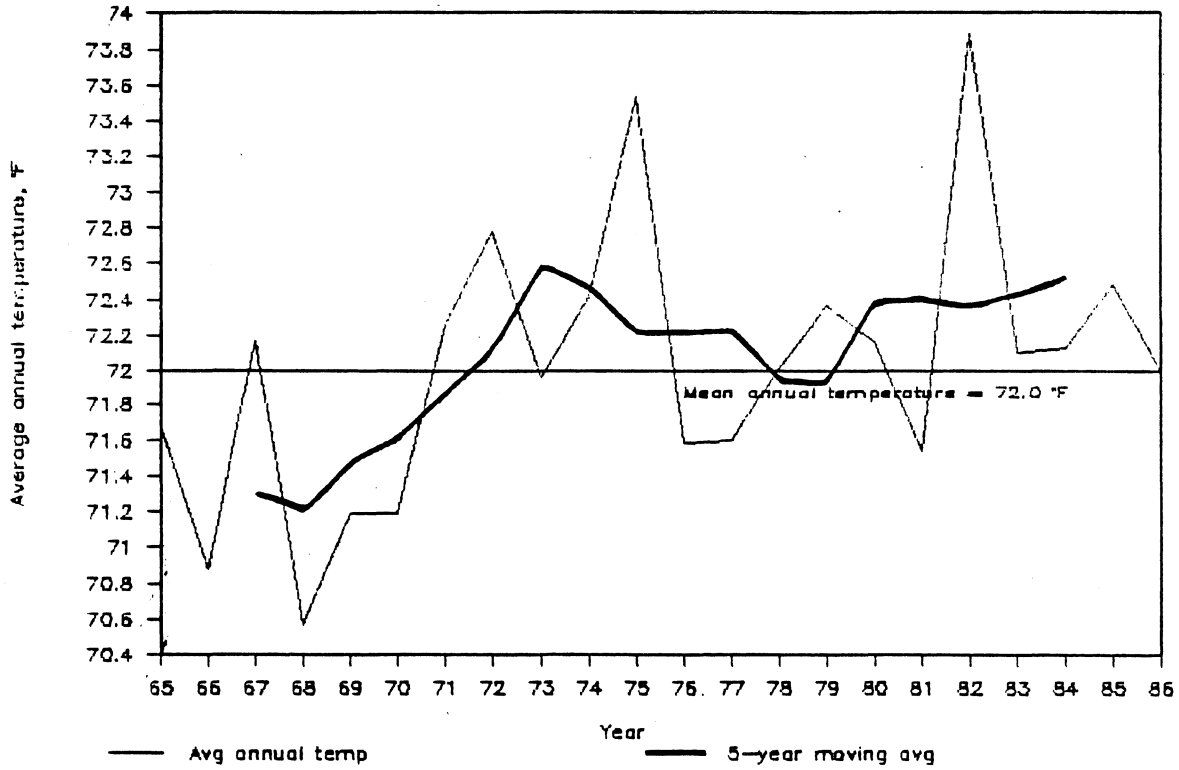

Figure 4-11. Average annual temperatures--Vero Beach 4W (1965-1979).

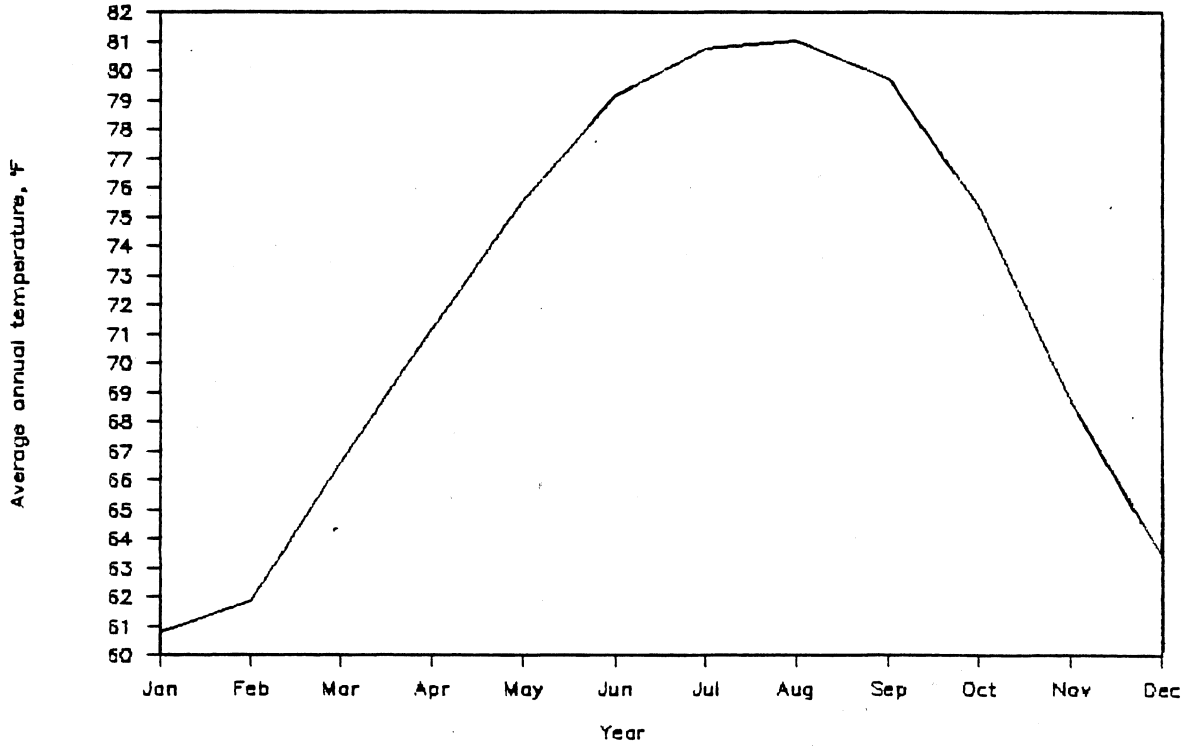

Figure 4-12. Average monthly temperatures--Vero Beach 4W (1965-1979).

Table 4-6. Annual and average monthly wind movement--Vero Beach 4W (1965-1986) and IRC-12 (1982-1986).

Year	Annual wind movement, miles	5-Yr moving average, miles
1965	14496	
1966	16159	
1967	14869	14713
1968	14246	14550
1969	13796	13831
1970	13682	13307
1971	12562	12995
1972	12251	12043
1973	12683	11510
1974	9036	11488
1975	11018	11631
1976	12452	11350
1977	12964	11899
1978	11279	11769
1979	11780	11640
1980	10369	10952
1981	11806	11178
1982	9527	11339
1983	12410	11296
1984	12583	11176
1985	10156	
1986	11205	
Avg	12333	

Month	Average monthly wind movement, miles
Jan	1229
Feb	1321
Mar	1409
Apr	1224
May	1048
Jun	903
Jul	755
Aug	700
Sep	746
Oct	904
Nov	1024
Dec	1071
Annual	12333

Notes: Statistics through 1979 compiled by HISARS; those for 1980 and thereafter obtained from NOAA's Climatological Data: Florida. Long-term averages used for missing months in computing annual sums.

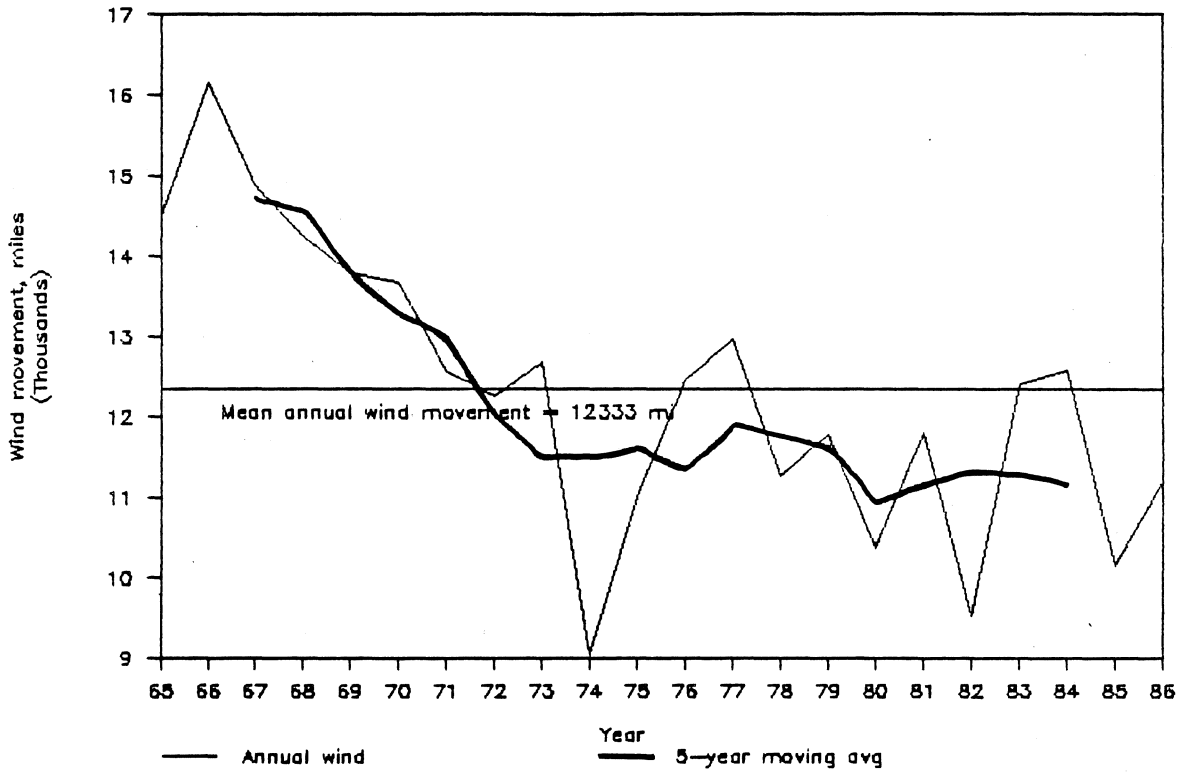

Figure 4-13. Annual wind movement--Vero Beach 4W (1965-1979).

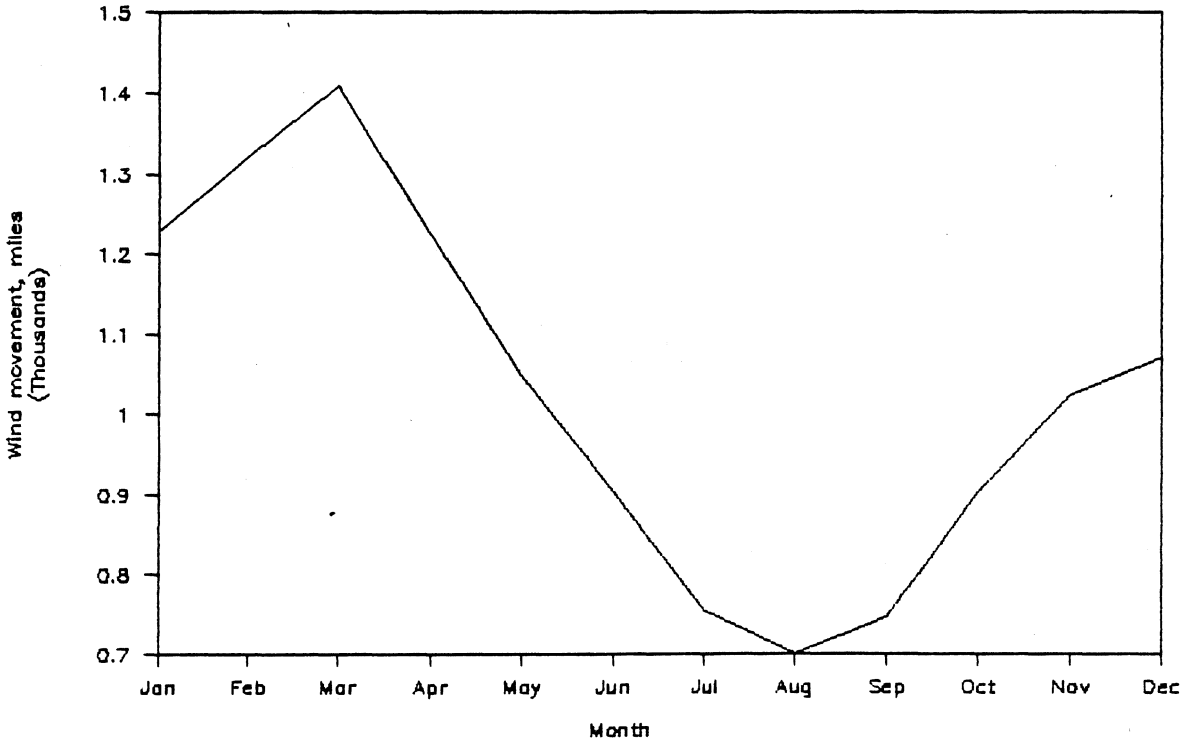

Figure 4-14. Average monthly wind movement--Vero Beach 4W (1965-1979).

inches to a maximum in 1986 of 70.07 inches (Table 4-7). During this period, an increasing trend in annual pan evaporation is visible (Figure 4-15). Long-term monthly averages range from 2.64 inches of pan evaporation in December to a peak of 6.81 inches in May (Figure 4-16).

Selection of Study Periods and Time Steps

In choosing study periods for model calibration and short-term simulations, a time step was desired that demonstrated four tidal points daily. These tidal points are spread on the average approximately five hours between two points and seven hours between the other two. In order to insure a time step smaller than the five-hour tide, a four-hour increment was chosen. The spreadsheet software used for data analysis and modeling is Lotus 1-2-3 on an AT microcomputer. The 640-kilobyte random access memory (RAM) available allowed modeling periods of approximately forty days with this time step. Longer periods may be modeled by recalculating shorter intervals, converting these formulas to values using 1-2-3's Range Value command, and continuing. The available database covered the period 10/84 to 10/86 with several gaps in both rainfall and water level data. This narrowed the choice down to three periods of useful size, which also were of about 40 days in length.

Short-Term Modeling Period	Dates	Length (days)
A	06/24/85 - 08/04/85	42
B	08/01/86 - 09/08/86	39
C	11/26/84 - 01/05/85	39

Period C was selected for calibration, as it covered a dry period which minimized error from using Vero Beach 4W rainfall data as

Table 4-7. Annual and average monthly pan evaporation--Vero Beach 4W (1965-1986) and IRC-12 (1982-1986).

Year	Annual pan evaporation, inches	5-Yr moving average, inches
1965	51.76	
1966	52.98	
1967	57.96	53.25
1968	52.84	54.20
1969	50.73	55.31
1970	56.51	55.57
1971	58.49	56.25
1972	59.29	57.54
1973	56.24	58.26
1974	57.17	58.43
1975	60.11	59.04
1976	59.32	59.29
1977	62.34	59.66
1978	57.50	60.88
1979	59.02	62.26
1980	66.20	62.15
1981	66.22	63.92
1982	61.80	65.84
1983	66.38	66.51
1984	68.58	67.28
1985	69.56	
1986	70.07	
Avg	60.05	

Month	Average monthly pan evaporation, inches
Jan	2.86
Feb	3.79
Mar	5.46
Apr	6.49
May	6.81
Jun	6.35
Jul	6.43
Aug	6.07
Sep	5.25
Oct	4.58
Nov	3.32
Dec	2.64
Annual	60.05

Notes: Statistics through 1979 compiled by HISARS; those for 1980 and thereafter obtained from NOAA's Climatological Data: Florida. Long-term averages used for missing months in computing annual sums.

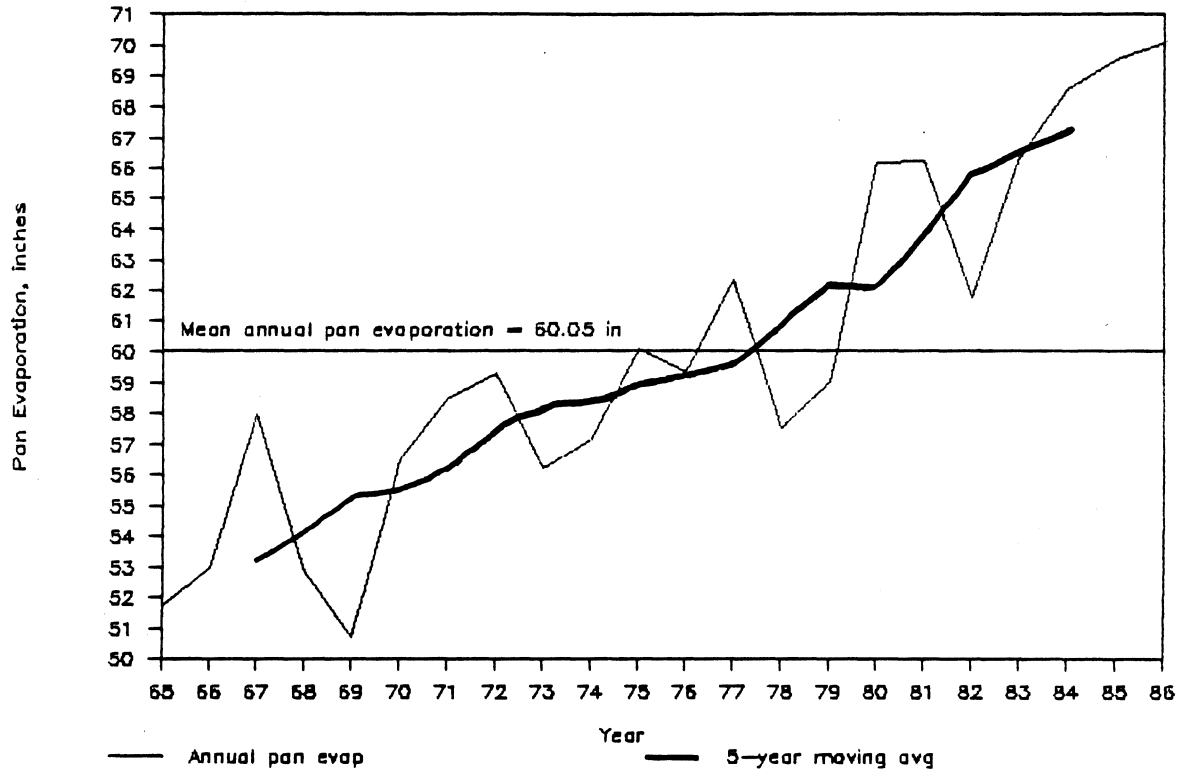

Figure 4-15. Annual pan evaporation--Vero Beach 4W (1965-1979).

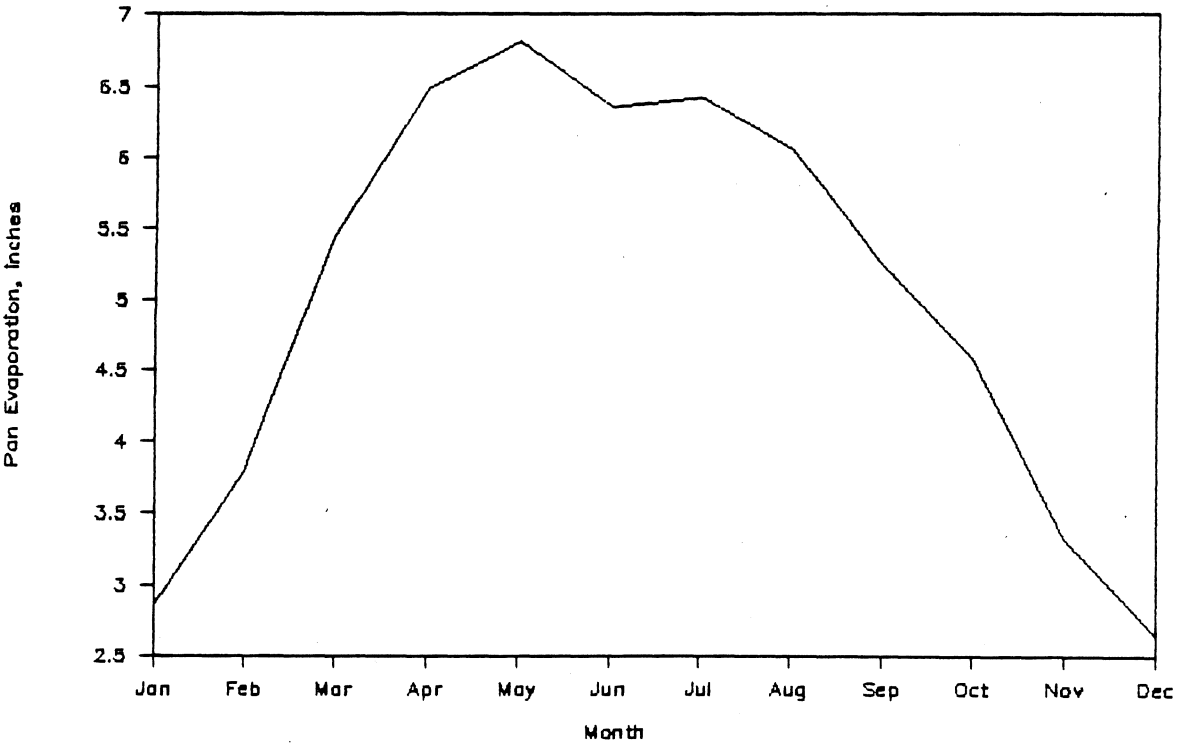

Figure 4-16. Average monthly pan evaporation--Vero Beach 4W (1965-1979).

estimates for rainfall at IRC-12. During this period, water levels were unmanaged and flow occurred freely through the two culverts. Period A water levels were also unmanaged and remained rather low, quickly responding to tides and rainfall. Flapgate risers were in place during period B which maintained high water levels, decoupling the impoundment from the tides. Pumping did not occur in any of the three periods. As both the latter periods had unique characteristics, it was decided to test the calibrated model (from period C) on both periods A and B.

In order to simulate an entire year to provide long-term analyses, 1985 was chosen as it is best covered by the database, allowing simulation results to be compared with measured data where available.

Stage-Area-Volume Analysis

Topography

Marsh elevations, excluding depressions, range from -0.35 to 1.80 feet NGVD, with most elevations falling between 0.40 and 0.70 feet. As described earlier in the section covering site location and selection, a dam encloses most of the impoundment. A typical vertical profile (Figure 4-17) shows the gradual slope toward the upland hammock with an occasional pond. An increased gradient to the uplands marks the impoundment's undiked eastern and northern boundaries.

A typical section across the dike and perimeter ditch was illustrated earlier in Figure 4-3. The dike averages approximately ten feet across with an elevation of 3 feet NGVD; the ditch ranges from three to ten feet across with a highly variable bottom elevation, measured at 0.44 feet NGVD at the south culvert.

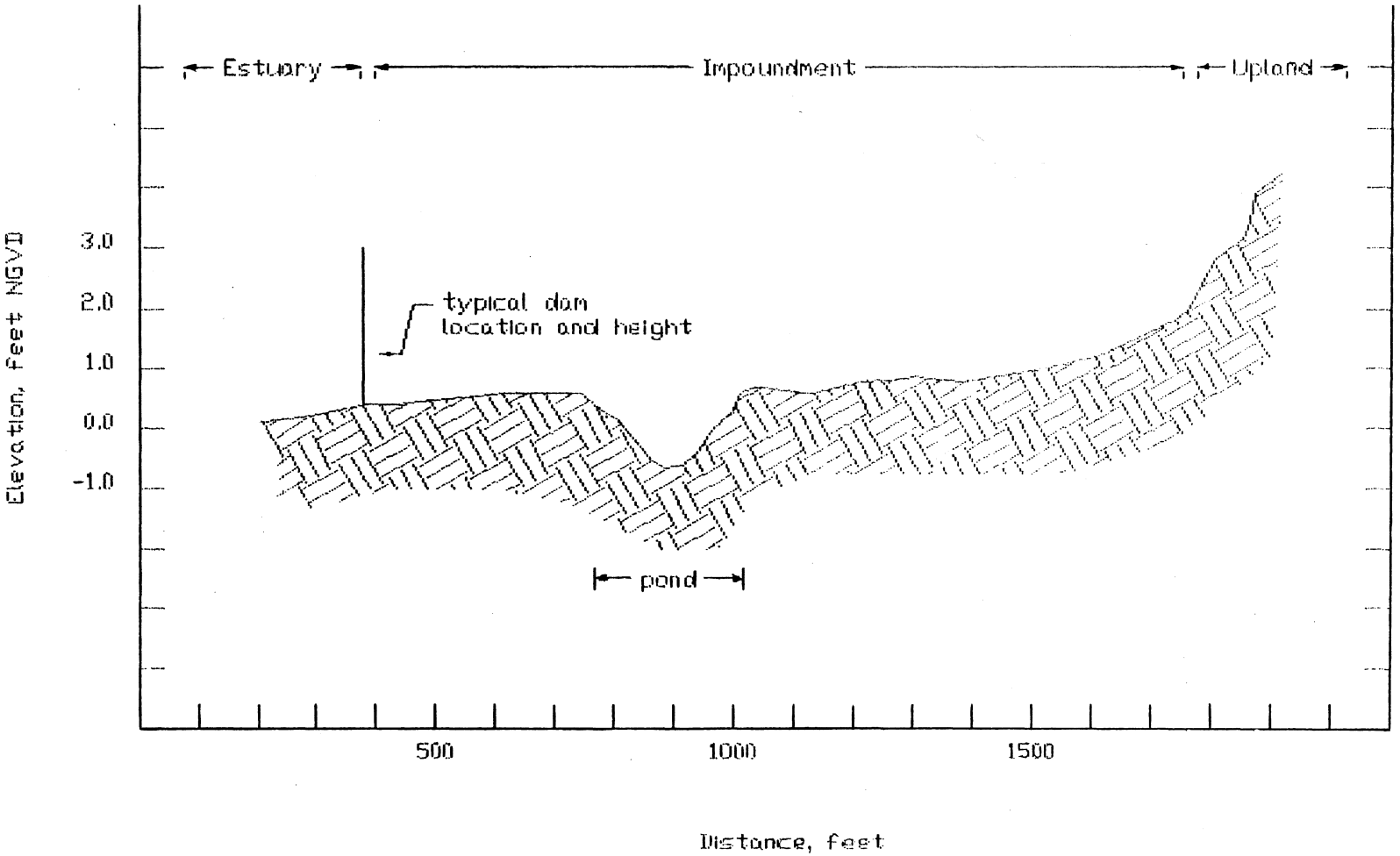

Figure 4-17. Typical vertical profile of Indian River County Impoundment No. 12.

Historical Stage Records

Impoundment stage as recorded in the perimeter ditch at the south culvert was analyzed to determine the historical range. Measurements of high and low tides producing four daily observations over two years ranged from a minimum of -5.28 inches NGVD to a maximum of 24.09 inches (Figure 4-18). The distribution over this period is quite symmetrical about the long-term average of 8.13 inches.

Areas of marsh inundation at discrete stages have been determined for IRC-12 by ground-truthing water coverage at established elevations, given as a series of hand-prepared maps (Carlson and Vigliano, 1984). AutoCAD, a graphics design software package, was used on the microcomputer to digitize this information. This was performed in order to prepare maps useful for future modifications and reporting purposes, and in order to quantify the relative land and water areas at different stages. The digitized maps (Figures 4-19a through 4-19f) show water coverage at stages 0.45, 0.55, 0.60, 0.75, 0.90, and 1.0 feet NGVD, spanning the range from minimum coverage to near total inundation.

Area vs. Stage

The computed water areas as percentages of total marsh area (Table 4-8) were plotted against stage, showing little coverage (less than 10%) at stages less than 0.45 feet NGVD (Figure 4-20). After this point, water area increases rapidly until reaching approximately 45% coverage at about 0.60 feet; the rate of increase then drops, with water area

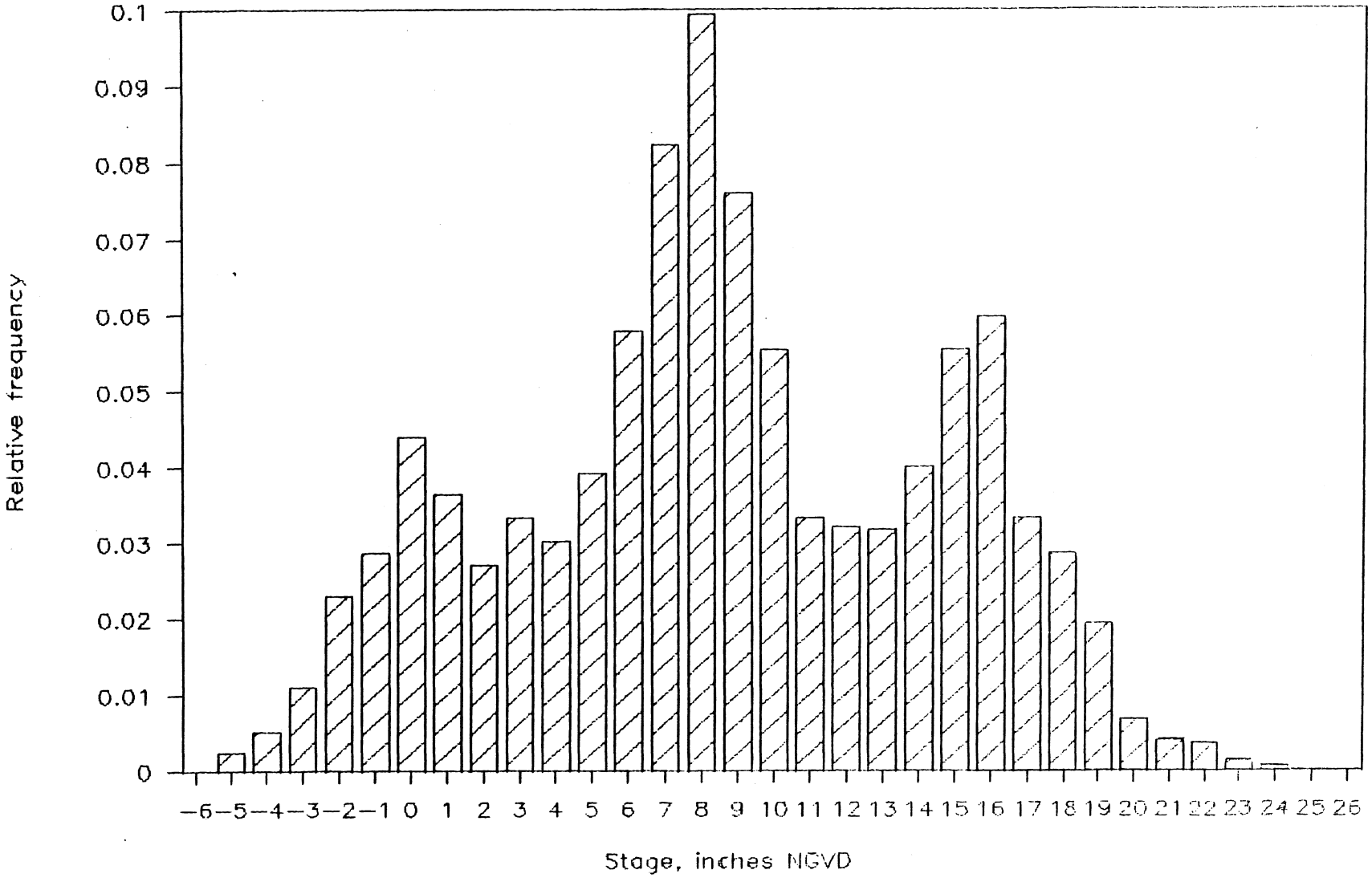

Figure 4-18. Impoundment stage frequency distribution of high and low tide observations--IRC-12 September 1984--October 1986.

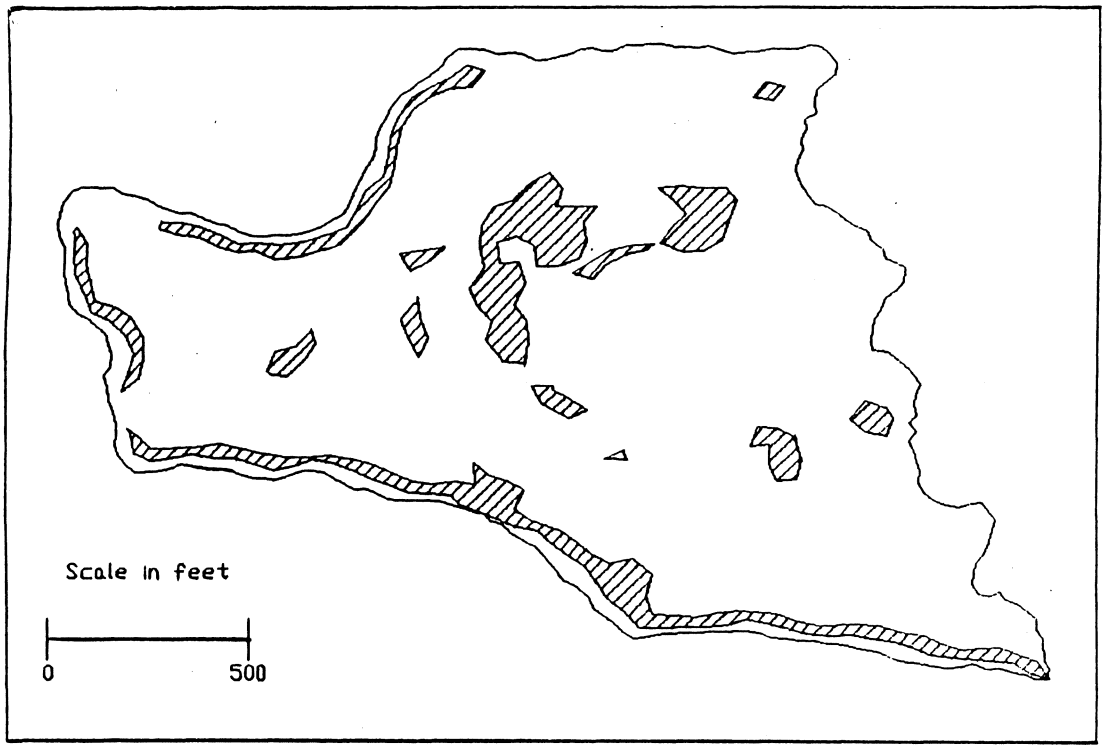

Figure 4-19a. Water area (shaded) of IRC-12 at stage of 0.45 feet NGVD.

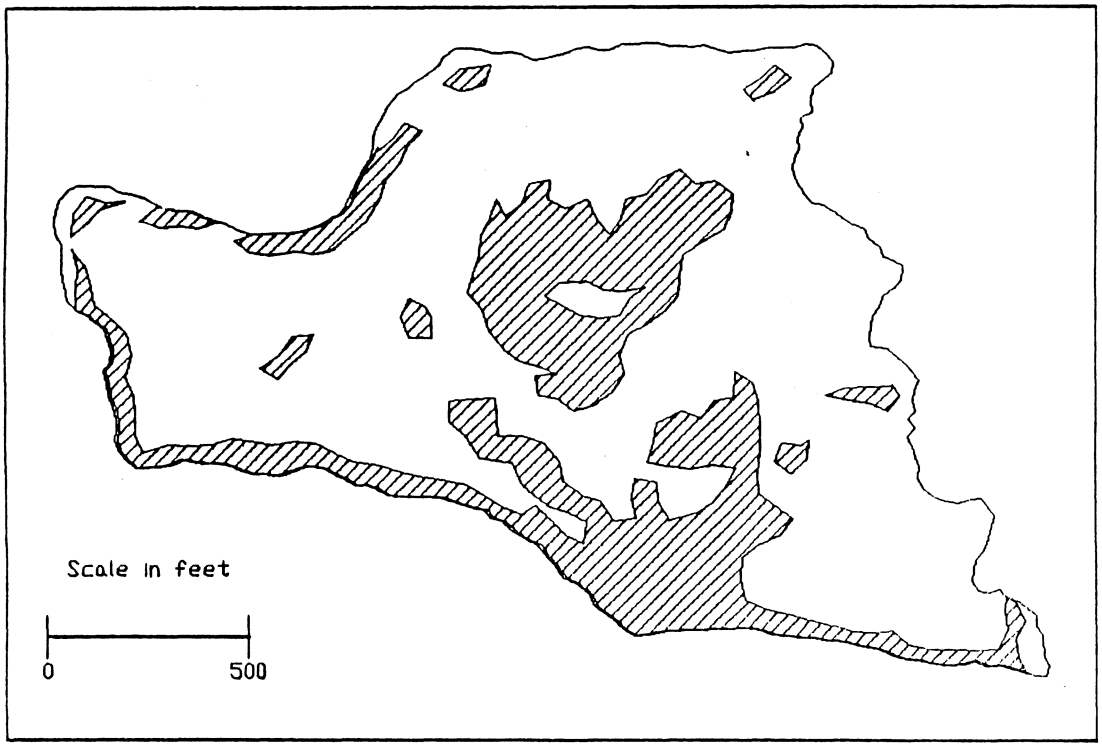

Figure 4-19b. Water area (shaded) of IRC-12 at stage of 0.55 feet NGVD.

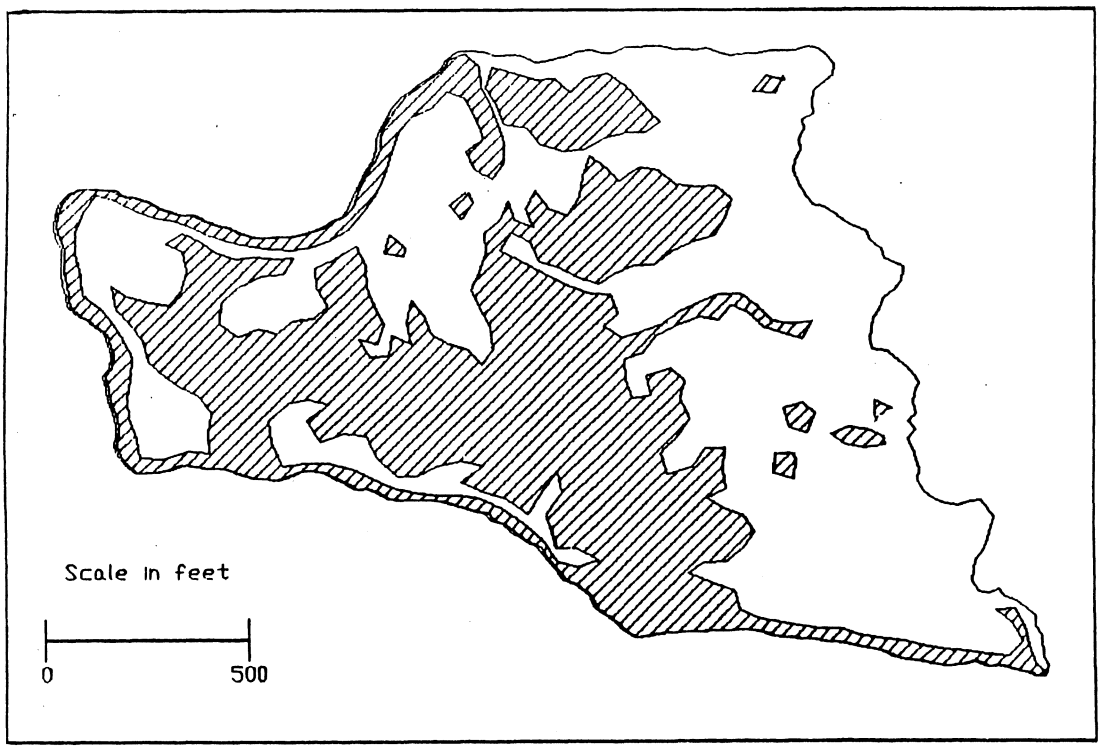

Figure 4-19c. Water area (shaded) of IRC-12 at stage of 0.60 feet NGVD.

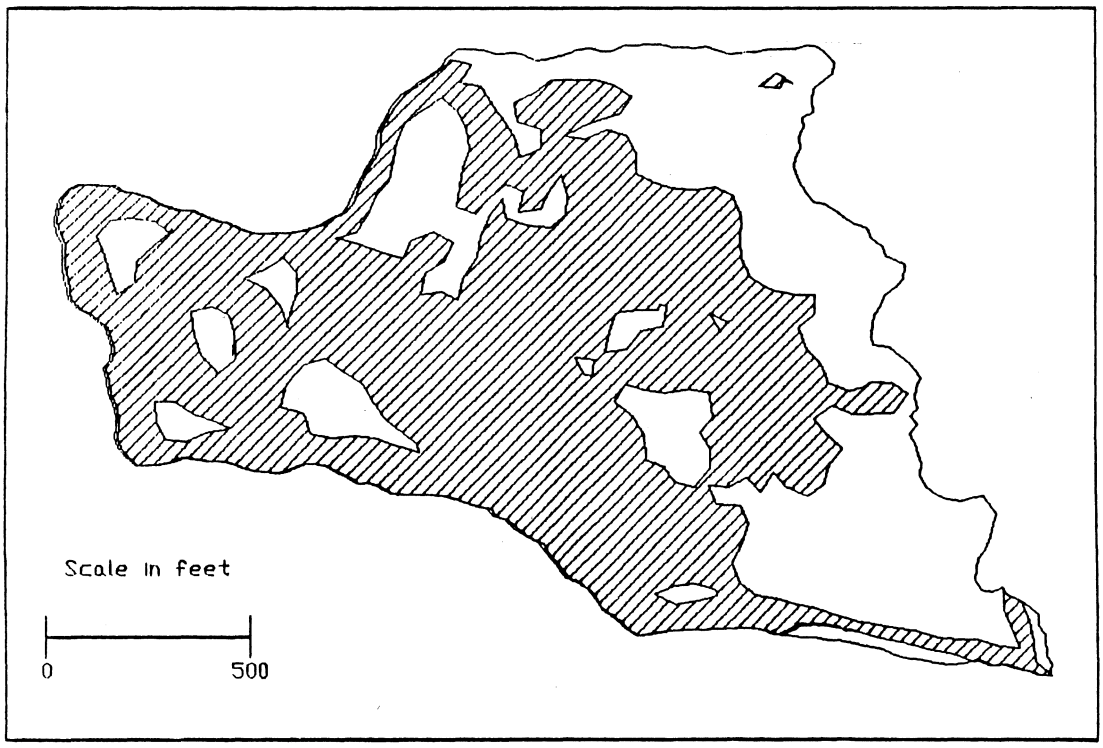

Figure 4-19d. Water area (shaded) of IRC-12 at stage of 0.75 feet NGVD.

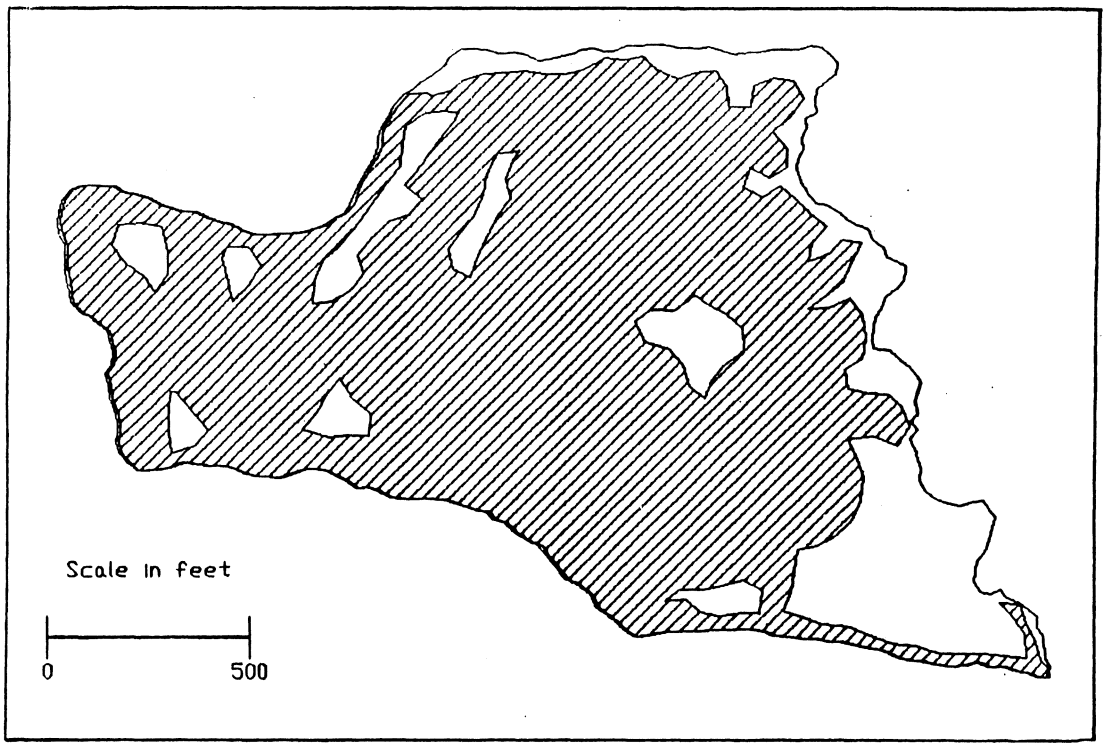

Figure 4-19e. Water area (shaded) of IRC-12 at stage of 0.90 feet NGVD.

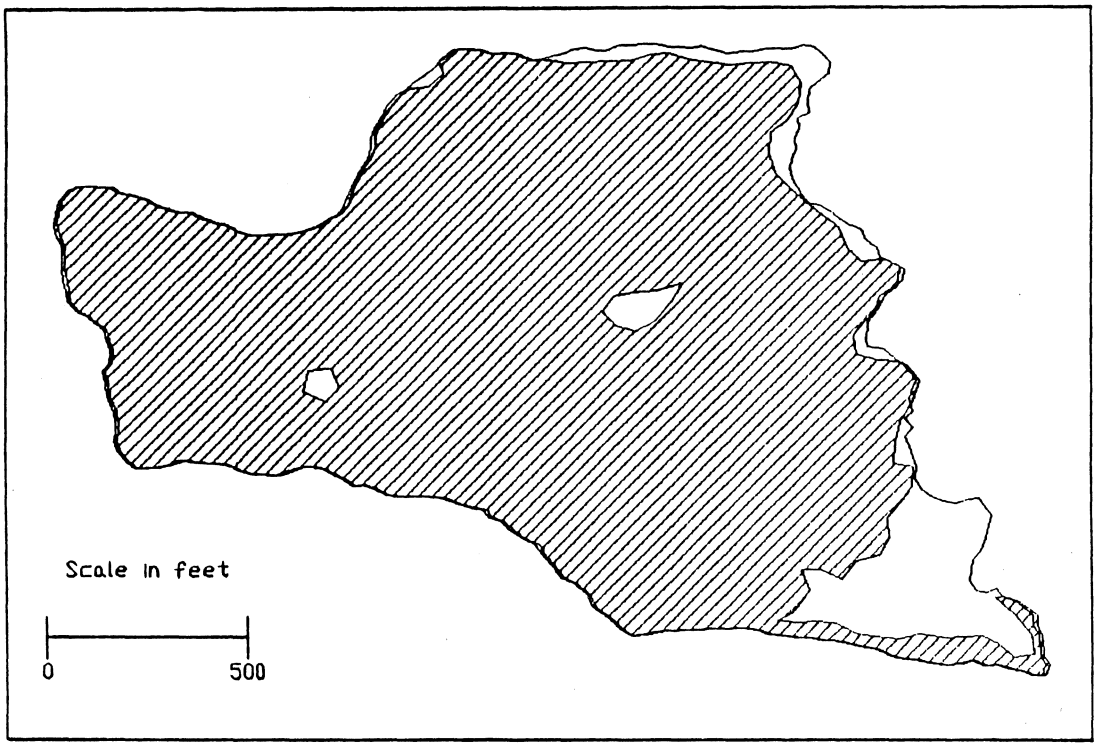

Figure 4-19f. Water area (shaded) of IRC-12 at stage of 1.00 feet NGVD.

Table 4-8. Area and perimeter vs. stage calculations for IRC-12.

Total impounded area = 2178000 ft^2
Total impounded perimeter = 7527 ft

Stage h, ft	Measured water perimeter, ft	Measured water area, %	Estimated water area, %	Calculated water area, %
-0.44			7.00	7.00
0.45	13438	11.15		10.66
0.55	15664	27.63		32.34
0.60	21021	44.96		44.75
0.75	16621	61.68		61.72
0.90	14070	77.92		78.69
1.00	9266	90.60		90.60
1.80			93.00	93.00

Notes: Measured areas are those digitized from maps prepared by Carlson and Vigliano (1984).

Estimated areas are rough estimates of minimum and maximum inundation percentages.

Calculated areas are generated by "if-then" equation containing containing four linear functions obtained by regressing four stage intervals:

h, feet = impoundment stage

Calculated area, % = @if(h<-0.44,7.00,
@if(h<0.45,4.663*h+9.052,
@if(h<0.60,216.76*h-86.880,
@if(h<1.00,113.14*h-23.137,
3*h+87.6))))

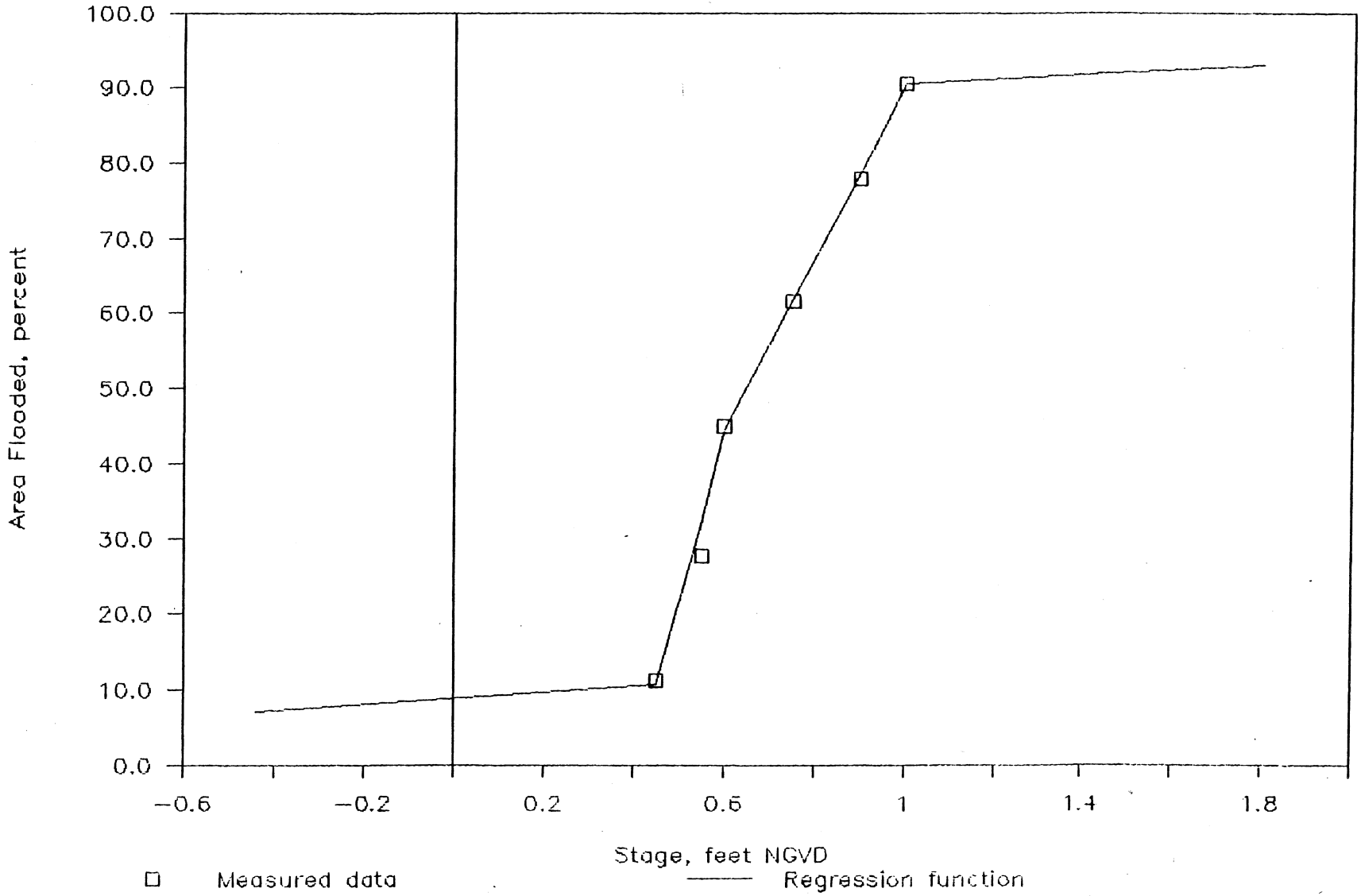

Figure 4-20. Water area vs. stage--IRC-12.

steadily increasing at a relatively constant rate through 91% coverage at 1.0 ft.

Water area is known to be small and very slow in increasing until 0.45 feet is attained and again shows very little change after 1.0 foot. Rough estimates were therefore added to Table 4-8 for minimum inundation of 7.00% at the lowest recorded stage of -0.44 feet NGVD and maximum inundation of 93.00% at the highest recorded stage of 1.80 feet. The result provides the relationship seen in Figure 4-20.

Several methods may be used at this point in formulating a single relationship for water area as a function of stage that may be incorporated into a simulation model. One possible method uses Lotus 1-2-3's lookup table feature, which allows values to be interpolated from actual or expanded data. To this end, a smooth curve is fitted to the plotted observed areas and regular smaller increments are estimated. A function can then be written which combines linear interpolation with the database lookup function to return an estimate of water area for an a single stage value.

This method is useful in that it uses the original data and eliminates curve-fitting. A function is, however, particularly simple to fit in this case as the graph may be closely approximated by four linear segments. This was the method chosen here as it was found to require less memory and spreadsheet recalculation time than a lookup operation. Water area as a function of stage therefore can be expressed as:

$$A(h) = \begin{cases} ah+b \; ; \; h < h_1 \\ ch+d \; ; \; h_1 \leq h < h_2 \\ eh+f \; ; \; h_2 \leq h < h_3 \\ gh+i \; ; \; h_3 \leq h \end{cases} \qquad [4\text{-}1]$$

where $A(h)$ = area of water coverage, % total impoundment area;

h = impoundment stage, feet; and

h_i = stage where $A(h)$ curve shows significant change in slope.

Equation 4-1 may be expressed in 1-2-3 as a nested @IF(cond,x,y) function placed in a single spreadsheet cell:

```
A(h) = @IF(h<h1,a*h+b,
       @IF(h<h2,c*h+d,
       @IF(h<h3,e*h+f,
       g*h+i)))                                    [4-2]
```

Version 2 of 1-2-3 provides an extremely easy-to-use linear regression operation; this was performed for each of the four selected ranges of values using $h_1 = 0.45$, $h_2 = 0.60$, and $h_3 = 1.00$. The following regression constants for these four intervals were generated:

a = 4.663	c = 216.76	e = 113.14	g = 3.000
b = 9.052	d = -86.880	f = -23.137	i = 87.60

Perimeter vs. Stage

The length of soil-water interface, or water perimeter, as a function of stage may be a useful relationship to quantify, particularly to those studying mosquito breeding or other biological processes. The same digitization process described above produced several perimeter values for different stages, which are found in Table 4-8.

As impoundment stage increases, numerous irregular "tendrils" are created, causing a rapid rise in water perimeter (Figure 4-21). Beyond

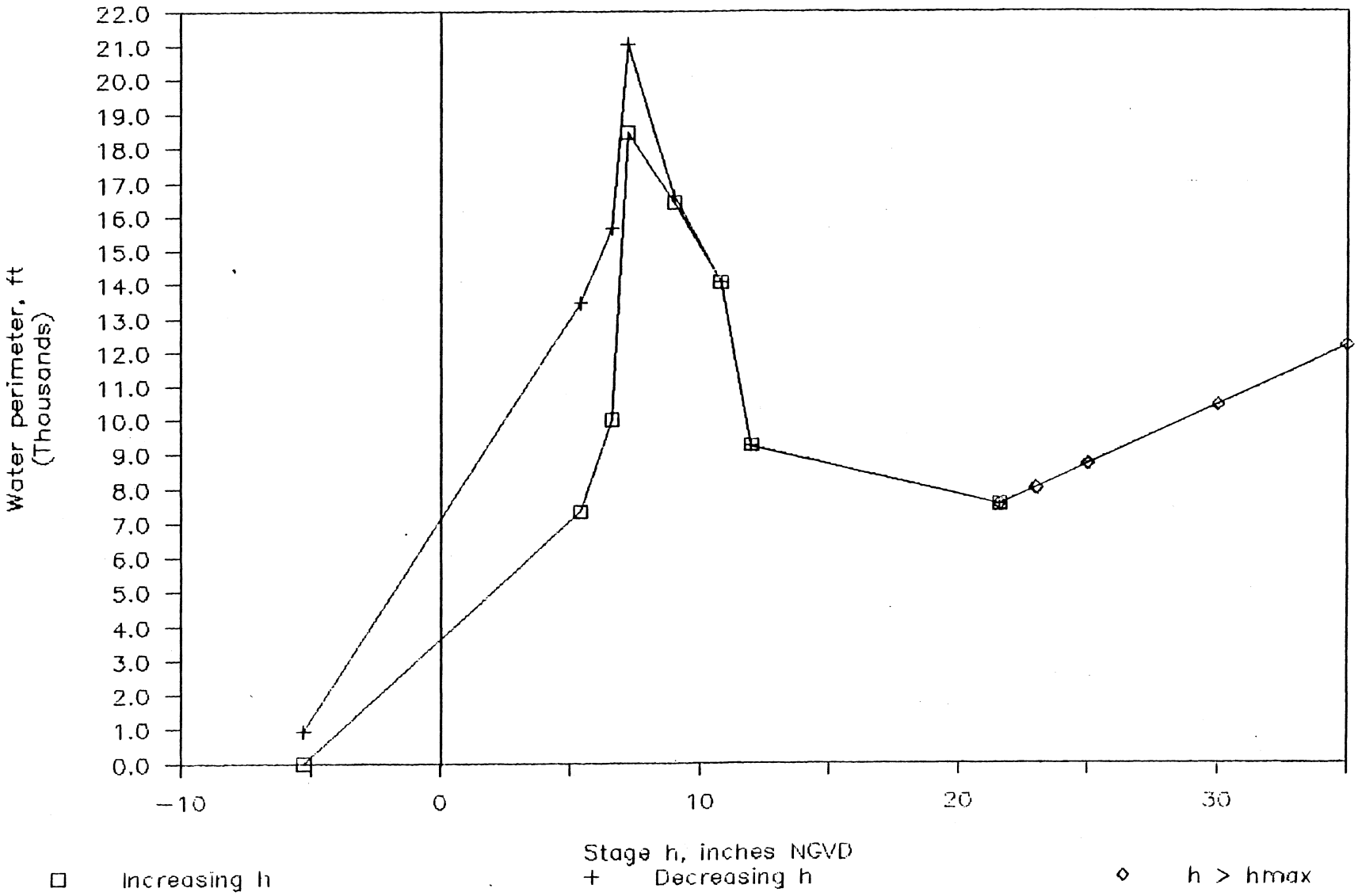

Figure 4-21. Water perimeter vs. stage--IRC-12.

a maximum point, these tendrils begin to coalesce and water perimeter decreases with increasing stage. When stage exceeds the maximum ground elevation of the impoundment and water spills out beyond the impoundment basin, perimeter is assumed to resume increasing. For Figure 4-21, beyond 1.80 feet NGVD the spreading water area is modeled as a circular area increasing as a function of stage and ground slope.

As the water recedes from total inundation, the curve takes a somewhat different shape as ponds disconnect from the receding waters and remain filled. The maximum water perimeter is higher with the addition of these ponds; the curve returns to a minimum which reflects permanent ponds within the impoundment.

Most impoundments of similar topography should generate a similar peaked curve; a smoother topography would yield a flatter curve. A lookup table or curve-fitting procedure could be used to approximate this relationship if required for modeling purposes.

Volume vs. Stage

In order to determine the manner in which water flow throughout the marsh moves toward the outlet and affects the stage as recorded in the perimeter ditch at this point, water storage, or volume, as a function of stage within the impoundment is required.

Calculations based on the digitized water areas are summarized in Table 4-9. In order to generate a curve, water areas were calculated for fifteen increments of impoundment stage covering the recorded range of -0.44 to 1.80 feet NGVD. The change in volume per change in stage is

Table 4-9. Volume vs. stage calculations--IRC-12.

		Estimation of cumulative volume as a function of stage			Regression analysis input		Curve Fit V(h), ft^3		Iterations	
							Curve 1 V=ah+b	Curve 2 V=ch^d	hcrit= 0.474 Vcrit= 204820	Resulting Combined Curves
Stage h, ft	Est area, ft^2	dh, ft	dV, ft^3	Cum V, ft^3	ln(h)	@ln ln(V)	a= 197000 b= 111403	c= 835530 d= 1.88	hcrit, ft	Calc V, ft^3	Calc h, ft
-0.44	151371	--	--	30000		10.31	24723		0.450	24723	-0.41
-0.20	175982	0.24	39282	69282		11.15	72003		0.468	72003	-0.21
0.00	196456	0.20	37244	106526		11.58	111403		0.473	111403	-0.02
0.20	216929	0.20	41338	147865		11.90	150803		0.474	150803	0.19
0.45	242629	0.25	57445	205309	-0.80	12.23	200052	185568	0.474	200052	0.47
0.55	686723	0.10	46468	251777	-0.60	12.44		270846	0.474	270846	0.53
0.60	922819	0.05	40239	292016	-0.51	12.58		319101	0.474	319101	0.57
0.75	1344262	0.15	170031	462047	-0.29	13.04		485890		485890	0.73
0.90	1713868	0.15	229360	691406	-0.11	13.45		685079		685079	0.90
1.00	1960200	0.10	183703	875110	0.00	13.68		835530		835530	1.02
1.20	1981980	0.20	394218	1269328	0.18	14.05		1178053		1178053	1.25
1.40	1992870	0.20	397485	1666813	0.34	14.33		1575122		1575122	1.44
1.60	2003760	0.20	399663	2066476	0.47	14.54		2025767		2025767	1.62
1.80	2014650	0.20	401841	2468317	0.59	14.72		2529165		2529165	1.78
2.00	2025540	0.20	404019	2872336	0.69	14.87		3084600		3084600	1.93

For estimation of area, see Table 4-9. Below are calculations used in estimating stage-volume curve to be fitted:

dh(i), ft = h(i)-h(i-1)
dV(i), ft^3 = 0.5*dh(i)*[V(i)+V(i-1)]
Cum V(i), ft^3 = V(i-1)+dV(i)

Calculated volume generated by @if statement containing linear & power functions below obtained by regressing two h intervals. Iteration used to find curve break (hcrit).

Curve 1 V(h), ft^3 = $a*h+$b
Curve 2 V(h), ft^3 = $a*h+$b
hcrit iterations = (($a_1*hcrit+$b_1)/$a_2)^(1/$b_2)
Combined V(h), ft^3 = @if(h<0.474,a_1*h+b_1,$a_2*h^$b_2)
Check: Calc h, ft = @if(V<$Vcrit,(V-$b)/$a,(V/$c)^(1/$d))

calculated by:

$$dV = Adh \qquad [4\text{-}3]$$

which for each incremental rise in stage i may be estimated by:

$$V_i = 0.5(A_i+A_{i-1})(h_i-h_{i-1}) \qquad [4\text{-}4]$$

Cumulative volume was summed for each increase in stage, which when plotted against the corresponding stage yielded the curve in Figure 4-22. From this curve an initial volume estimate at the minimum stage was made, indicating the existence of semi-permanent ponds within the marsh. Two curves were used to approximate this relationship. The first is a linear segment through a stage of approximately 0.45 feet:

$$V(h) = ah+b \qquad [4\text{-}5]$$

where V(h) = volume of water stored within impounded area, ft^3;
h = impoundment stage, feet NGVD; and
a,b = parameters;

followed by a power function of the form:

$$V(h) = ch^d \qquad [4\text{-}6]$$

where c,d = parameters.

Regressions were performed using 1-2-3 on the both the linear portion of the curve and the linearized equation of the power function:

$$\ln(V) = \ln(a) + b[\ln(h)]; \qquad [4\text{-}7]$$

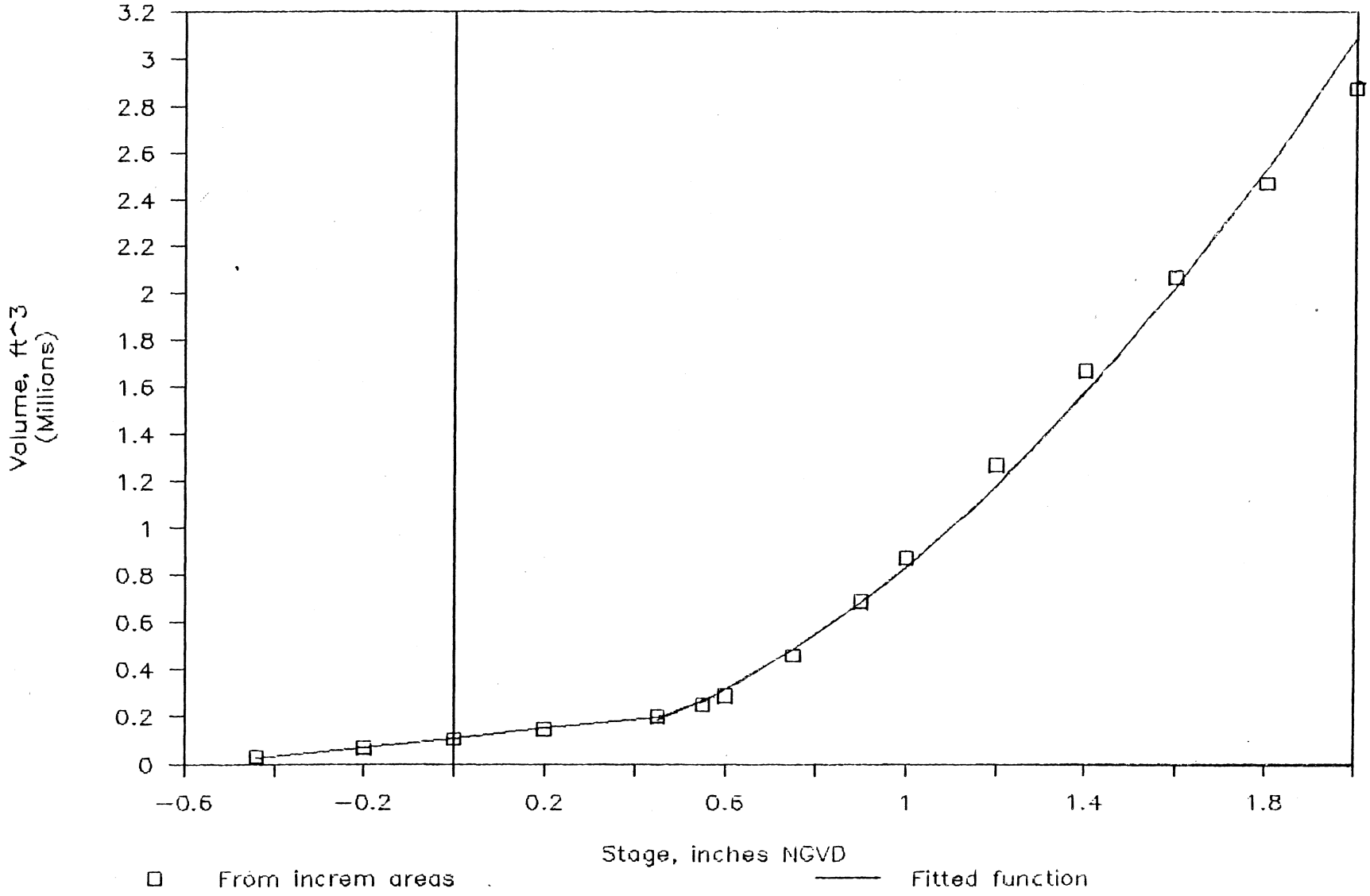

Figure 4-22. Water volume vs. stage--IRC-12.

yielding parameter values of:

$$a = 197000 \qquad c = 835530 \qquad b = 111403 \qquad d = 1.88$$

An @IF statement was used to combine the two portions of the curve. In order to find the stage at which the curve changes, so that:

$$V_i = \begin{cases} ah_i + b \; ; \; h_i < h_{crit} \\ ch_i^d \; ; \; h_i \geq h_{crit} \end{cases} \qquad [4\text{-}8]$$

where h_{crit} = stage at which curve changes from linear to power function;

the two equations were set as an equality, with the resulting expression solved iteratively for h_{crit} (Table 4-9), found to be 0.474 ft. A 1-2-3 expression could then be written to solve for stage given a known volume:

$$h_i = @IF(V<Vcrit,(V-b)/a, (V/c)\hat{}(1/d)) \qquad [4\text{-}9]$$

Calculated volumes using equation 4-8 are compared with values estimated from the data in Figure 4-22.

Hydrologic Components of Model

Impoundment Water Levels

Water levels were continuously monitored by Harbor Branch Foundation (HBF) personnel outside the Indian River Lagoon and estuary inlets of the culvert throughout the study period. Discrete times and stages were digitized from these tracings at 4-6 hour intervals by HBF.

Because of the desirability of knowing the head difference between simultaneous lagoon and impoundment water levels in order to calculate flow through the culvert, the data were interpolated for regular time increments.

Linear interpolation estimates for water levels at desired regular time steps were made as follows:

for: $t_1 < t < t_2$

$$h(t) = h_2-[(h_2-h_1)/(t_2-t_1)](t_2-t) \qquad [4\text{-}10]$$

where $h(t)$ = water surface elevation at time t; and

$(h_2-h_1)/(t_2-t_1)$ = rate of change in water surface elevation over time interval t_1 to t_2.

Both the HBF original data and the spreadsheet table in which the interpolations were calculated may be found for each study period in Appendix B. In the original data table a spreadsheet column was prepared in which dh/dt is first calculated separately between each pair of data points. The 1-2-3 vertical lookup function @VLOOKUP(x,range,column number) operates on time t, scanning the lookup table of measured data, finding the two nearest digitized times t_1 and t_2, and interpolating between the associated levels for the water level h(t). Equation 4-10 is expressed in the spreadsheet as:

```
h(t) = @VLOOKUP(T,RANGE,3)-
       @VLOOKUP(T,RANGE,6)*
       (@VLOOKUP(T,RANGE,2)-T)                    [4-11]
```

Tidal Flow

A tidal model was generated by assuming five principal tidal components and calibrating them to fit tidal height data taken in Indian River Lagoon outside the south culvert to IRC-12 during the study year 1985. Measurements were generally recorded four times daily on high and low tides.

A table of harmonic constants was set up (Table 4-10) with amplitude and phase angle varied as calibration parameters and period maintained constant for each tidal component. A table of calculations (Table 4-11) begins with the observation times in 1-2-3's serial date/time format. The column of measured tidal heights is followed by a column of moving averages calculated over 21 tidal points by copying down a single 1-2-3 @AVG(range) function. This smoothed out diurnal and semi-diurnal fluctuations sufficiently to make monthly trends more apparent.

The remainder of the table consists of the model calculations. Each tidal component j is calculated for each time t by:

$$h_j(t) = n\sin[2\pi t/(T+\phi)] \qquad [4\text{-}12]$$

where t = time, days;

$h_j(t)$ = contribution to total tidal height of tidal component j at time t, inches;

n = amplitude, inches;

T = period, days; and

ϕ = phase angle, radians.

A spreadsheet usage note: by using the correct combination of relative and fixed cell addresses, only one sine function needs to be

Table 4-10. Harmonic constants of principal tidal components--Indian River lagoon at IRC-12.

	Long-period			Short-period	
	Monthly	Semi-annual	Annual	Semi-diurnal	Diurnal
Amplitude n, inches:	2.50	3.8	7.8	4.67	1.85
Time angle, radians:	4.712	3.93	3.14	4.45	5.24
Period T, hours:	708.73	4380	8760	12.48	24.96
Period T, days:	29.53	182.5	365	0.52	1.04

Note: For time angle calculations, 31048 = 31-Dec-84 midnight = 0.

Table 4-11. Tidal model calibration of Indian River lagoon at IRC-12.

AVG	7.96	7.96	8.05	8.03	4.77
STD	5.67	6.88	6.58	4.59	2.68
MAX	22.22	26.99	30.72	20.02	13.11
MIN	-1.45	-7.52	-3.62	-1.63	0.00

Date	Time	Monthly	Semi-annual	Annual	Semi-diurnal	Diurnal	Net Long Trends	Resul-tant	Meas HOUT	21-Tide Mov Avg Meas HOUT	@Abs (dH)
26-Nov-84	21:08	-0.93	1.56	4.43	4.12	0.74	13.96	18.82	15.78		
27-Nov-84	00:45	-1.01	1.54	4.42	1.14	1.79	13.86	16.78	22.28		6.50
27-Nov-84	05:09	-1.09	1.52	4.40	-4.29	1.21	13.73	10.64	16.03		6.26
27-Nov-84	08:58	-1.17	1.50	4.38	3.18	-0.45	13.61	16.35	12.48		3.55
27-Nov-84	12:46	-1.24	1.48	4.36	2.13	-1.73	13.50	13.91	21.83		9.35
27-Nov-84	16:59	-1.32	1.46	4.34	-4.66	-1.42	13.38	7.30	19.90		1.93
27-Nov-84	20:35	-1.39	1.44	4.32	1.47	0.05	13.28	14.81	12.31		7.59
28-Nov-84	00:36	-1.46	1.42	4.31	3.36	1.59	13.17	18.12	17.22		4.91
28-Nov-84	05:00	-1.54	1.40	4.29	-4.61	1.55	13.05	9.98	15.48		1.74
28-Nov-84	08:37	-1.60	1.38	4.27	0.43	0.16	12.95	13.54	10.00		5.48
28-Nov-84	12:25	-1.67	1.36	4.25	4.23	-1.42	12.85	15.66	16.87	16.73	6.87
28-Nov-84	17:14	-1.75	1.34	4.23	-4.49	-1.61	12.72	6.63	20.47	16.67	3.60
28-Nov-84	20:27	-1.80	1.32	4.21	-1.09	-0.46	12.64	11.09	13.70	16.25	6.78
29-Nov-84	01:15	-1.87	1.30	4.19	3.82	1.52	12.52	17.86	16.15	16.48	2.46
29-Nov-84	04:52	-1.92	1.28	4.17	-3.54	1.77	12.43	10.66	18.29	16.61	2.13
29-Nov-84	08:40	-1.97	1.26	4.16	-1.66	0.57	12.34	11.25	13.60	16.13	4.69
29-Nov-84	12:41	-2.03	1.24	4.14	4.65	-1.19	12.25	15.72	15.73	16.00	2.13
29-Nov-84	17:05	-2.08	1.22	4.12	-3.12	-1.80	12.15	7.23	22.56	16.09	6.82
29-Nov-84	20:42	-2.13	1.20	4.10	-2.61	-0.77	12.07	8.70	16.50	15.79	6.06
30-Nov-84	00:54	-2.17	1.18	4.08	4.67	1.09	11.98	17.74	14.34	15.89	2.16

entered in the first tidal component column of the first time step row. This is copied across to all components (assuming the table of constants is ordered the same), then the first row including the remaining calculations is copied down through all time steps.

Calibration began with long-term trends. Monthly, semi-annual and annual components were summed and added to the long-term average h_{avg} (8.9 inches NGVD). This "net long trends" column then was graphed in superposition with the 21-tide moving average column. Amplitudes and phases of the long-term components were then varied, the worksheet recalculated, and the graph redisplayed to obtain the best possible visual match (Figure 4-23). The resulting long-term components may be seen separated in Figure 4-24. These figures illustrates the seasonal tides combining to form the fall high tides which typically appear in September. Lowest tides occur in March and April, followed by a smaller peak in May with relatively low summer levels.

Diurnal and semi-diurnal components were added to the net long-term trends to provide the total tidal height, which is expressed as:

$$h(t) = \Sigma h_j(t) + h_{avg} \qquad [4\text{-}13]$$

where $h(t)$ = total tidal height, inches NGVD; and

h_{avg} = long-term mean tidal height, inches NGVD.

Period C, planned as the simulation model calibration period due to its complete data set, was used to calibrate the short-term trends. The resultant column of total tidal height was graphed along with the measured tidal height for Period C and monitored, while short-term harmonic constants alone were varied and the worksheet recalculated until a similarity in short-term trends was obtained (Figures 4-25 and 4-26).

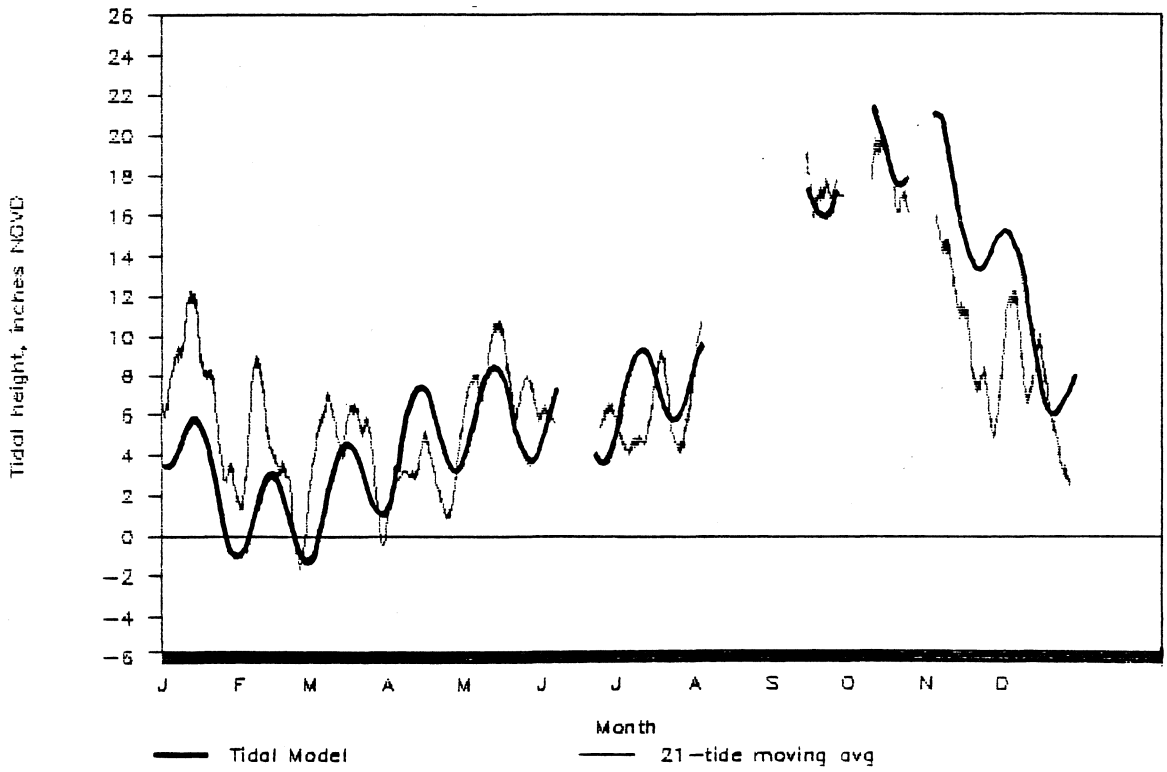

Figure 4-23. Tidal height Indian River lagoon at IRC-12--long-period model with 21-tidal-point moving average January-December 1985.

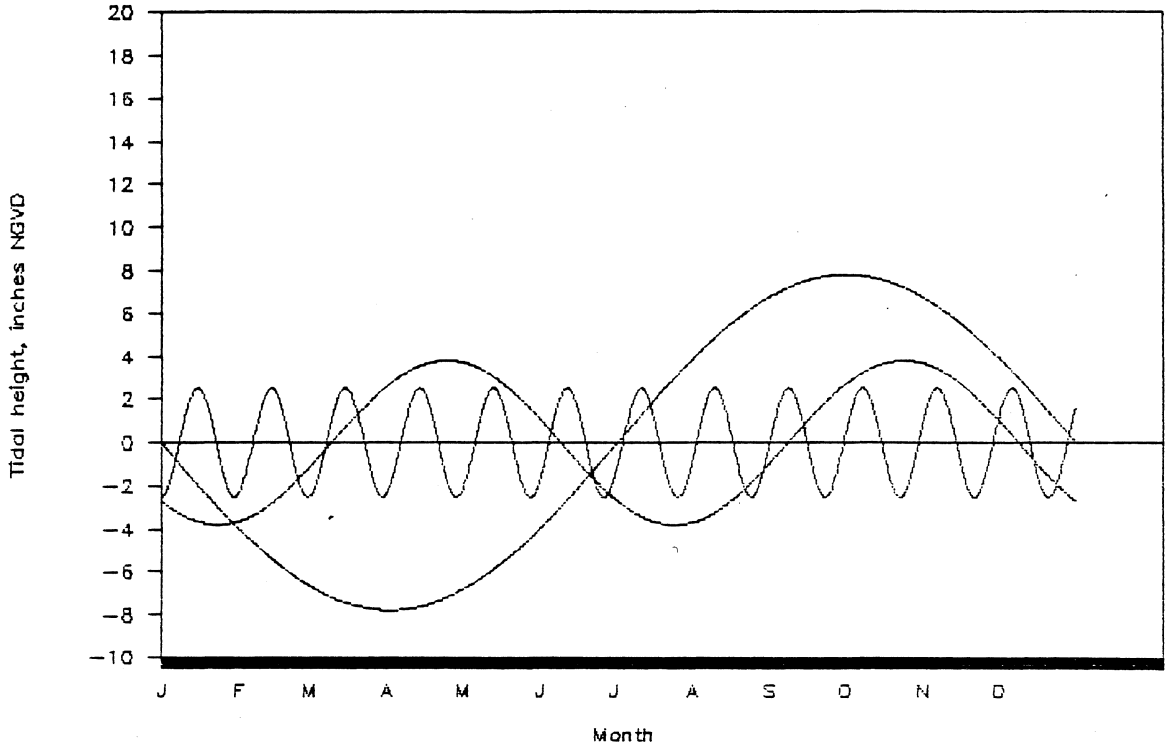

Figure 4-24. Tidal components Indian River lagoon at IRC-12--long-period model January-December 1985.

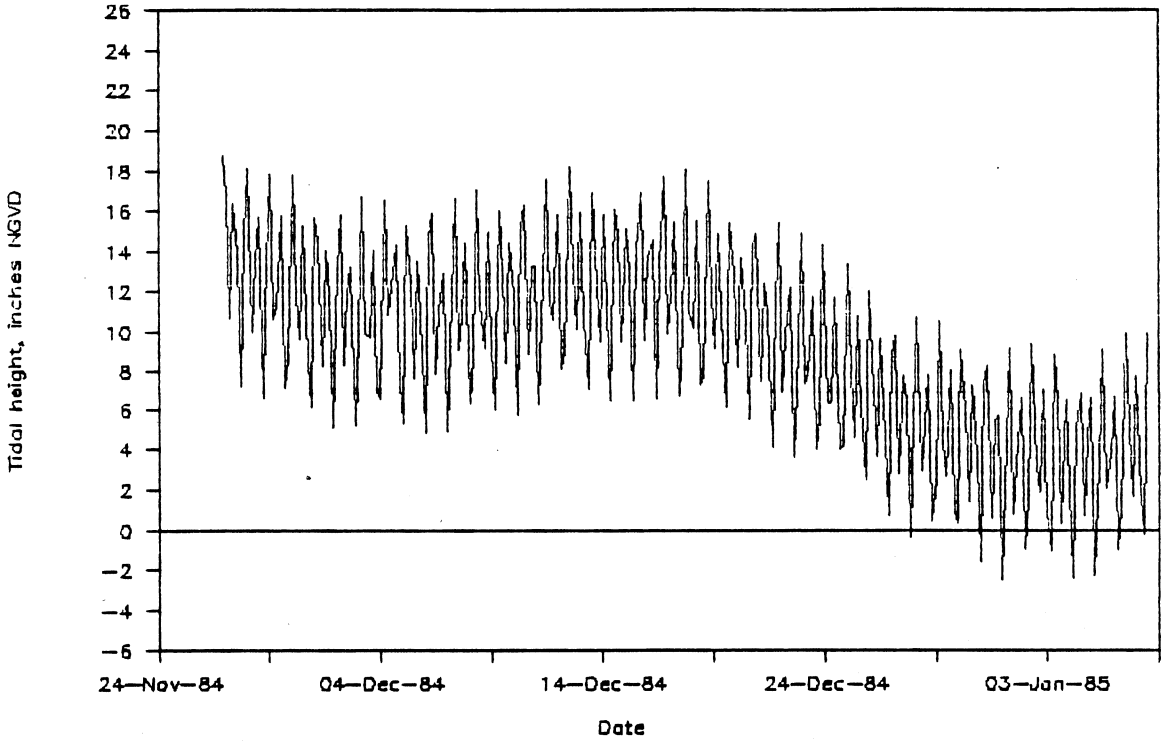

Figure 4-25. Tidal height Indian River lagoon at IRC-12--short-period model Period C (11/27/84-01/06/85).

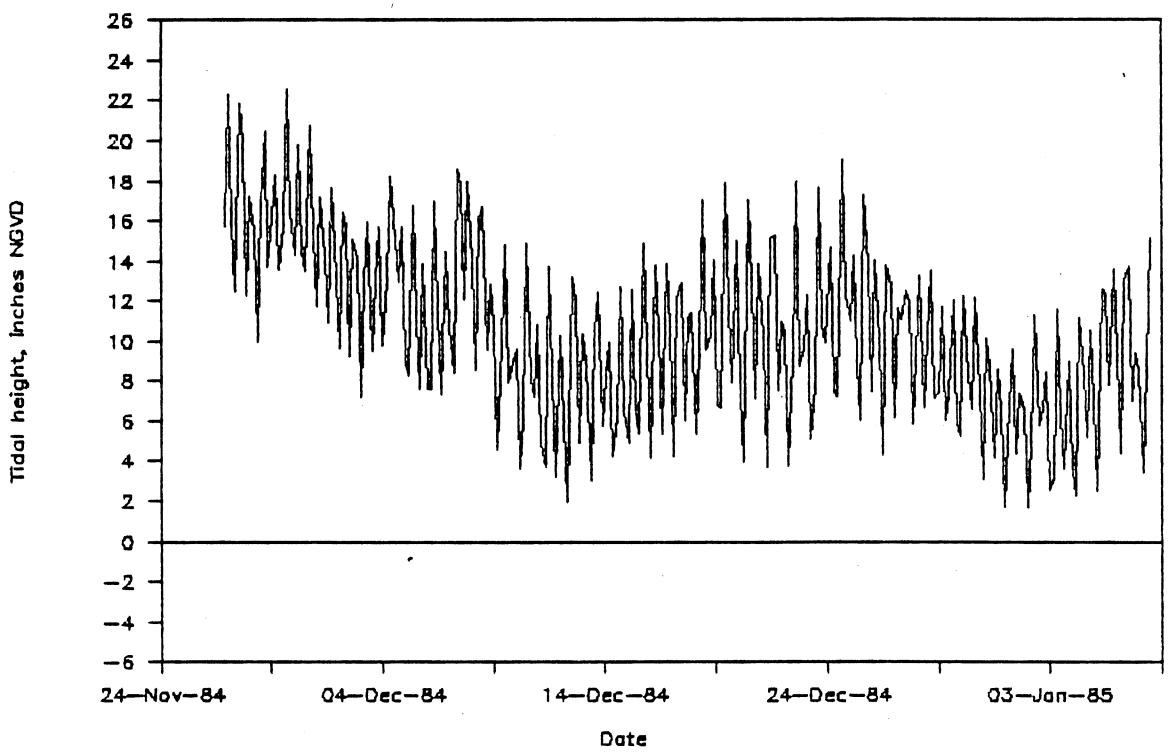

Figure 4-26. Tidal height Indian River lagoon at IRC-12--Period C (11/27/84-01/06/85).

A tidal range of approximately 10 inches was indicated by taking the average of tidal height differences between tidal points over Period C.

Rainfall

As discussed earlier in this chapter in the climate and hydrology section, rain data were collected in a tube gauge within the impoundment by Indian River County Mosquito Control District personnel twice weekly (see location in Figure 4-2). Since hourly precipitation data (HPD) from the Vero Beach 4W station were to be used in the simulation for a more accurate time distribution of rainfall, it was desired to review the possible study periods for which complete data sets existed to determine when precipitation had been most similar between the two sites.

In order to accomplish this, HPD data for study periods A-C were summed for each IRC-12 collection date. This provides, of course, only a rough comparison; HPD data were summed at 8 a.m. of the morning of the IRC-12 collection date, while IRC's actual collection times varied and are not available. It must also be assumed that some evaporation loss from the IRC-12 gauge would consistently occur, and overflows may be a possibility.

Once this was done, both sites were summed monthly (Table 4-12) and compared in Figure 4-27. Where some IRC-12 sampling periods extended across adjacent months, the totals are found in the month that the measurement was made. The same shift therefore occurs in the Vero Beach 4W totals.

Three months of 1985 contained gaps in HPD data. For the purposes of this comparison, daily records from NOAA's Climatological Data: Florida for Vero Beach 4W were substituted for missing HPD data. These

Table 4-12. Comparison of monthly rainfall totals--Vero Beach 4W and IRC-12 January-December 1985.

Month	Monthly rainfall, inches	
	IRC-12	VB4W
Jan	1.80	0.87 *
Feb	0.20	0.43 *
Mar	2.65	2.10
Apr	6.30	5.20
May	2.80	1.60
Jun	2.45	3.00
Jul	9.40	10.20
Aug	3.85	6.20
Sep	11.95	12.50
Oct	5.95	4.10
Nov	6.80	1.60
Dec	1.60	2.65 *
Annual	55.75	50.45

Notes: IRC-12 data collected semiweekly by Indian River Mosquito Control District. Since time distribution unknown between measurements, sampling months may not correspond exactly to calendar months.

Vero Beach 4W data are from NOAA's Hourly Precipitation Data: Florida. Asterisked months have incomplete hourly data; daily records from NOAA's Climatological Data: Florida were used instead. All data were totaled to correspond to IRC-12 sampling months.

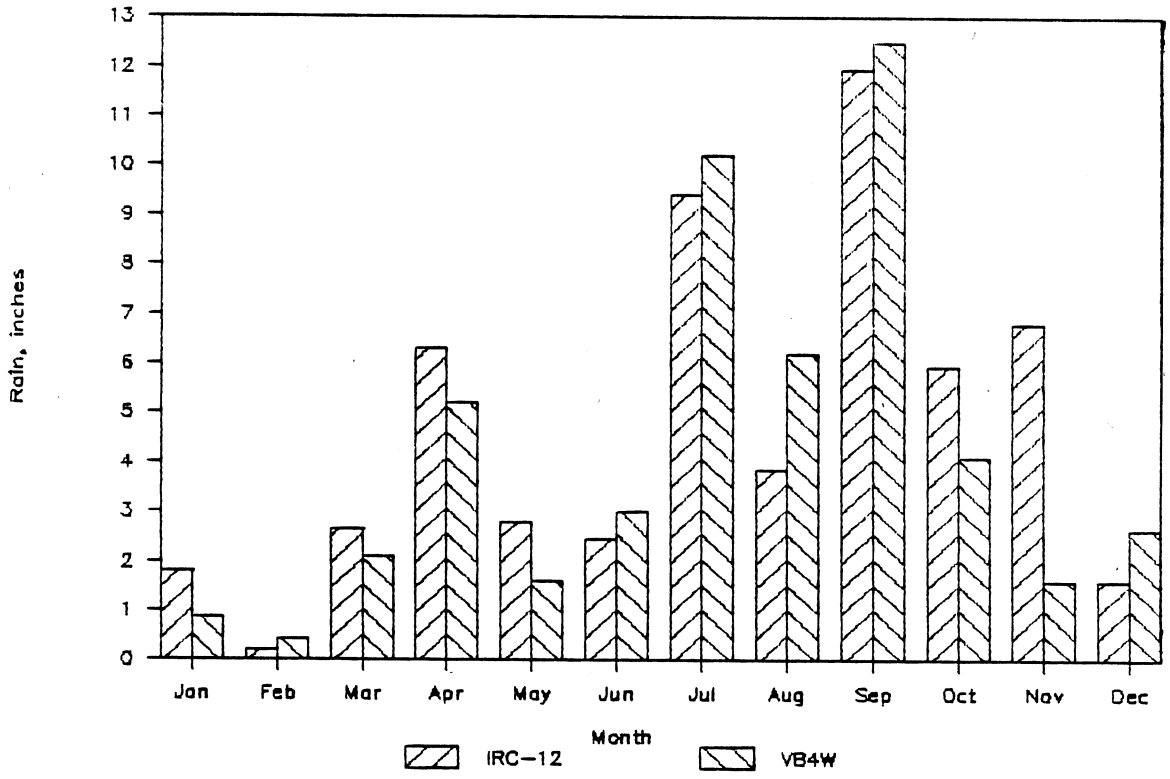

Figure 4-27. Comparison of rainfall--monthly totals January-December 1985 Vero Beach 4W and IRC-12.

measurements are not taken from the same gauge, but are positioned at approximately the same site; analysis of several periods showed little variation between the two. For 1985, Vero Beach 4W recorded 50.45 inches of rainfall, while IRC-12 totaled 55.75 inches.

The semiweekly sums described above are compared for each study period in Figures 4-28a through 4-28c. It can be seen that some rain events match up well, while some are fairly disparate. Period C (11/26/84-01/07/85) shows the closest similarity, aided by the small number of rain events; this was therefore chosen for the calibration period. HPD data used for each of the study periods are presented in Appendix B, as is the table which modifies these for model input.

Grouping these hourly records into four-hour time steps was simplified by use of 1-2-3's @INDEX(range,column,row) function, which returns the value of the cell in a specified range at the intersection of the specified column and row. The range called for by the function consists of the single column of hourly data, named here HPD. A column of numbers was generated using the Data Fill command to give the last row number (called here PROW) of each four-hour group. For a one-column range, the column number will always be zero. Thus, @INDEX($HPD,0,PROW) returns the one-hour precipitation at time t, and the four-hour precipitation for time t can be calculated in one cell by:

$$P^4(t) = \text{@SUM(@INDEX(\$HPD,0,PROW)+}$$
$$\text{@INDEX(\$HPD,0,PROW-1)+}$$
$$\text{@INDEX(\$HPD,0,PROW-2)+}$$
$$\text{@INDEX(\$HPD,0,PROW-3)} \qquad [4\text{-}14]$$

where $P^4(t)$ = four-hour precipitation ending at time t.

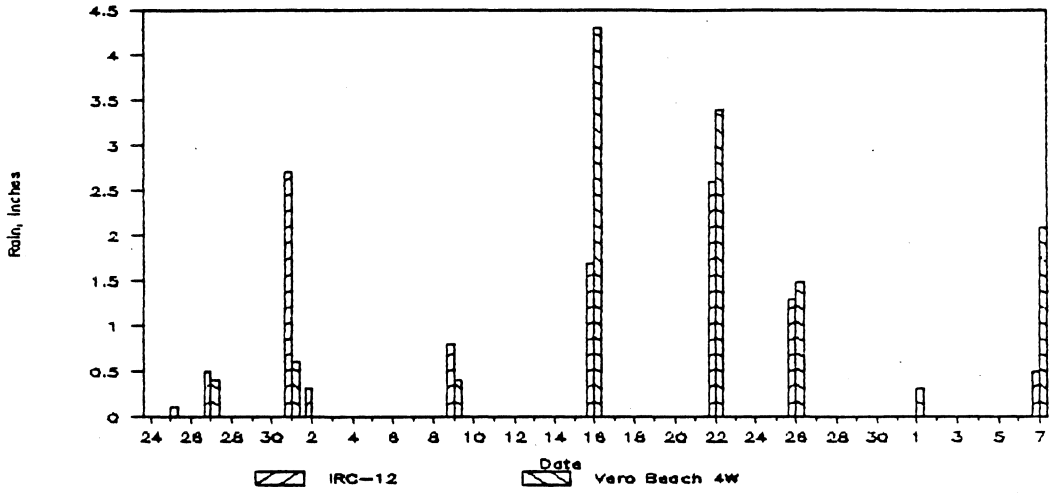

Figure 4-28a. Comparison of rainfall--semiweekly totals for Period A (06/23/85-08/04/85) Vero Beach 4W and IRC-12.

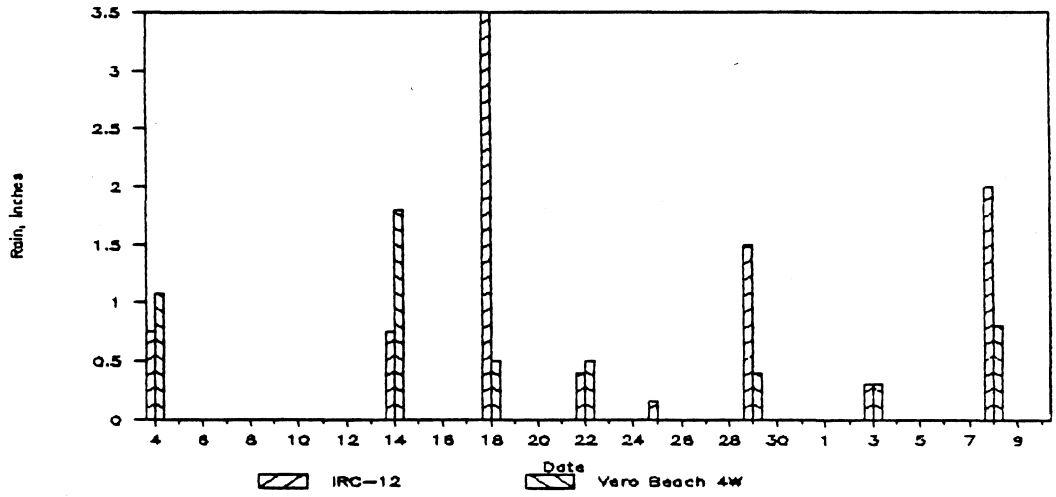

Figure 4-28b. Comparison of rainfall--semiweekly totals for Period B (08/01/86-09/08/86) Vero Beach 4W and IRC-12.

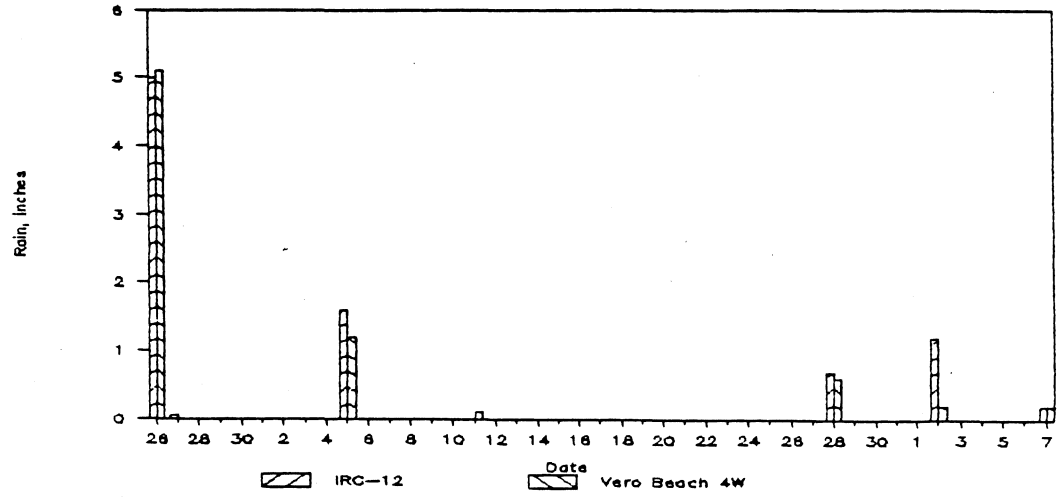

Figure 4-28c. Comparison of rainfall--semiweekly totals for Period C (11/26/84-01/05/85) Vero Beach 4W and IRC-12.

Copying this cell down the required number of time steps provides the model input needed for precipitation.

Evapotranspiration

Daily pan evaporation data from the Vero Beach 4W climatological station, described earlier in the climate and hydrology discussion, were incorporated into a model for potential evapotranspiration (ET). First, however, it was desired to distribute each single daily pan evaporation (PE) measurement over several simulation time steps. For a four-hour time step, this was performed by equally distributing the daily pan evaporation over the three daylight intervals ending at 12 noon, 4 p.m., and 8 p.m. Since PE measurements are made at 8 a.m. on the stated date, this daily total is assumed to cover the previous day's daylight intervals.

A variation of the spreadsheet method described earlier for calculating four-hour precipitation was used. In that method, a column of numbers (3,7,11...) was generated which provided the last row number (named PROW) of each four-hour block of hourly data. Each value of PROW acted as an input variable to the @INDEX function which summed the specified four rows. In this method, the time column was first generated using Data Fill. A column of numbers named EROW was then produced which a) evaluates each time step, determining if the associated interval is a daylight interval; b) gives the row number for the correct day's PE measurement if a daylight interval, and c) returns 0, an "empty" row, for non-daylight intervals. The cell entry producing this column for each time t is:

```
EROW(t) = @IF(@HOUR(T)<12
          #OR#@HOUR(T)>20,
          0,@ROUND(T,0)-31222                                    [4-15]
```

This equation demonstrates the advantages of using 1-2-3's serial date format. The @HOUR(time number) function is used to return the hour (1-24) of the serial date to aid in the evaluation of daylight intervals. The @ROUND(x,n) function strips the decimal portion off the serial date, leaving a whole number which, when reduced by a constant, acts as the row number for the @INDEX(range,column,row) function. The input range is the original column of daily PE, named here E. The column which actually returns the appropriate four-hour PE for the desired time step is then created with a simple

$$PE_4 = @INDEX(\$E,0,EROW)/3 \qquad [4\text{-}16]$$

These were then utilized in an evapotranspiration (ET) model which considers percentage of inundated area in which:

$$[\text{Total ET}] = [\text{ET from land area}] + [\text{ET from water area}] \qquad [4\text{-}17]$$

Since water area as a function of stage has been determined, equation 4-17 can be expressed for period i with four-hour intervals as:

$$ET_i = ET_{w.i}A_{w.i} + ET_{s.i}A_{s.i} \qquad [4\text{-}18]$$

where ET_i = total ET over the impoundment during period i;

$ET_{w.i}$ = ET over water areas during period i;

$ET_{s.i}$ = ET over exposed soil areas during period i;

$A_{w.i}$ = water area at end of period i; and

$A_{s.i}$ = exposed soil area at end of period i.

ET over water areas is assumed to be equivalent to a maximum possible ET for a given site, which is some fraction of the pan evaporation measurement. Thus,

$$ET_{w.i} = (ETMAX)PE_i \qquad [4\text{-}19]$$

where PE_i = pan evaporation during period i; and

ETMAX = coefficient indicating maximum possible fraction of PE for site, a calibration parameter.

For land areas, pan evaporation is modified both by the ETMAX coefficient and by depth to the water table (Figure 4-29):

$$ET_{s.i} = [ETMAX-ETRATE(h_{grd}-h_{wt.i})]PE_i \qquad [4\text{-}20]$$

where ETRATE = coefficient reducing ET with increasing depth to water table, a calibration parameter;

$h_{wt.i}$ = water table elevation at end of period i; and

h_{grd} = average ground elevation over impoundment.

For the purposes of estimating ET, water table elevation is approximated by the impoundment stage h at the previous time step:

$$h_{wt.i} \sim h_{i-1} \qquad [4\text{-}21]$$

Combining equations 4-18 through 4-21 gives the complete expression for estimation of ET over the impounded area for period i:

$$ET_i = (ETMAX)PE_iA_{w.i} + [ETMAX-ETRATE(h_{grd}-h_{i-1})]PE_iA_{s.i} \qquad [4\text{-}22]$$

In the simulation, water area fraction over total marsh area is calculated at each time step using the model of water area as a function of

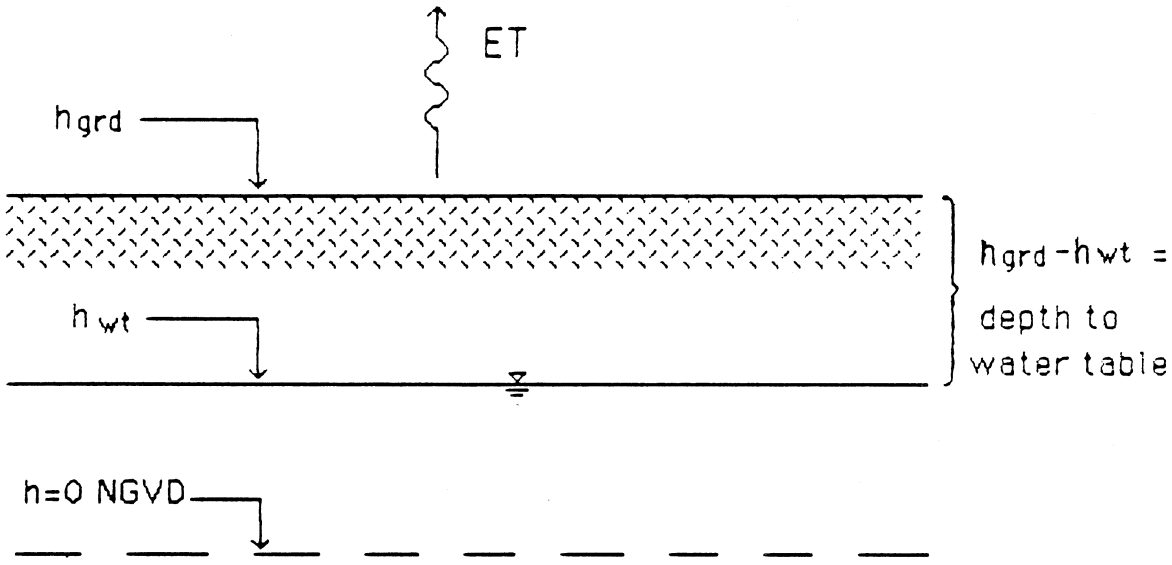

Figure 4-29. Evapotranspiration model.

stage described earlier. The following modification of Equation 4-22 is used in each spreadsheet cell:

$$ET_i = (ETMAX)PE_iA_{w.i})+ [ETMAX-ETRATE(h_{grd}-h_{i-1})]PE_i(1-A_i) \quad [4\text{-}23]$$

where $A_i = A_{w.i}$ = fraction of water area over total impoundment area at end of period i.

Infiltration

As water table data are not available for this site, infiltration estimates are limited in reliability. Before a sensitive infiltration model would be structured, it was preferred to use a simple model to test sensitivity of the model to percolation. Total infiltration as a simple function of stage and average ground elevation was estimated by:

$$F_i = (FRATE)\max(h_{grd}-h_{wt.i},0)A_i \quad [4\text{-}24]$$

where F_i = infiltration during period i;

FRATE = infiltration coefficient giving ratio of infiltration rate to depth to water table, a calibration parameter.

Infiltration would be at a maximum when a large water area exists but tidal height is low; $h_{wt.i}$ is therefore approximated here by tidal height outside the south culvert, $h_{out.i}$ (Figure 4-30).

Water Control Structures

Flow in and out of the culvert is a function of the difference in head between the estuary and the impoundment, the culvert length and diameter, friction due to roughness within the culvert and local energy

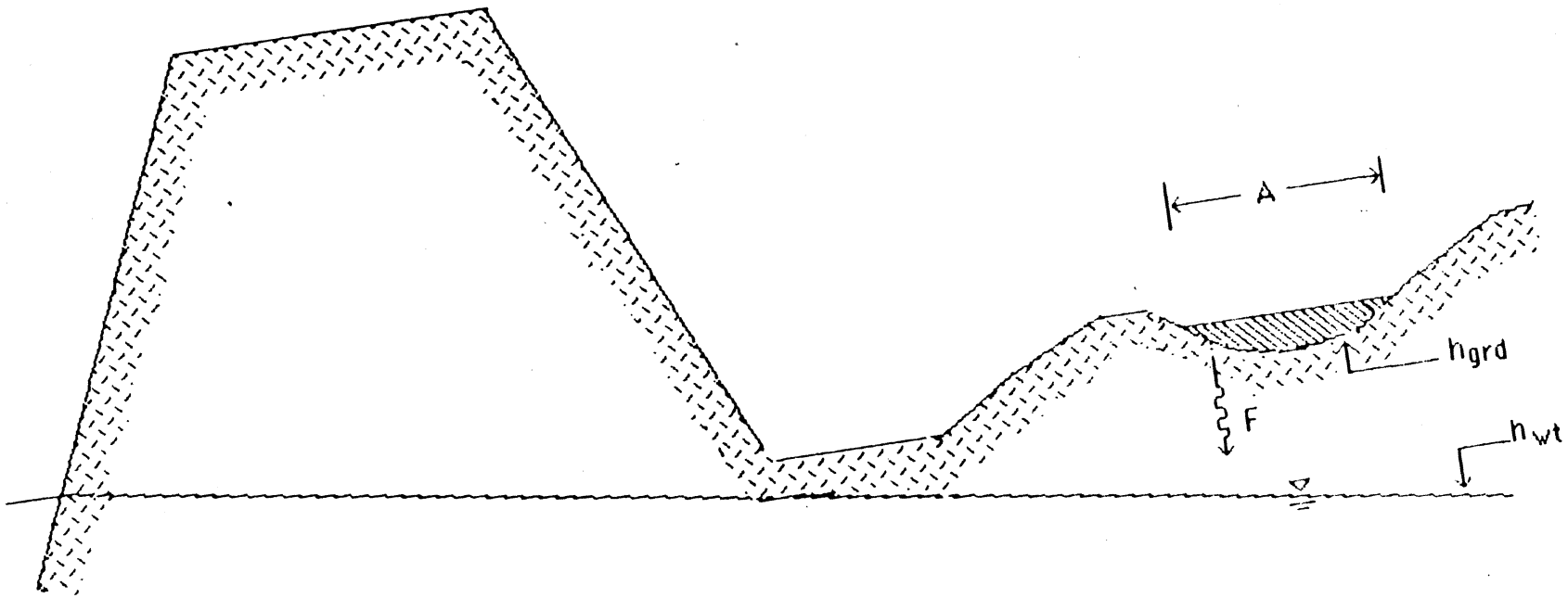

Figure 4-30. Infiltration model.

losses at the orifices. The characteristic pipe equation is developed using Manning's equation:

$$V = MR^{2/3}S^{1/2} \qquad [4\text{-}25]$$

where V = mean velocity;

M = coefficient for Manning's formula;

R = hydraulic radius; and

S = slope of energy grade line.

The coefficient M is generally expressed using the Manning coefficient n. For a closed corrugated metal storm drain flowing partly full, n ranges from 0.021 to 0.030, with 0.024 considered normal (Christenson, 1984). For English units:

$$M = 1.486/n$$

where n = Manning coefficient of roughness ~ 0.24.

The slope of the energy grade line is defined as

$$S = \Delta H/L$$

where ΔH = head loss due to friction; and

L = pipe length.

Head loss is thus given by

$$\Delta H = LV^2/(MR^{4/3})$$

To include losses at the pipe or culvert orifices, a local loss term is added to the head loss expression:

$$\Delta H = LV^2/(MR^{4/3}) + \Sigma\zeta\, V^2/(2g) \qquad [4\text{-}26]$$

where $\Sigma\zeta$ = sum of local loss coefficients; and

g = acceleration due to gravity.

The following estimates are generally made for local losses in a circular pipe, yielding an estimate for $\Sigma\zeta$ of 1.78:

Re-entrant inlet: $\zeta = 0.78$ Outlet: $\zeta = 1.00$

Substituting $V = Q/A$ into equation 4-26 yields:

$$\Delta H = [L/(MR^{4/3}A^2) + \Sigma\zeta/(2gA^2)]Q^2$$

The following expression may be given for flow:

$$Q = (\Delta H/P)^{1/2} \qquad [4\text{-}27]$$

where P_v = characteristic pipe value = $L/(M^2R^{4/3}A^2) + \Sigma\zeta/(2gA^2)$.

Hydraulic radius is defined for a pipe as:

$$R = A/P$$

where A = cross-sectional water area of pipe; and

P = wetted perimeter.

The P-value can therefore be rewritten as:

$$P_v = LM^{-2}P^{4/3}A^{-10/3}) + \Sigma\zeta\, A^{-2}/(2g)$$

The next step is to find cross-sectional area as a function of depth of water in a partially-filled pipe. For a circular cross sectional area, an angle θ is defined (Figure 4-31) such that:

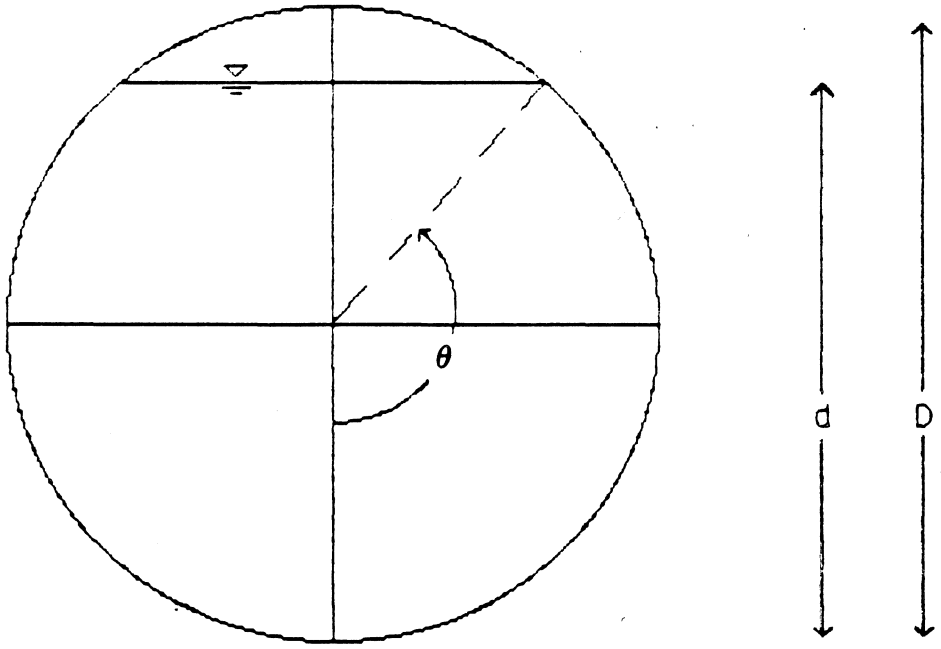

Figure 4-31. Definition of angle θ created by water surface within partially-filled circular pipe.

$$d = (D/2)(1-\cos\theta) \quad [4\text{-}28]$$

where d = depth of water in pipe; and

D = diameter of pipe.

The following expressions can then be written for cross-sectional water area and wetted perimeter as functions of θ (Christenson, 1984):

$$A_i = (D^2/4)(\theta_i - \cos\theta_i \sin\theta_i) \quad [4\text{-}29]$$

$$P = \theta D$$

The latter substitution for wetted perimeter is made into the expression for P-value to be used in the spreadsheet as:

$$P_{v.i} = LM^{-2}(\theta_i D)^{4/3} A_i^{-10/3}) + \Sigma\zeta A_i^{-2}/(2g) \quad [4\text{-}30]$$

Mean depth in the pipe is estimated by averaging the depths at either end; depths are obtained by subtracting the culvert elevation from water elevations at either end while maintaining a maximum depth equal to the pipe diameter (Figure 4-32):

$$d = 0.5[\min(D, h_{in} - h_{cul}) + \min(D, h_{out} - h_{cul})]$$

where h_{in} = water elevation measured outside culvert's impoundment opening;

h_{out} = tidal elevation measured outside culvert's estuary opening; and

h_{cul} = culvert elevation.

Substituting into equation 4-28 and rearranging:

$$\theta_i = \cos^{-1}\{1 - [\min(D, h_{in.i-1} - h_{cul}) + \min(D, h_{out.i} - h_{cul})]/D\} \quad [4\text{-}31]$$

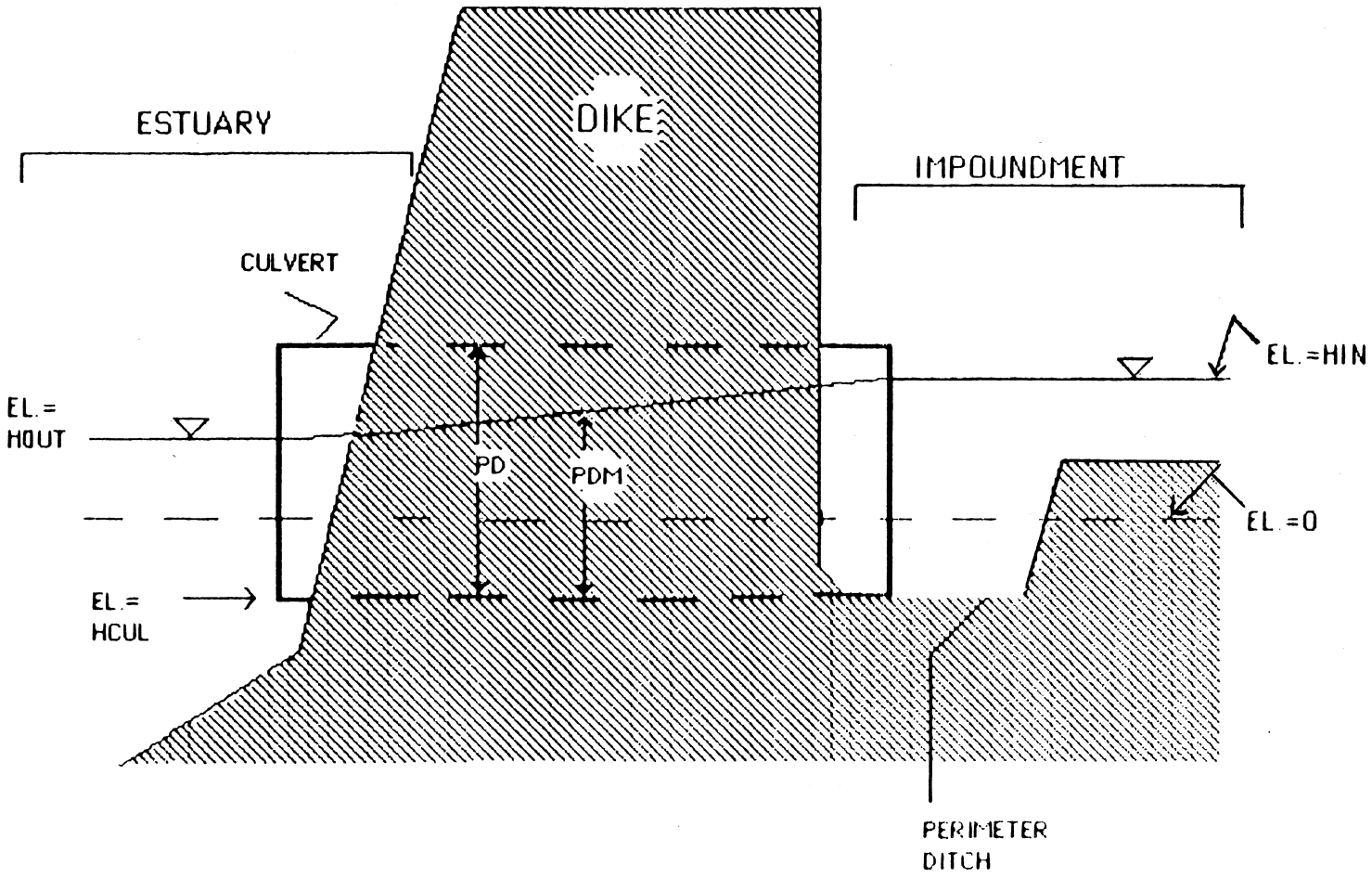

Figure 4-32. Estimation of mean culvert depth.

Upon initially determining the head difference at each step as:

$$\Delta H_i = (h_{out.i} - h_{in.i-1}) \qquad [4\text{-}32]$$

flow through the culvert can be determined after successively evaluating values for depth angle θ (equation 4-31), cross-sectional water area of pipe A (equation 4-29), and pipe characteristic value P_v (equation 4-30). Since for each period i h_{out} is an input at the beginning of the calculations and h_{in} is the final calculation, the following are used for computing Q_i as shown in equation 4-32:

$h_{out} = h_{out.i}$ (from period i)

$h_{in} = h_{in.i-1}$ (from period i-1)

For the final flow calculations, equation 4-27 is expanded to include if-then statements which a) look at the sign of ΔH to determine flow direction and b) determine the presence of a flapgate preventing flow out of the impoundment (FPG=1 indicates installed flapgate, FPG=0 means none).

Flows calculated in this manner were found in daily tides to permit water to flow in too readily on daily high tides, in turn flowing out too slowly with low tides. A simple calibration parameter was introduced to account for variation between inflows and outflows due to contribution of bottom slope in the impoundment. This adds to ΔH for outflows and subtracts from ΔH for inflows.

$$Q_{in.i} = |\Delta H_i - R_{st}\Delta H_i|^{1/2}/P_{v.i} \quad ; \Delta H_i > 0$$
$$0 \quad ; \Delta H_i \leq 0 \qquad [4\text{-}33]$$

$$Q_{out.i} = |\Delta H_i + R_{st}\Delta H_i|^{1/2}/P_{v.i} \quad ; \Delta H_i < 0 \text{ and FPG} = 1$$
$$0 \quad ; \Delta H_i \geq 0 \text{ or FPG} = 0. \qquad [4\text{-}34]$$

A culvert with a flapgate attached to permit one-way flow only into the impoundment may additionally have a riser board structure attached at the culvert's impoundment opening (Figure 4-33). Water trapped by the flapgate within the impoundment may be released over the riser, thus allowing control of water levels. Flow over the riser board is estimated using the formula for flow over a sharp-crested weir (White, 1979):

$$Q_r = (2/3)C_w bh(2gh)^{1/2}$$

where C_w = weir coefficient $\simeq$ 0.611;

b = width of riser board; and

h_c = water elevation above weir crest; or

$$Q_r = 0.5761g^{1/2}bh_c^{3/2}$$

The water elevation above the weir crest is estimated by:

$$h_c = h_{in}-h_{rb}$$

where h_{in} = impoundment stage; and

h_{rb} = elevation of riser board.

Flow over the riser board at time step t_i may be expressed as:

$$Q_r = 0.5761g^{1/2}b\max[h_{in}-h_{rb},0]^{3/2} \qquad [4\text{-}35]$$

Setting the constant h_{rb} to an extremely high value eliminates riser flow when not in place.

Integration of the above models into the spreadsheet simulation, with the associated 1-2-3 expressions, is summarized in the following section.

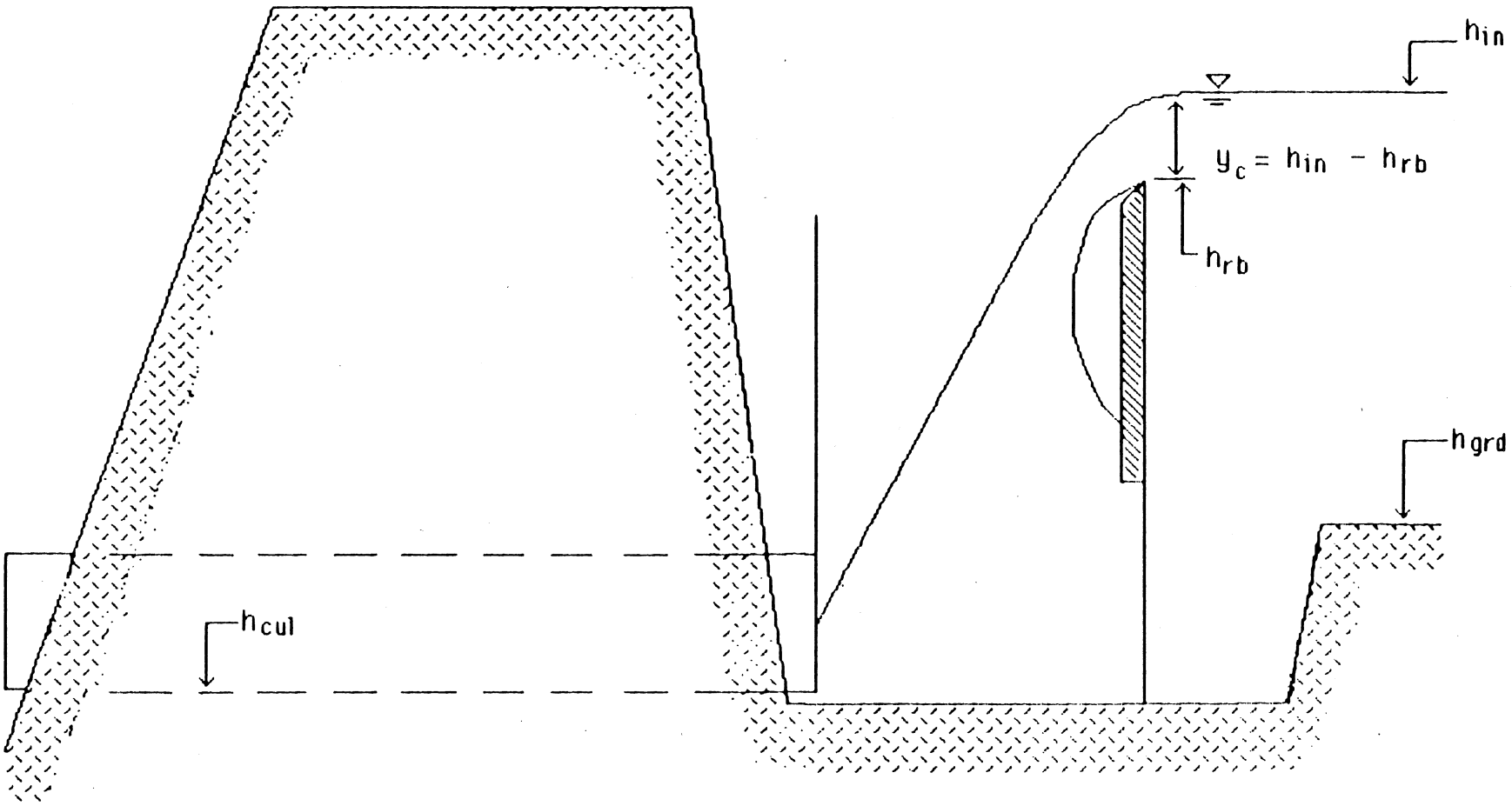

Figure 4-33. Flow over riser board attached to culvert.

Structure of Simulation Model

The program run used to calibrate the simulation model, the 39-day Period C with four-hour time steps, is used in this section to explain the structure and summarize the calculations of the model. Constants and parameters used by the model are listed in Table 4-13. Once calibrated to the values shown for Period C, all remained constant for all model runs with the exceptions of time step (DT), flapgate on/off toggle (FPG), riser elevation (HRB), and riser width (RW). Upon altering any of these and recalculating the spreadsheet, the new summary statistics and hydrograph are immediately available.

To prepare the model, all parameters and constants are entered as shown in Table 4-13. Table 4-14 is a printout of a portion of the calibration run with column letters and row numbers as they appear in the spreadsheet. Column A contains the serial dates (not shown), which may be generated by a Data Fill command. Columns E-H and column AC are input data, generally brought into the worksheet using 1-2-3's File Import for an ASCII file or File Combine for another 1-2-3 file. Columns B-D and columns I-AB contain all necessary calculations in their top row (row 17); this row is copied down the required number of time steps and the worksheet recalculated. Finally, each statistic in the summary of results table must be checked to be certain its input range includes the entire period.

A row by row, column by column description for periods i-1 and i is presented next, summarizing each calculation as follows: a) mathematical notation as developed earlier in this chapter; b) spreadsheet notation using spreadsheet variable names; and c) spreadsheet notation using cell references (except for constants, whose names will continue to be used

Table 4-13. Hydrodynamic simulation constants and parameters for calibration run.

Impoundment and Model Constants

HGRD	Average elevation, inches NGVD	=	7.68
AREA	Area, acres	=	50.0
A	Stage-volume coefficient	=	0.0109
B	Stage-volume exponent	=	0.3597
C	Stage-volume coefficient 2	=	-0.563
D	Stage-volume exponent 2	=	5.05E-06
DT	Model timestep, seconds	=	14400

Hydrologic Parameters

ETMAX	Maximum ET coefficient	=	1.00
ETRATE	Water table drop ET coefficient	=	0.00
FRATE	Infiltration coefficient	=	0.00
RST	Resistance coefficient	=	0.690

Water Control Structures

	CULVERT NUMBER	=	1
PD1	Diameter, feet	=	1.5
HCUL1	Elevation, inches	=	-5.3
PL1	Length, feet	=	22.3
PN1	Manning's n	=	0.024
LMS1	PL1*(1.486/PN1)^-2	=	0.0058
ZETA1	Sum of local loss coefficients	=	1.78
FPG1	Flapgate on (=1) or off (=0)	=	0
HRB1	Riser board elevation, inches NGVD*	=	100.00
RW1	Riser width, feet	=	0.00
	CULVERT NUMBER	=	2
PD2	Diameter, feet	=	1.5
HCUL2	Elevation, inches	=	-9.6
PL2	Length, feet	=	39.4
PN2	Manning's n	=	0.024
LMS2	PL2*(1.486/PN2)^-2 (self-calculating)	=	0.0103
ZETA2	Sum of local loss coefficients	=	1.78
FPG2	Flapgate on (=1) or off (=0)	=	0
HRB2	Riser board elevation, inches NGVD*	=	100.00
RW2	Riser width, feet	=	0.00

*Set at 100 for no riser board.

Water Control Operations

PR	Pump rate, cfs	=	
PT	Minimum pumping time, hours	=	

Table 4-14. Hydrodynamic simulation spreadsheet model.

	B	C	D	E	G	H	I	J	K	L	M	N	O	P	Q	R	S	T	U	V	W	X	Y	Z	AA	AB	AC
1																											
2	FILENAME			:		SIMCOAT																					
3	IMPOUNDMENT ID:					IRC-12																					
4	PERIOD MODELED:					11/26/84 - 01/05/85 (Period C)																					
5	RUN DESCRIP			:		Calibration run; uses tidal data.																					
6						39 days, 4-hr timesteps.																					
7																											
8																											
9								Culvert 1						Culvert 2													
10					Pan Evap																						
11				HOUT,	E,	P,	DH,	THETA,	PA,	PV, s^2	QIN,	QOUT,	QR,	THETA,	PA,	PV, s^2	QIN,	QOUT,	QR,	QNET,	WA, frac-	ET,	Infil F,	dV, 1000	Cum V, 1000	Calc HIN,	Meas HIN,
12	Mo	Day	Hr	in	in	in	ft	rad	ft^2	/ft^5	cfs	cfs	cfs	rad	ft^2	/ft^5	cfs	cfs	cfs	in	tion	in	in	ft^3	ft^3	in	in
13																											
14																											
15																											
16	11	27	0																						3117	23.06	23.06
17	11	27	4	17.68	0.00	0.00	-0.4	3.1	1.8	0.016	0.0	6.9	0.0	3.1	1.8	0.021	0.0	6.0	0.0	-1.0	0.93	0.00	0.00	-186	2931	22.32	22.33
18	11	27	8	13.38	0.00	0.00	-0.7	3.1	1.8	0.016	0.0	8.9	0.0	3.1	1.8	0.021	0.0	7.7	0.0	-1.3	0.93	0.00	0.00	-240	2690	21.48	21.18
19	11	27	12	19.32	0.02	0.00	-0.1	3.1	1.8	0.016	0.0	3.7	0.0	3.1	1.8	0.021	0.0	3.2	0.0	-0.6	0.92	0.02	0.00	-104	2586	21.10	20.38
20	11	27	16	20.35	0.02	0.00	-0.1	3.1	1.8	0.016	0.0	2.6	0.0	3.1	1.8	0.021	0.0	2.2	0.0	-0.4	0.92	0.02	0.00	-74	2512	20.83	20.35
21	11	27	20	13.56	0.02	0.00	-0.6	3.1	1.8	0.016	0.0	8.1	0.0	3.1	1.8	0.021	0.0	7.0	0.0	-1.2	0.92	0.02	0.00	-221	2292	19.97	19.45
22	11	28	0	16.48	0.00	0.00	-0.3	3.1	1.8	0.016	0.0	5.6	0.0	3.1	1.8	0.021	0.0	4.8	0.0	-0.8	0.92	0.00	0.00	-150	2142	19.36	18.57
23	11	28	4	15.88	0.00	0.00	-0.3	3.1	1.8	0.016	0.0	5.6	0.0	3.1	1.8	0.021	0.0	4.8	0.0	-0.8	0.92	0.00	0.00	-150	1992	18.72	17.98
24	11	28	8	10.95	0.00	0.00	-0.6	2.7	1.7	0.015	0.0	8.5	0.0	3.1	1.8	0.021	0.0	7.2	0.0	-1.2	0.92	0.00	0.00	-226	1765	17.70	17.02
25	11	28	12	16.10	0.04	0.00	-0.1	3.1	1.8	0.016	0.0	3.8	0.0	3.1	1.8	0.021	0.0	3.3	0.0	-0.6	0.92	0.04	0.00	-108	1657	17.18	16.27
26	11	28	16	19.54	0.04	0.00	0.2	3.1	1.8	0.016	2.0	0.0	0.0	3.1	1.8	0.021	1.7	0.0	0.0	0.3	0.92	0.04	0.00	46	1703	17.40	16.76
27	11	28	20	14.65	0.04	0.00	-0.2	3.1	1.8	0.016	0.0	5.0	0.0	3.1	1.8	0.021	0.0	4.3	0.0	-0.7	0.92	0.04	0.00	-140	1563	16.71	16.44
28	11	29	0	15.51	0.00	0.00	-0.1	3.1	1.8	0.016	0.0	3.3	0.0	3.1	1.8	0.021	0.0	2.8	0.0	-0.5	0.91	0.00	0.00	-88	1475	16.25	15.68
29	11	29	4	17.77	0.00	0.00	0.1	3.1	1.8	0.016	1.6	0.0	0.0	3.1	1.8	0.021	1.4	0.0	0.0	0.2	0.91	0.00	0.00	42	1518	16.48	15.89
30	11	29	8	14.43	0.00	0.00	-0.2	3.1	1.8	0.016	0.0	4.3	0.0	3.1	1.8	0.021	0.0	3.7	0.0	-0.6	0.91	0.00	0.00	-115	1403	15.87	15.52
31	11	29	12	15.37	0.02	0.00	.0	3.1	1.8	0.016	0.0	2.1	0.0	3.1	1.8	0.021	0.0	1.8	0.0	-0.3	0.91	0.02	0.00	-61	1342	15.53	14.86
32	11	29	16	20.86	0.02	0.00	0.4	3.1	1.8	0.016	3.0	0.0	0.0	3.1	1.8	0.021	2.6	0.0	0.0	0.4	0.91	0.02	0.00	75	1417	15.94	15.22
33	11	29	20	17.68	0.02	0.00	0.1	3.1	1.8	0.016	1.7	0.0	0.0	3.1	1.8	0.021	1.5	0.0	0.0	0.2	0.91	0.02	0.00	41	1458	16.16	15.86
34	11	30	0	14.81	0.00	0.00	-0.1	3.1	1.8	0.016	0.0	3.5	0.0	3.1	1.8	0.021	0.0	3.0	0.0	-0.5	0.91	0.00	0.00	-93	1365	15.66	15.32
35	11	30	4	18.54	0.00	0.00	0.2	3.1	1.8	0.016	2.2	0.0	0.0	3.1	1.8	0.021	1.9	0.0	0.0	0.3	0.91	0.00	0.00	58	1423	15.98	15.41
36	11	30	8	15.68	0.00	0.00	.0	3.1	1.8	0.016	0.0	1.6	0.0	3.1	1.8	0.021	0.0	1.4	0.0	-0.2	0.91	0.00	0.00	-43	1380	15.74	15.42
37	11	30	12	13.68	0.03	0.00	-0.2	3.1	1.8	0.016	0.0	4.3	0.0	3.1	1.8	0.021	0.0	3.7	0.0	-0.6	0.91	0.03	0.00	-121	1258	15.05	14.65
38	11	30	16	18.90	0.03	0.00	0.3	3.1	1.8	0.016	2.5	0.0	0.0	3.1	1.8	0.021	2.2	0.0	0.0	0.4	0.91	0.03	0.00	61	1320	15.40	14.75
39	11	30	20	16.23	0.03	0.00	0.1	3.1	1.8	0.016	1.2	0.0	0.0	3.1	1.8	0.021	1.0	0.0	0.0	0.2	0.91	0.03	0.00	25	1345	15.55	15.15

rather than cell addresses). In some cases variable nomenclature for spreadsheet usage has been modified slightly from that which appears in the mathematical notation.

A spreadsheet usage note: In first preparing a model such as this, the calculation is first typed in and edited as text, using the variable names as shown in the following example for the DV calculation in Column Z:

(QNET+P-ET-F)*43560*$AREA/12/1000

This expression is preceded with a label prefix to indicate that a string follows. Cells containing constants as listed in Table 4-13 are named using 1-2-3's \Range Name Create, e.g. the cell where the impoundment area is input has been named AREA. Constants are preceded with a dollar sign ($), indicating a cell whose address is absolute, rather than relative; that is, in copying down a calculation, the row number should not change. Next the first cell in each column is named with the column heading name; in this example, the first cells (in Row 17) of columns V, H, X, Y and Z are named QNET, P, ET, F, and DV. The string expression, placed above the table area (Row 15) is copied down to the first row of the table area (Row 17). It is then edited to remove the label prefix, and the resulting calculation shows the range names for the first row. This technique aids greatly in a) entering and editing expressions, b) documentation (using \Range Transpose across Row 15 creates a convenient table of calculations that may be placed elsewhere in the spreadsheet) and c) debugging. Upon completion this row may be formatted as "hidden" to improve the table's appearance. In cases where calculations depend upon values obtained in the preceding timestep,

range names will be spread over the first two rows of the table, as will be seen below.

Row 16 (Period i-1)

Column A--Serial Date. Constant interval time t_i, in decimal portion of a day. Generated with \Data Fill.

Column B--Month. Uses the @month(serial date) function to return month of the year (1-12):

```
month = @month(A16)
```

Column C--Day. Uses the @day(serial date) function to return day of the month (1-31):

```
day   = @day(A16)
```

Column D--Hour. Uses the @hour(serial date) function to return hour of the day (0-23):

```
hour  = @hour(A16)
```

Column AA--Cumulative Volume CUM V. Total impoundment volume, 1000 ft^3. Initial volume for simulation estimated by rearranging stage-volume function (equation 4-8) to solve for volume using initial stage from next column:

```
Cum V = @if(HIN/12<0.474,
          (HIN/12-$C)/$D,
          ((HIN/12)/$A)^(1/$B))/1000

      = @if(AB16/12<0.474,
          (AB16/12-$C)/$D,
          ((AB16/12)/$A)^(1/$B))/1000
```

Column AB--Calculated Stage HIN. Initial estimate of impoundment stage h_{in}, inches NGVD, (elevation of water surface in perimeter ditch at south culvert). For these runs obtained from known stage in adjacent column:

Init HIN = +AC16

Column AC--Measured Stage HIN. Impoundment stage h_{in}, inches NGVD, measured in perimeter ditch at south culvert. Imported from data file where raw data was interpolated for desired time steps. For comparison only; not used in calculations with the exception of providing the initial entry in column AB.

Row 17 (Period i)

Column A--Serial Date. A continuation of the \Data Fill operation begun in row 16.

Column B--Month. Copied down from row 16.

Column C--Day. Copied down from row 16.

Column D--Hour. Copied down from row 16.

Column E--Measured HOUT. Tidal elevation h_{in} at time t_i, inches NGVD, measured in the Indian River Lagoon outside south culvert. Imported from data file where raw data was interpolated for desired time steps. Not utilized in runs using tidal model.

Column F--Tidal Model HOUT (not shown). Tidal elevation h_{out}, inches NGVD, generated by tidal model. Values imported from data file

where these were calculated for each time step using harmonic constants. Not utilized in runs using tidal data, as in this example.

Column G--Pan Evaporation PE. Four-hour pan evaporation PE, inches, for the indicated interval if daylight hours; imported from data file where these were calculated for each time step.

Column H--Precipitation P. Four-hour precipitation P_4, inches, for the indicated interval; imported from data file where these were calculated for each time step.

Column I--DH. Head difference ΔH, inches, between impoundment and estuary water levels (equation 4-32):

$$\Delta H_i = (h_{out.i} - h_{in.i-1})$$

$$= (HOUT-HIN)/12$$

$$= (E17-AB16)/12$$

Column J--THETA. Angle θ, radians, formed by water surface in partially-filled culvert (equation 4-31):

$$\theta_i = \cos^{-1}\{1-[\min(D,h_{in.i-1}-h_{cul})+ \min(D,h_{out.i}-h_{cul})]/D\}$$

$$= @acos(1-(@min(\$PD1*12,HIN-\$HCUL1)+ @min(\$PD1*12,HOUT-\$HCUL1))/(\$PD1*12))$$

$$= @acos(1-(@min(\$PD1*12,AB16-\$HCUL1)+ @min(\$PD1*12,E17-\$HCUL1))/(\$PD1*12))$$

Column K--Pipe area PA. Cross-sectional water area A, ft^2, of culvert (equation 4-29):

$$A_i = (D^2/4)(\theta_i - \cos\theta_i \sin\theta_i)$$

$$= \$PD1\hat{}2/4*(THETA1-@cos(THETA1)*@sin(THETA1))$$

= $PD^2/4*(J17)*@sin(J17))

Column L--P-value PV. Characteristic pipe value P_v, sec^2/ft^5 (equation 4-30):

$$P_{v.i} = LM^{-2}(\theta_i D)^{4/3} A_i^{-10/3}) + \Sigma\zeta A^{-2}/(2g)$$

To minimize computer memory usage, the following calculation is made outside the model in the water control structure parameters table producing a 1-2-3 variable called "LMS":

$$LMS = LM^{-2}$$

thus,

$$P_v = \$LMS*(THETA*\$PD)^1.333*PA^-3.333+\$ZETA*PA^-2/64.348$$

$$= \$LMS*(J17*\$PD)^1.333*K17^-3.333+\$ZETA*K17^-2/64.348$$

Column M--QIN. Culvert flow into impoundment Q_{in}, ft^3/sec (equation 4-33):

$$Q_{in.i} = \begin{cases} |\Delta H_i - R_{st}\Delta H_i|^{1/2}/P_{v.i} & ; \ \Delta H_i > 0 \\ 0 & ; \ \Delta H_i \leq 0 \end{cases}$$

= @if(DH>0,@sqrt(@abs(DH-DH*$RST)/PV),0)

= @if(I17>0,@sqrt(@abs(I17-I17*$RST)/L17),0)

Column N--QOUT. Culvert flow out of impoundment Q_{out}, ft^3/sec (equation 4-34):

$$Q_{out.i} = \begin{cases} |\Delta H_i + R_{st}\Delta H_i|^{1/2}/P_{v.i} & ; \ \Delta H_i < 0 \text{ and } FPG = 1 \\ 0 & ; \ \Delta H_i \geq 0 \text{ or } FPG = 0 \end{cases}$$

= @if(DH<0#and#$FPG=0,@sqrt(@abs(DH+DH*$RST)/PV),0)

= @if(I17<0#and#$FPG=0,@sqrt(@abs(I17+I17*$RST)/L17),0)

Column O--QR. Flow over flapgate riser Q_r, ft^3/sec (equation 4-35):

$$Q_{r.i} = 0.5761 g^{1/2} bmax(h_{in.i-1} - h_{rb}, 0)^{3/2}$$

$$= 0.5761*5.672*\$RW*@max(0,(HIN-\$HRB)/12)\hat{}1.5$$

$$= 0.5761*5.672*\$RW*@max(0,(AB16-\$HRB)/12)\hat{}1.5$$

Columns P-U. Repeat Columns J-O for each culvert.

Column V--QNET. Sum of culvert and riser inflows and outflows reported as total volume over period in inches:

$$QNET = (QIN1+QIN2-QOUT1-QOUT2-QR1-QR2)*\$DT*12/(43560*\$AREA)$$

$$= (M17+S17-N17-T17-017-U17)*\$DT*12/(43560*\$AREA)$$

Column W--Water area WA. Fraction of water area over total marsh area (equation 4-1):

$$A_i = \begin{cases} ah_{i-1}+b \; ; \; h_{i-1} < h_1 \\ ch_{i-1}+d \; ; \; h_1 \leq h_{i-1} < h_2 \\ eh_{i-1}+f \; ; \; h_2 \leq h_{i-1} < h_3 \\ gh_{i-1}+i \; ; \; h_{i-1} \geq h_3 \end{cases}$$

$$= @if(HIN<=5.40,0.393*HIN+9.02,$$
$$@if(HIN<=7.20,18.063*HIN-87.69,$$
$$@if(HIN<=12.00,9.450*HIN-23.14,$$
$$0.208*HIN+88)))/100$$

$$= @if(AB16<=5.40,0.393*AB16+9.02,$$
$$@if(AB16<=7.20,18.063*AB16-87.69,$$
$$@if(AB16<=12.00,9.450*AB16-23.14,$$
$$0.208*AB16+88)))/100$$

Column X--Evapotranspiration ET. Four-hour evapotranspiration ET, inches (equation 4-23):

$$ET_i = (ETMAX)PE_i)A_i +$$
$$[ETMAX-ETRATE(h_{grd}-h_{i-1})]PE_i(1-A_i)$$

= ($ETMAX*WA+
($ETMAX-$ETRATE*@max(0,$HGRD-HIN))*(1-WA))*E

= ($ETMAX*W17+
($ETMAX-$ETRATE*@max(0,$HGRD-AB16))*(1-W17))*G17

Column Y--Infiltration F. Four-hour infiltration F, inches (equation 4-24):

$$F = (FRATE)\max(h_{grd}-h_{out.i}),0)A_i$$

= $FRATE*(@max($HGRD-HOUT,0)*WA

= $FRATE*(@max($HGRD-E17,0)*W17

Column Z--DV. Net change in volume over period i, 1000 ft^3, by summing all inflows and outflows:

DV = (QNET+P-ET-F)*43560*$AREA/12/1000

= (V17+H17-X17-Y17)*43560*$AREA/12/1000

Column AA--Cumulative volume. Each cell adds the change in volume for period i to the cumulative volume from period i-1:

Cum V = @max(0,V+DV)

= @max(0,AA16+Z17)

Column AB--Calculated HIN. Calculated impoundment stage h_{in}, inches NGVD, (elevation of water surface in perimeter ditch at south culvert). From equation 4-8:

$$h_i = \begin{cases} aV_i+b & ; V_i < V_{crit} \\ cV_i^d & ; V_i \geq V_{crit} \end{cases}$$

= @if(V<204.820,($A+$B*V*1000)*12,
($C*(V*1000)^$D)*12)

```
= @if(AA17<204.820,($A+$B*V*1000)*12,
  ($C*(AA17*1000)^$D)*12)
```

Column AC--Measured HIN. A continuation of input data set for comparison, if available.

Calibration of Simulation Model

The choices of three short (approximately 40-day) modeling periods A, B, and C along with a one-year modeling period for simulation runs were detailed earlier in this chapter under Selection of Study Periods and Time Steps. This section also explained the choice of period C, a 39-day span from 11/26/84 to 01/05/85, for the calibration run.

Table 4-15 shows the complete model summary area for this calibration run, which consists of the following groups: 1) impoundment and model constants, 2) hydrologic parameters, 3) simulation results, and 4) variables describing water control structures and operations. Groups (1), (2), and (4) are input variables, as first listed in Table 4-13; Group (3) summarizes the output.

Calibration was performed by varying the hydrologic parameters while monitoring both the output summary comparing predicted and actual stages and screen graphics superimposing these two time series. The simulation for this period required approximately twenty seconds of recalculation time upon entering a changed parameter; the statistics and graphics are generated automatically. Actual measurements of tidal height in the estuary over the period were used.

A close match of the predicted and actual stages was obtained (Figure 4-34) with the hydrologic parameters shown in Table 4-15. The simplest case proved to offer the closest approximations, where the

Table 4-15. Simulation input/output summary for Period C calibration run.

FILENAME : SIMCDAT
IMPOUNDMENT ID: IRC-12
PERIOD MODELED: 11/26/84 - 01/05/85 (Period C)
RUN DESCRIP : Calibration run; uses tidal data. 39 days, 4-hr timesteps.

Impoundment and Model Constants

HGRD	Average elevation, inches NGVD	=	7.68
AREA	Area, acres	=	50.0
A	Stage-volume coefficient	=	0.0109
B	Stage-volume exponent	=	0.3597
C	Stage-volume coefficient 2	=	-0.563
D	Stage-volume exponent 2	=	5.05E-06
DT	Model timestep, seconds	=	14400

Hydrologic Parameters

ETMAX	Maximum ET coefficient	=	1.00
ETRATE	Water table drop ET coeff	=	0.00
FRATE	Infiltration coefficient	=	0.00
RST	Resistance coefficient	=	0.690

Simulation Results

Predicted Water Levels (HIN), inches

			Predicted	Actual
	Mean	=	9.5	9.5
	Std	=	3.8	3.5
	Max	=	22.3	22.3
	Min	=	0.9	0.8

Summary of Inflows/Outflows and Continuity Check, inches

QIN1	Culvert 1 in	=	21.8
QOUT1	Culvert 1 out	=	28.2
QR1	Riser 1 out	=	0.0
QIN2	Culvert 2 in	=	20.8
QOUT2	Culvert 2 out	=	28.7
QR2	Riser 2 out	=	0.0
QNET	Net discharge in	=	-14.4
P	Precipitation	=	2.3
ET	Evapotranspiration	=	3.8
	Infiltration	=	0.0
	QNET+P-ET-F	=	-15.8
	dS/dt	=	-15.8

Table 4-15--continued.

FILENAME : SIMCDAT
IMPOUNDMENT ID: IRC-12
PERIOD MODELED: 11/26/84 - 01/05/85 (Period C)
RUN DESCRIP : Calibration run; uses tidal data.
39 days, 4-hr timesteps.

Water Control Structures and Operations

Structures

	CULVERT NUMBER	=	1
PD1	Diameter, feet	=	1.5
HCUL1	Elevation, inches	=	-5.3
PL1	Length, feet	=	22.3
PN1	Manning's n	=	0.024
LMS1	PL1*(1.486/PN1)^-2	=	0.0058
ZETA1	Sum of local loss coefficients	=	1.78
FPG1	Flapgate on (=1) or off (=0)	=	0
HRB1	Riser board elevation, inches NGVD*	=	100.00
RW1	Riser width, feet	=	0.00
	CULVERT NUMBER	=	2
PD2	Diameter, feet	=	1.5
HCUL2	Elevation, inches	=	-9.6
PL2	Length, feet	=	39.4
PN2	Manning's n	=	0.024
LMS2	PL2*(1.486/PN2)^-2	=	0.0103
ZETA2	Sum of local loss coefficients	=	1.78
FPG2	Flapgate on (=1) or off (=0)	=	0
HRB2	Riser board elevation, inches NGVD*	=	100.00
RW2	Riser width, feet	=	0.00

*Set at 100 for no riser board.

Operations

PR	Pump rate, cfs	=
PT	Minimum pumping time, hours	=

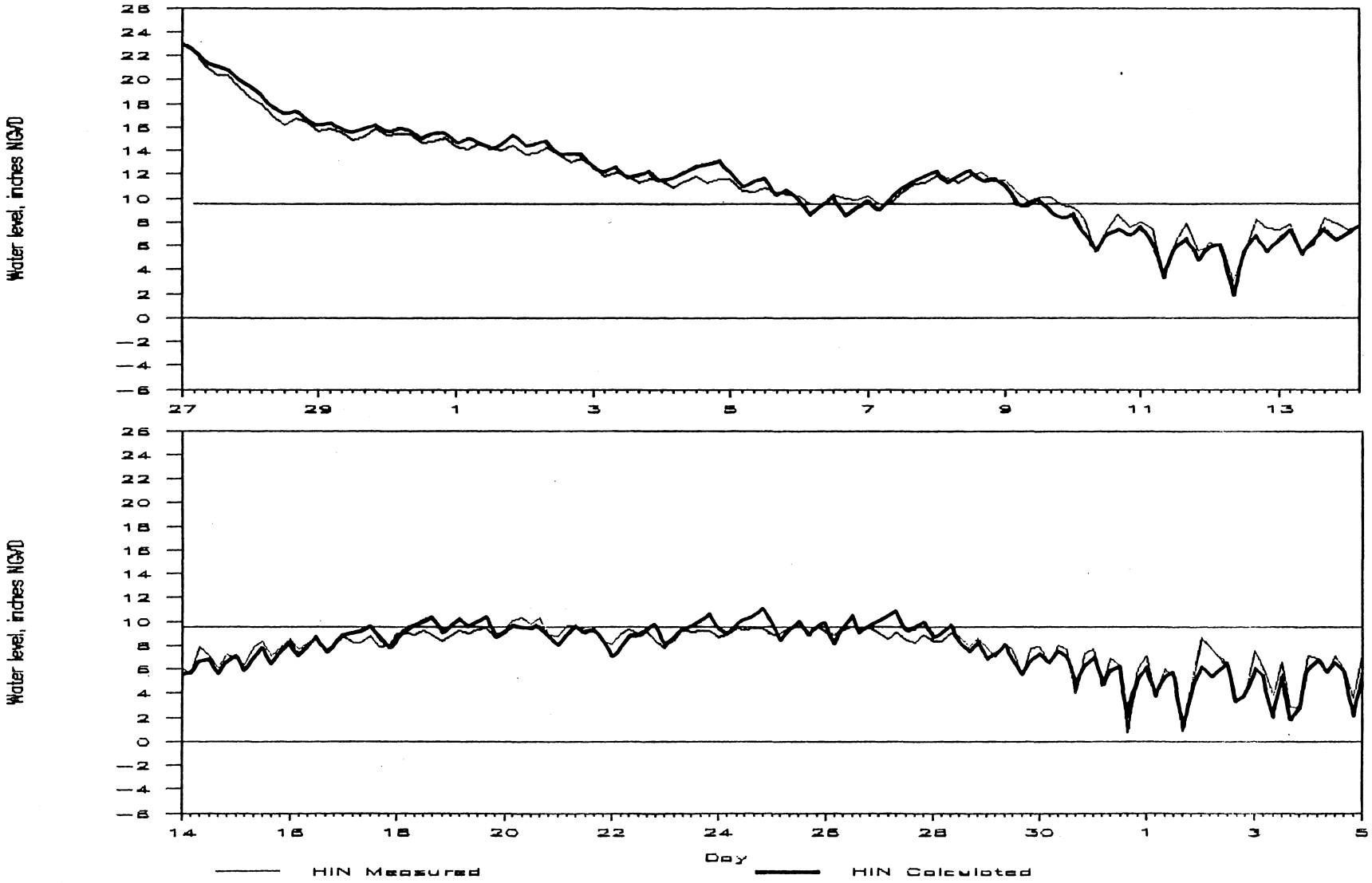

Figure 4-34. Simulated vs. measured IRC-12 stage for calibration period C (11/26/84-01/05/85) using tidal data.

infiltration and evapotranspiration coefficients were very small. Evapotranspiration at the impoundment is thus approximated here by unreduced pan evaporation measurements, while infiltration was determined to be neglible. A resistance coefficient of 0.690 was chosen.

Actual and predicted stages (HIN) over the period shared a mean of 9.5 inches NGVD and a maximum of 22.3 inches. Predicted minimum stage was 0.9 inches; virtually the same as the actual low of 0.8. Standard deviations were 3.8 for the predicted range of stages and 3.5 for the actual. The inflow/outflow summary gave the expected picture of an impoundment draining after the fall high tides with little winter rain. The sum of flows through the culverts was a net 14.4 inches discharged out of the impoundment into the estuary, with 3.8 inches of evapotranspiration and 2.3 inches of rainfall for the period. Diurnal and semidiurnal tidal fluctuations are not significant until the stage has dropped below about six inches NGVD, even then approaching a tidal range of only around five inches.

A continuity check calculated by summing the inflows and outflows and comparing with the change in storage over the entire period shows a balanced water budget with a net loss of 15.8 inches.

Simulation Results

Short Period Simulations using Tidal Data

Using the above calibration parameters and holding all other input variables constant, similar runs were performed for the other two short-term modeling periods, A and B. Output summaries for remaining simulation runs may be found in Appendix B, with only the hydrographs shown here.

Period A, a 42-day period during the unmanaged 1985 summer mosquito breeding season (06/24/85-08/04/85), showed low impoundment water levels with predicted and actual means of 4.2 and 3.9 inches respectively (Figure 4-35). Daily fluctuations are therefore more evident, but longer-period tidal variation overall is insignificant, with net flow into the impoundment totaling 0.6 inch. Rainfall (11.6 inches) and ET (10.5 inches) dominate, with rainfall events triggering the peaks seen in the hydrograph. The predicted maximum stage is approximately 3 inches greater than that recorded; this difference is most directly due to the significance of rainfall here and the higher rainfall recorded at the Vero Beach 4W climatological station than at the impoundment.

Water was trapped in the impoundment by flapgates during the managed summer of 1986; Period B (08/01/86-09/08/86) is a 39-day portion of this summer. The model input in Appendix B for this period shows a change in values for the water control structures and operations section: flapgates are set on, with riser board elevations and widths specified for each culvert. Water levels were maintained at high levels with no tidal influence (Figure 4-36); predicted and actual mean stages were 13.2 and 15.2 inches respectively. The summary of inflows and outflows shows that slightly more flow into the impoundment occurred through Culvert 1 (South Culvert), with spillage over the riser back into the estuary occurring only at this culvert. This is in accordance with observations made at the time. Combined flow into the impoundment was 10.2 inches, and outflow over the riser was 6.0 inches, resulting in a net inflow of 4.2 inches. Together with a similar inflow of 4.5 inches from rainfall, this balanced with ET loss of 7.3 inches to yield

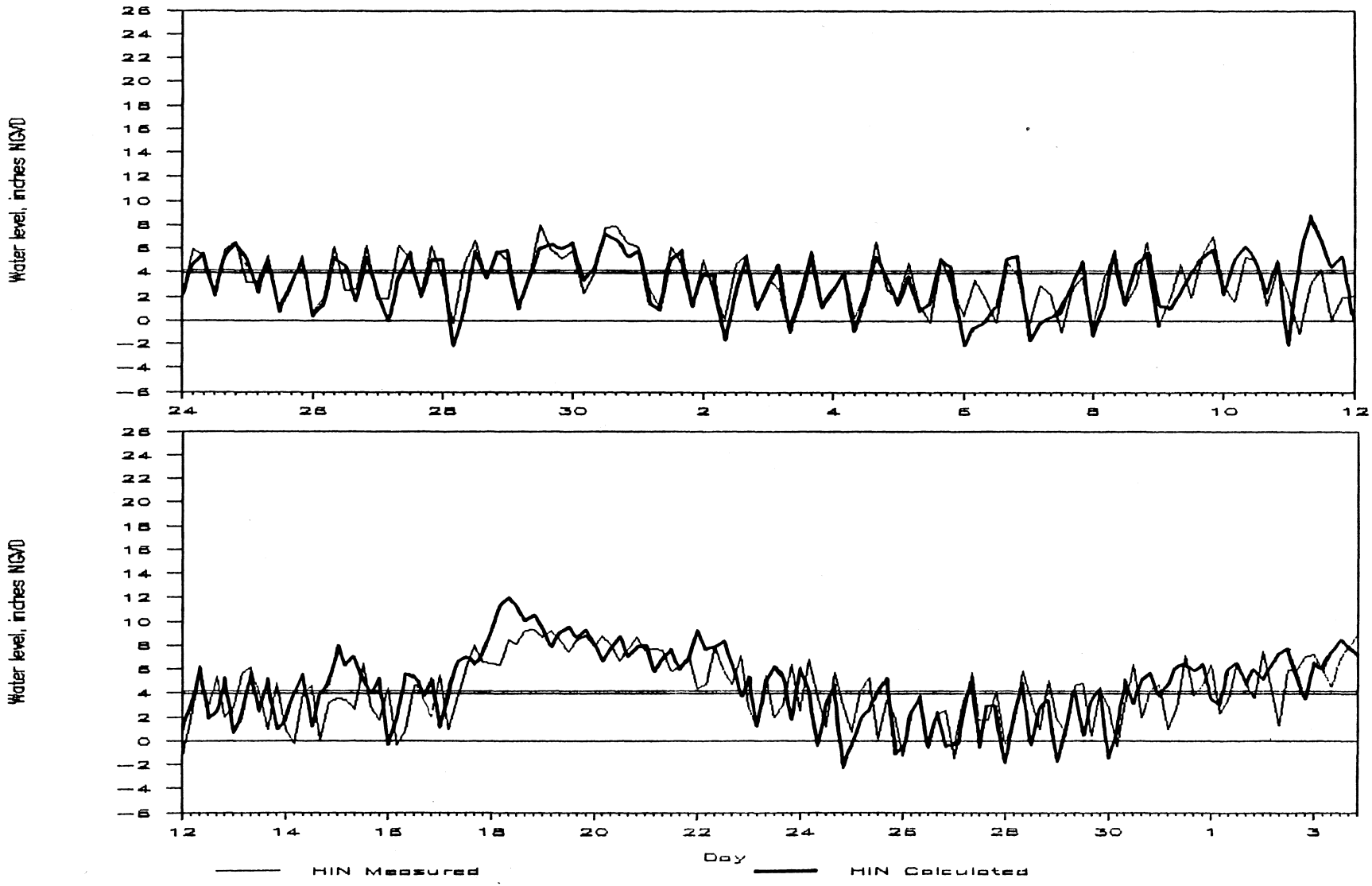

Figure 4-35. Simulated vs. measured IRC-12 stage for period A (06/24/84-08/04/85) using tidal data.

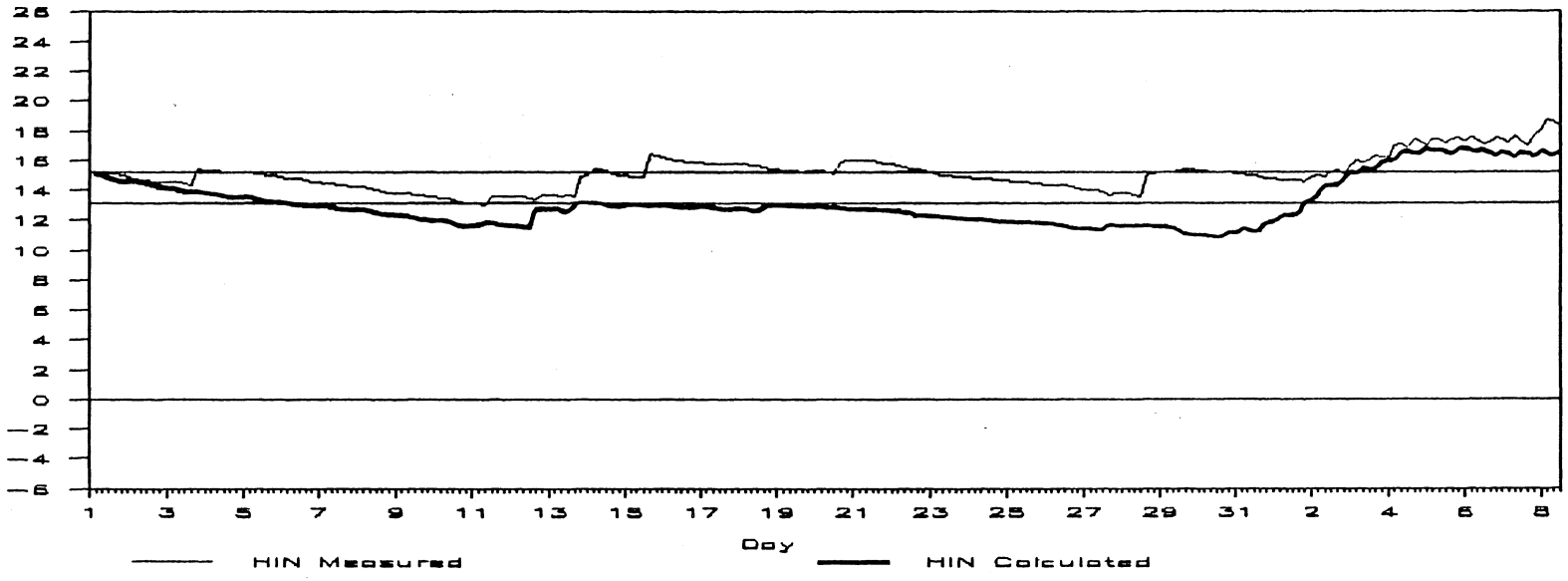

Figure 4-36. Simulated vs. measured IRC-12 stage for period B (08/01/86-09/08/86) using tidal data.

relatively constant water levels. The trend of slowly falling stage from ET and riser spillage, punctuated with rainfall peaks, is clearly evident. As before, differences in time and volume of rainfall events between Vero Beach 4W and IRC-12 prevent a more precise match.

Short Period Simulations using Tidal Model

As a major goal of this modeling process was to simulate one entire year, and even the best year of data (1985) had gaps in tidal observations amounting to approximately one-third of the year, a tidal model was required to produce this run. Impoundment stage observations were also incomplete for the year; thus additional assurance of the tidal model's reliability was sought through replacing the tidal data for Periods A, B, and C with the tidal model and comparing the results.

The results may be seen in Figures 4-37 through 4-39; though differences between the actual and predicted stage hydrographs are more pronounced, the tidal model seems to keep the simulation results within an acceptable range. The output summaries for these runs may be found in Appendix B.

Simulation of One Year using Tidal Model

Using the same methods and parameters as before, a year-long simulation was run employing the tidal model. 1985 was an entirely unmanaged year, so control structure variables were reset to indicate two permanently open culverts for the entire year with no pumping. Figure 4-40 shows the simulated hydrograph and the actual hydrograph where data were available. Summary statistics (Table 4-16) show a relatively good comparison; though hydrographs show a January peak missing from the

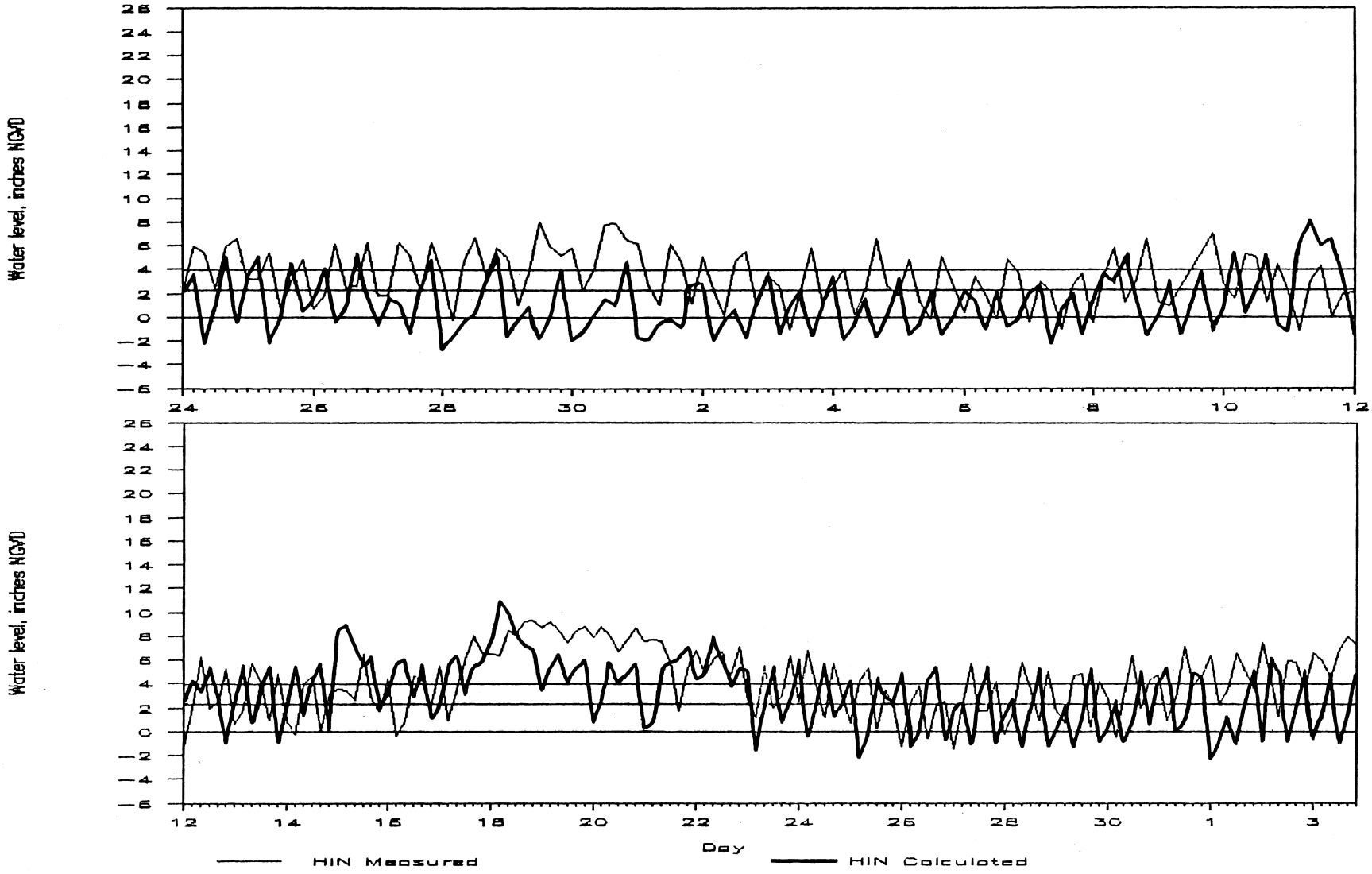

Figure 4-37. Simulated vs. measured IRC-12 stage for period A (06/24/85-08/04/85) using tidal model.

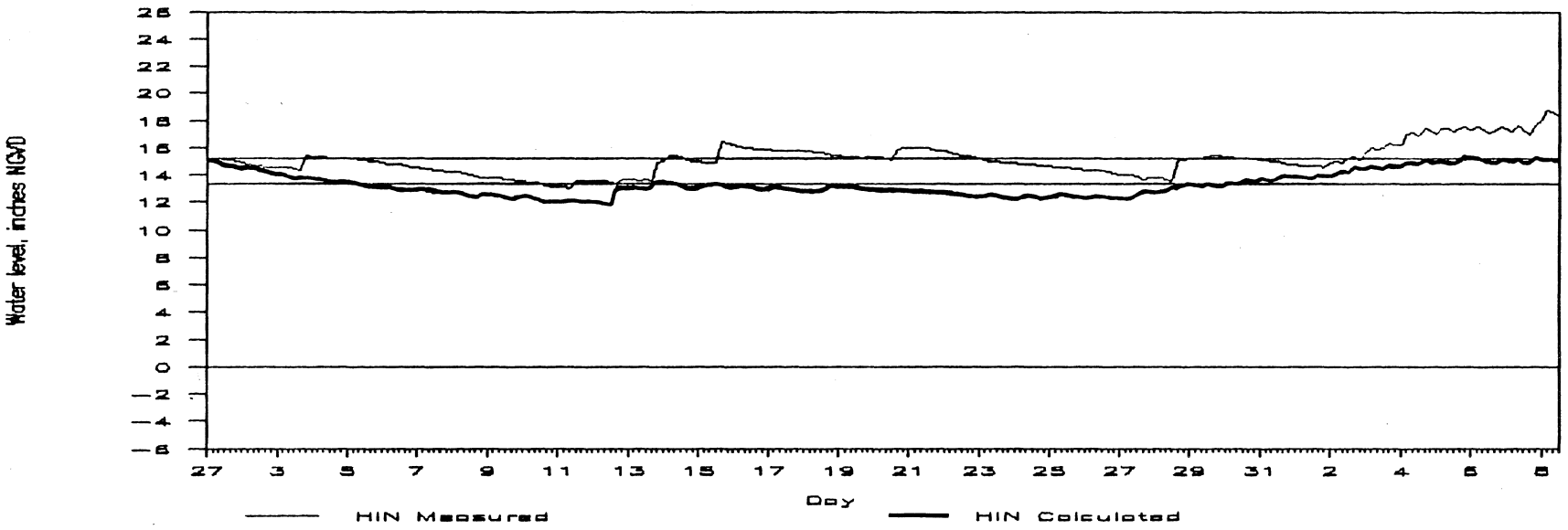

Figure 4-38. Simulated vs. measured IRC-12 stage for period B (08/01/86-09/08/86) using tidal model.

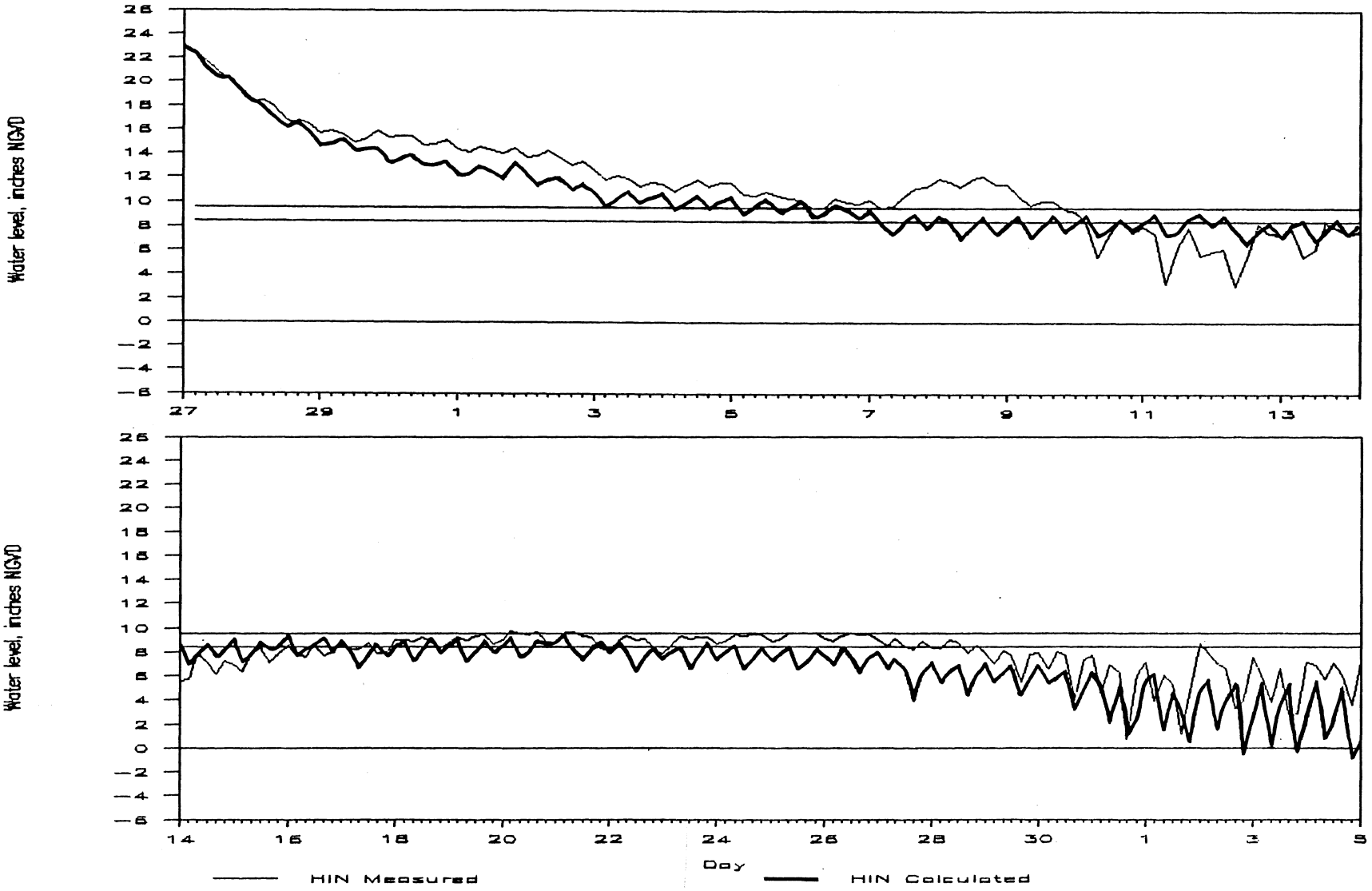

Figure 4-39. Simulated vs measured IRC-12 stage for period C (11/26/84-01/05/85) using tidal model.

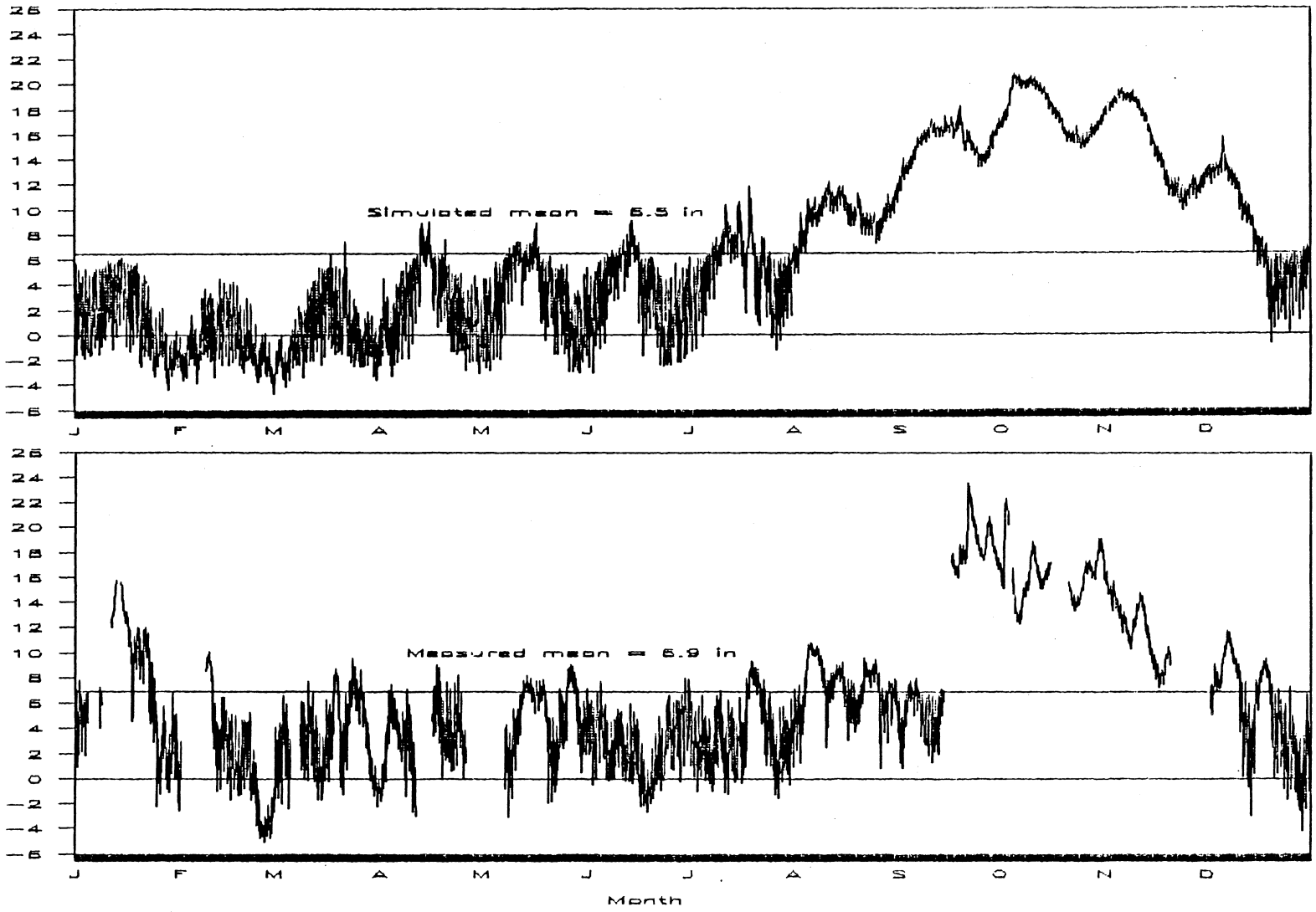

Figure 4-40. Simulated (top) and measured (bottom) IRC-12 stages for January-December 1985.

Table 4-16. Simulation input/output summary for January-December 1985.

FILENAME : SIMYRMOD
IMPOUNDMENT ID: IRC-12
PERIOD MODELED: Jan-Dec 1985
RUN DESCRIP : 365 day period, 8-hr timesteps. Uses tidal model, Vero Beach 4W precip and evap for 1985.

Impoundment and Model Constants

HGRD	Average elevation, inches NGVD	=	7.68
AREA	Area, acres	=	50.0
A	Stage-volume coefficient	=	0.0109
B	Stage-volume exponent	=	0.3597
C	Stage-volume coefficient 2	=	-0.563
D	Stage-volume exponent 2	=	5.05E-06
DT	Model timestep, seconds	=	14400

Hydrologic Parameters

ETMAX	Maximum ET coefficient	=	1.00
ETRATE	Water table drop ET coeff	=	0.00
FRATE	Infiltration coefficient	=	0.00
RST	Resistance coefficient	=	0.690

Simulation Results

Predicted Water Levels (HIN), inches

			Predicted	Actual
	Mean	=	1.8	3.9
	Std	=	2.7	4.5
	Max	=	9.2	15.6
	Min	=	-3.4	-4.9

Summary of Inflows/Outflows and Continuity Check, inches

QIN1	Culvert 1 in	=	18.6
QOUT1	Culvert 1 out	=	13.5
QR1	Riser 1 out	=	0.0
QIN2	Culvert 2 in	=	27.3
QOUT2	Culvert 2 out	=	21.7
QR2	Riser 2 out	=	0.0
QNET	Net discharge in	=	10.7
P	Precipitation	=	3.4
ET	Evapotranspiration	=	13.6
	Infiltration	=	0.0
	QNET+P-ET-F	=	0.5
	dS/dt	=	0.5

simulation. Annual predicted vs. actual means are 6.9 compared to 6.5 inches, standard deviations 6.7 to 5.6, maxima 20.8 to 23.5, and minima of -4.7 to -4.9. A more detailed summary giving additional annual statistics on key hydrologic components is presented in Table 4-17. Time series of input data for the year show the seasonal variations in ET, precipitation, and tides for 1985 (Figures 4-41 and 4-42). The simulated percent inundation or water area time series (Figure 4-43) is of particular interest in mosquito brood production.

Summary

Results of these simulation runs indicate that the model is sufficiently reliable to predict the study impoundment's response to a variety of management schemes. Within the constraints of two culverts at the stated locations, one may vary culvert dimensions, elevations, presence of flapgate risers, dimensions and elevations of riser boards. Within the obvious constraints of a one-dimensional model, the key limitation to this model as presented in this chapter is the neglect of isolated ponds. A method to remedy this problem will be given in the next chapter.

In order to extended this model to predict response to alternate culvert locations or to simulate a different impoundment entirely, it would be possible to add or subtract culverts as necessary to the existing model, or vary the impoundment specifications and tidal harmonic constants for a new impoundment. To maintain reliability, however, it would be necessary to establish new stage-area and stage-volume relationships. In the case of predicting response to the relocation or addition of a tidal connection where no data are available, an

Table 4-17. Summary of simulation results January-December 1985.

	ET, in	P, in	Meas HOUT, in	Tidal Model HOUT, in	Meas HIN, in	Calc HIN, in	WA, fraction	Culvert 1 QIN, cfs	Culvert 1 QOUT, cfs	Culvert 2 QIN, cfs	Culvert 2 QOUT, cfs
SUM	69.2	50.8	-	-	-	-	-	2587	2363	2843	2822
AVG	-	-	7.5	8.9	6.5	6.9	0.4	1.2	1.1	1.3	1.3
MAX	-	-	26.9	28.0	23.5	20.8	0.9	3.9	8.1	3.6	7.1
MIN	-	-	-3.2	-7.4	-4.9	-4.7	0.1	0.0	0.0	0.0	0.0
STD	-	-	5.7	7.3	5.6	6.7	0.4	1.2	1.7	1.2	1.9

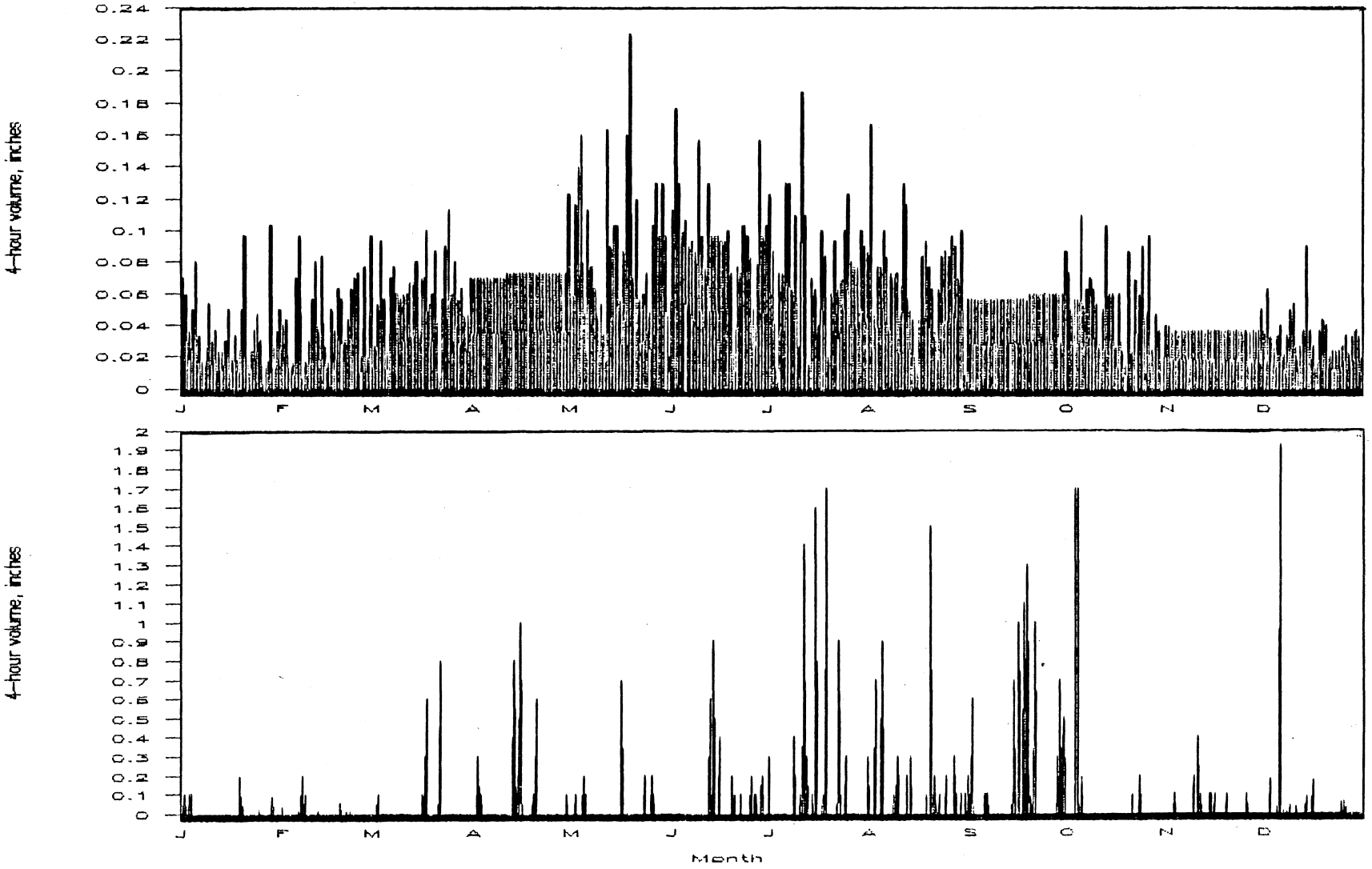

Figure 4-41. Four-hour evapotranspiration and precipitation model input estimates at IRC-12 for January-December 1985.

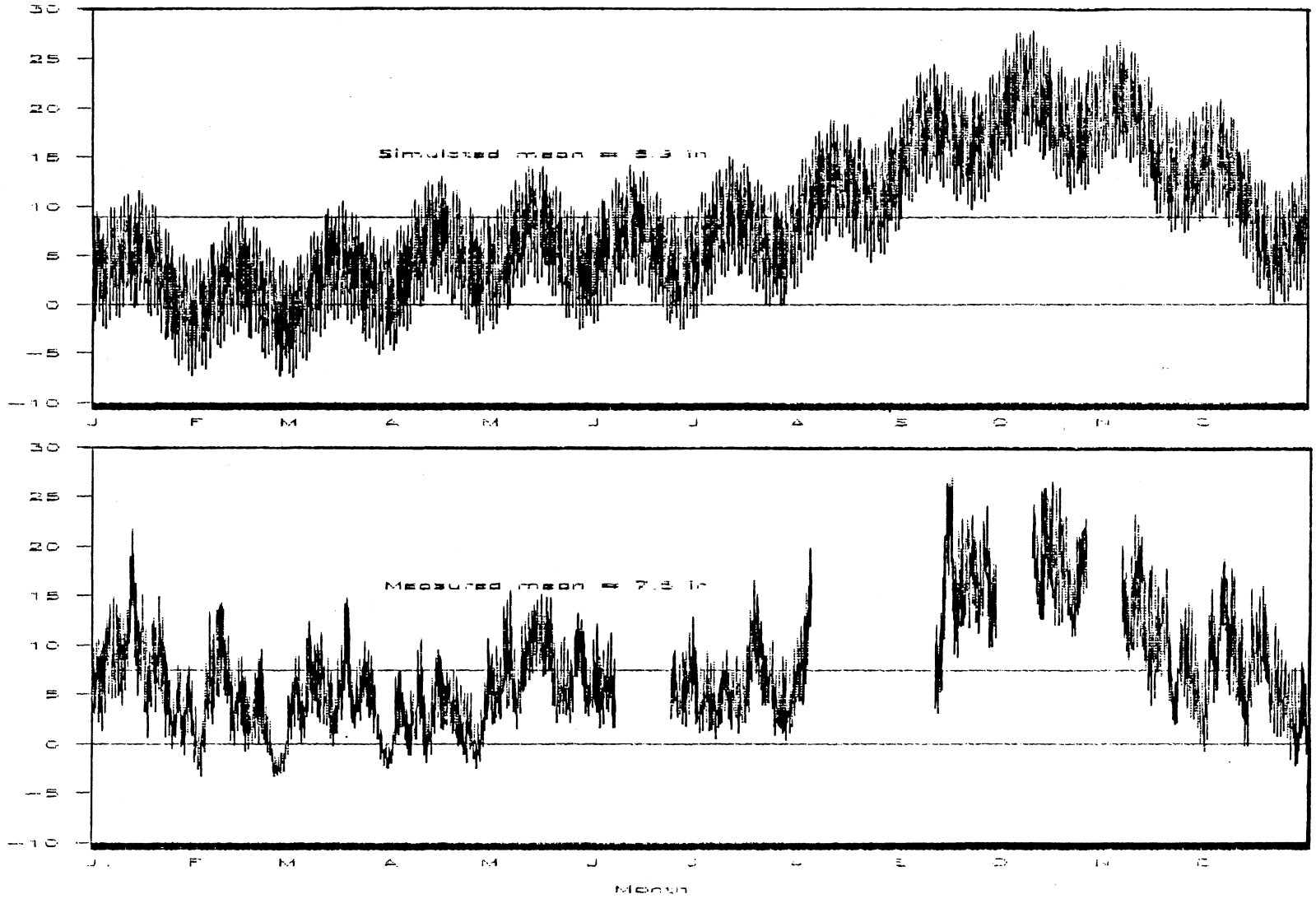

Figure 4-42. Tidal model (top) for simulation input and measured tidal height (bottom) of Indian River Lagoon at IRC-12 for January-December 1985.

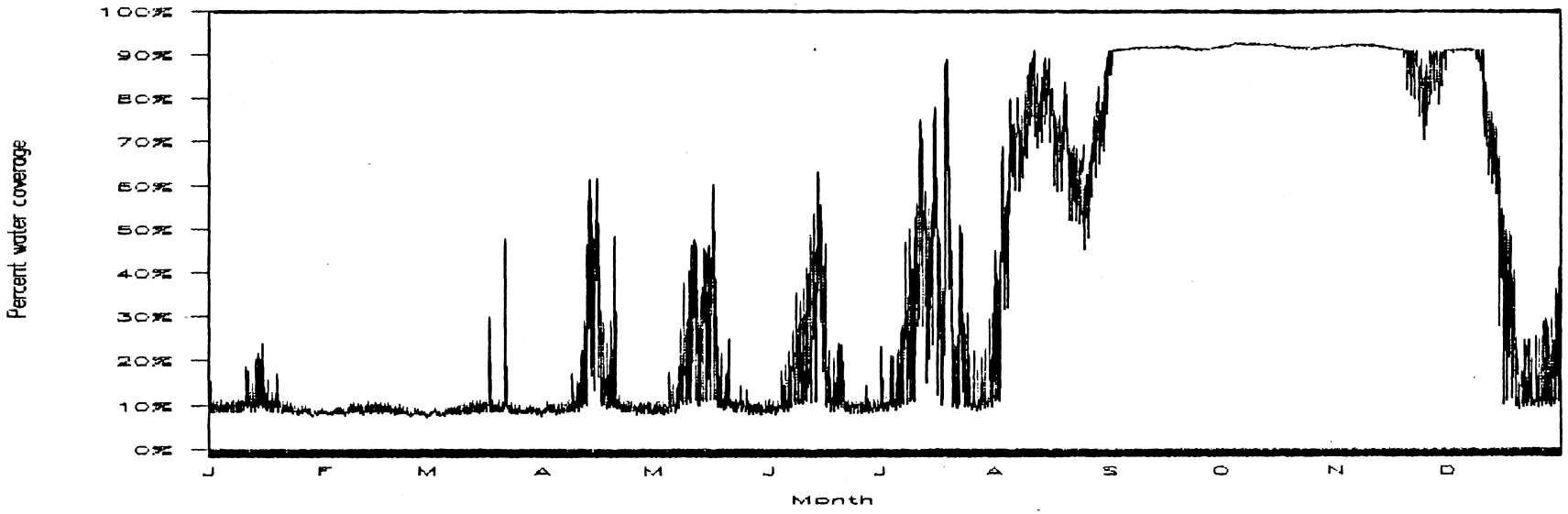

Figure 4-43. Simulated IRC-12 water area for January-December 1985.

additional modeling process is required which examines topography more closely. Without actually stepping over the boundary into the complexities of a two-dimensional model, a relatively simple additional process outlined in Chapter 6 can both generate predictive stage-area and stage-volume relationships, plus estimate the spatial distribution of water.

References

Bidlingmayer, W. L. and E. D. McCoy. 1978. An inventory of the salt-marsh mosquito control impoundments in Florida. Unpublished report to Fish and Wildlife Service, U. S. Department of the Interior.

Carlson, D. and P. O'Bryan. 1986. Impoundment management: mosquito sampling. Unpublished report. Indian River Mosquito Control District, Vero Beach, Florida.

Carlson, D. B. and R. R. Vigliano. 1984. Mosquito production in a salt marsh mosquito control impoundment under differing management regimes. Unpublished report. Indian River Mosquito Control District, Vero Beach, Florida.

Christensen, B. A. 1984. Analysis of partially filled circular storm sewers. Proceedings of Water for Resource Development, Hydraulics Division, American Society of Civil Engineers, New York, New York.

Fernald, E. A. and D. J. Patton, ed. 1984. Water resources atlas of Florida. Institute of Science and Public Affairs, Florida State University, Tallahassee, Florida.

Gilmore, R. G. 1984. Fish and macrocrustacean population dynamics in a tidally influenced impounded sub-tropical marsh. Unpublished report. Harbor Branch Foundation, Inc., Fort Pierce, Florida.

Gilmore, R. G. and D. J. Peters. 1986. Impoundment management: rotational management impoundment effects on fish, macrocrustacean and avian population dynamics and basic hydrological parameters. Unpublished report. Harbor Branch Oceanographic Institution, Fort Pierce, Florida.

Portier, K. M. 1981. Hydrologic information storage and retrieval system. University of Florida, Gainesville, Florida.

Rey, J. R., R. Crossman, T. Kain, S. Taylor, P. O'Bryan. 1986. Impoundment management: vegetation, zooplankton, and water quality. Unpublished report. Florida Medical Entomology Laboratory, Institute for Food and Agricultural Sciences, University of Florida, Vero Beach, Florida.

Rey, J. R., T. Kain, R. Crossman, F. Vose, and F. Perez. 1984. Zooplankton and marsh vegetation in a recently re-opened mosquito control impoundment. Unpublished report. Florida Medical Entomology Laboratory, Institute for Food and Agricultural Sciences, University of Florida, Vero Beach, Florida.

U. S. Geological Survey. 1956. 1:250:000 quadrangle map for Fort Pierce, Florida. Department of the Interior, Washington, D. C.

White, F. M. Fluid mechanics. 1979. McGraw-Hill Book Company, New York, NY.

CHAPTER 5
EXTENDING SIMULATION TO DISTINGUISH ISOLATED PONDS

Introduction

The general effectiveness of the current control structures and their operation policies can be revealed through an analysis of inundation levels, provided by the calibrated spreadsheet model presented in Chapter 4, for hydrologic conditions favorable to mosquito brood production. This model combines water in the impoundment which is tidally connected with isolated locations of standing water in a single volume calculation. However, mosquito larvae can hatch from isolated patches of stagnant water when they have been dry during the egg-laying season, while connected waters may have fluctuated too much to allow larval development. It would therefore be desirable to determine the frequency and extent of these potential breeding areas. This chapter presents a method to achieve lumped estimates of the percentage of wet-connected, wet-unconnected and dry areas for the entire impoundment at each time step.

Development of Connected/Isolated Water Budgets

In calculating the overall impoundment water budget for each time step, separate budgets must be maintained for water areas connected to a culvert and isolated ponds (Figure 5-1). When a water area is disconnected, or isolated, it is referred to here as a pond. Ponds

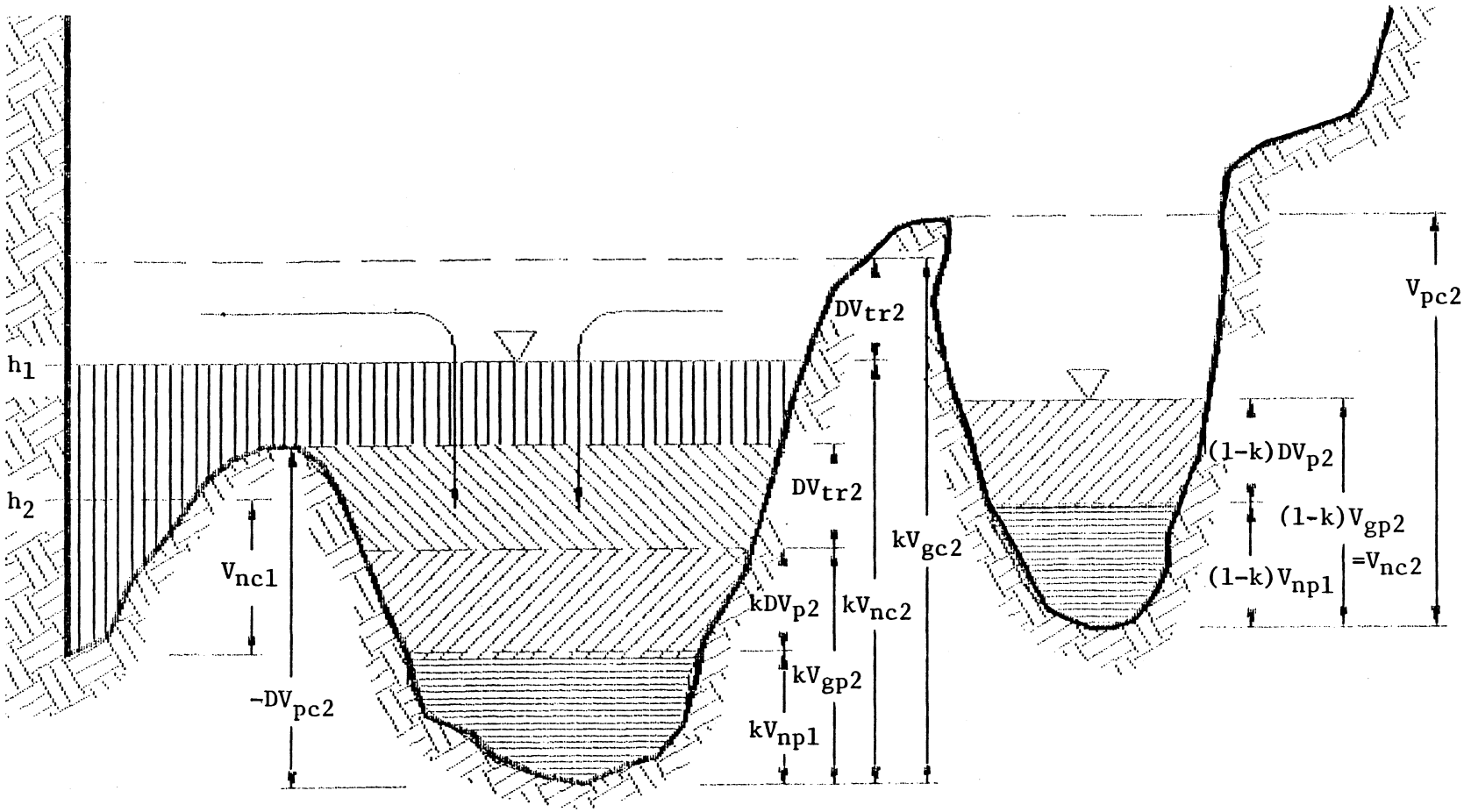

Note: Subscript 1 refers to period i-1; subscript 2 refers to period i (from t_{i-1} to t_i).

Figure 5-1. Illustration of connected/isolated water budget calculations.

connect and disconnect with fluctuating stage. Once this water merges with the surrounding connected water, then all its volume is connected water. Precipitation, evapotranspiration and infiltration volumes are therefore calculated separately for pond areas.

The stage as measured at the culvert is a function of the volume of connected water only:

$$h_i = f(V_{nc.i}) \qquad [5\text{-}1]$$

where h_i = stage at culvert at end of period i; and

$V_{nc.i}$ = net volume of water connected to tidal interaction at end of period i (after transfer to/from ponds is calculated).

The net volume of connected water is the corrected volume after calculating the extent to which flow between connected areas and ponds would have occurred:

$$V_{nc.i} = V_{gc.i} - DV_{tr.i} \qquad [5\text{-}2]$$

where $V_{gc.i}$ = gross volume of connected water at end of period i (before transfer to/from ponds calculated); and

$DV_{tr.i}$ = volume of water transferred during period i to/from ponds.

Gross volume of connected water is calculated by incrementing the previous net volume by that portion of the inflows and outflows to the impoundment that would affect connected areas:

$$V_{gc.i} = V_{nc.i-1} + DV_{c.i} \qquad [5\text{-}3]$$

where $DV_{c.i}$ = water volume gained by connected area during period i from sources other than transfer to/from ponds.

This incremental volume would consist of all components of the general water budget. Including conversion factors to express volume in cubic feet:

$$DV_{c.i} = (43560/12)\left[P_i(A_{cw.i}+A_{cd.i})-(ET_{w.i}+F_i)A_{cw.i}-ET_{d.i}A_{cd.i}\right]+ 3600Q_i(t_i-t_{i-1}) \qquad [5\text{-}4]$$

where P_i = precipitation during period i, inches;

$ET_{w.i}$ = evapotranspiration during period i, inches;

F_i = infiltration during period i, inches;

$A_{cw.i}$ = area of connected water during period i, acres;

$A_{cd.i}$ = dry connected area during period i, acres;

Q_i = combined net flow through water control structures during period i, cfs; and

t_i-t_{i-1} = length of period i, hours.

The above assumes the estimate that only precipitation falling directly upon a pond area will collect in a pond; rain falling upon connected dry areas is assumed to run off into connected water areas. In the model in Chapter 4, evapotranspiration for dry or exposed soil areas (ET_d) is calculated differently from that for water areas (ET_w), and the estimate is made that infiltration is limited to water areas.

A similar water budget is maintained for ponds, omitting the flow through water control structures from which these areas are isolated:

$$DV_{p.i} = (43560/12)\left[P_i(A_{pw.i}+A_{pd.i})-(ET_{w.i}+F_i)A_{pw.i}-ET_{d.i}A_{pd.i}\right] \qquad [5\text{-}5]$$

where $DV_{p.i}$ = water volume gained by ponds during period i from sources other than flows to/from connected areas; and

$A_{pd.i}$ = dry pond area during period i, acres.

Also in the same vein as for the connected areas, gross and net pond volumes are defined:

$$V_{gp.i} = V_{np.i-1} + DV_{p.i} \qquad [5\text{-}6]$$

where $V_{gp.i}$ = gross pond volume at end of period i (before transfer to/from connected areas is calculated); and

$V_{np.i-1}$ = net pond volume at end of period i-1 (after transfer to/from connected areas is calculated.

The volume of water transferred depends upon the number of ponds that newly connect or disconnect, and the extent to which these may have been partially filled from previous higher stages or rainfall. For a given stage rising in an empty impoundment, a specific percentage of the total pond volume or capacity will be exposed, beginning with 100% at the lowest water level and dropping to zero when the impoundment is inundated fully. This yields a curve of pond capacity vs. stage which may be predetermined through digitization of maps showing full ponds as they disconnect from a falling stage. Such a curve may also be obtained from analysis of the gridded representation of the impoundment.

To incorporate this curve into the simulation procedure, which produces stage as the final calculation at the end of each time step, one of the following methods could be used. Pond capacity could be given as a function of stage at the end of the previous time step:

$$V_{pc.i} = f(h_{i-1})$$

where $V_{pc.i}$ = dry capacity of isolated ponds exposed by given stage during period i.

This would, however, require the omission of the current time step's activities. An "interim" stage could be calculated based upon the gross volume outside the ponds;

$$h'_i = f(V_{gc.i})$$

where h'_i = interim stage.

The stage calculation, however, is a long and memory-intensive one. It would be preferable to compute pond capacity directly from the gross volume outside the ponds. Thus since

$$V_{pc.i} = f'(h'_i)$$
$$= f'[f(V_{gc.i})]$$

the following relationship should be determined:

$$V_{pc.i} = f'(V_{gc.i}) \qquad [5\text{-}7]$$

To find the volume of water which will connect or disconnect during period i, it will first be necessary to find how much pond capacity (regardless for now whether this capacity is already partially or fully filled with water) has been exposed by receding waters or covered with rising waters. This is simply the difference between the current and the previous pond capacities:

$$DV_{pc.i} = V_{pc.i} - V_{pc.i-1}$$

where $DV_{pc.i}$ = change in pond capacity over period i.

A coefficient k is defined here as:

$$k_i = -DV_{pc.i}/V_{pc.i}$$

where k_i = fraction of period i-1's pond volume which will connect or disconnect during period i

= (change in pond capacity)/(previous pond capacity).

Sufficient information is now known for period i to calculate how much water will connect or disconnect. From Figure 5-1, it can be seen that:

$$-DV_{pc.i} = DV_{tr.i} + k_i V_{gp.i}$$

Rearranging:

$$DV_{tr.i} = -DV_{pc.i} - k_i V_{gp.i} \qquad [5\text{-}8]$$

The net volume of connected water can then be calculated by rearranging equation 5-2:

$$V_{nc.i} = V_{gc.i} - DV_{tr.i} \qquad [5\text{-}9]$$

The final net pond volume is that portion of the gross pond volume not transferred to connected areas:

$$V_{np.i} = (1-k_i)V_{gp.i} \qquad [5\text{-}10]$$

Finally, the net volume of connected water is used to calculate stage for period i from the curve fitted to the function described in equation 5-1.

Summary

The maintenance of separate water budgets for connected and isolated pond areas and the calculation of the water transferred between the two at each time step adds a significant spatial dimension to the spreadsheet model of Chapter 4. Use of this method should also increase the accuracy of the total impoundment volume calculation and consequently the prediction of stage. Further knowledge of the spatial distribution of these areas may be helpful, however. The elevation of newly inundated areas and the specific location of isolated ponds are types of questions that can be answered more accurately through an in-depth look at the topography of the impoundment.

The model depicted here is most useful if provided with several stage-volume functions defining a variety of tidal connection combinations. This ability also requires further topographic analysis; both these enhancements are addressed in Chapter 6.